UNIVERSITY OF OKLAHOMA

GRADUATE COLLEGE

RESPONSES OF TOTAL AND ACTIVE SOIL MICROBIAL COMMUNITIES TO CLIMATE WARMING

A DISSERTATION

SUBMITTED TO THE GRADUATE FACULTY

in partial fulfillment of the requirements for the

Degree of

DOCTOR OF PHILOSOPHY

By

JIAJIE FENG
Norman, Oklahoma
2019

RESPONSES AND FEEDBACKS OF TOTAL AND ACTIVE SOIL MICROBIAL COMMUNITIES TO CLIMATE WARMING

A DISSERTATION APPROVED FOR THE
DEPARTMENT OF MICROBIOLOGY AND PLANT BIOLOGY

BY THE COMMITTEE CONSISTING OF

Dr. Jizhong Zhou, Chair

Dr. Shaorong Liu

Dr. Heather R. McCarthy

Dr. Lee R. Krumholz

Dr. Bradley S. Stevenson

Dedication

To Dr. Jingjing Xu

My companion, friend, and partner,

from whom I have been away for so long, and will be with forever

Acknowledgment

During this memorable journey exploring the boundary of both science and myself, I have been enjoying the honor to receive kind help and inspiring support, without which it would be impossible for me to finish this journey. I would like to sincerely acknowledge all of you who brought me here, and wish you all the best in the future.

First of all I may dedicate my great thanks to my advisor, Dr. Jizhong Zhou, for giving me the chance of this memorable journey and supporting me with both helpful advices and funding. Thank you for pointing out the correct orientations when I was about to make wrong choices, and for your continuous urges for progress, which I felt annoyed but has also been aware how they had reminded me I was in a serious journey. Your intriguing advice and sincere attitude to science will echo throughout my career.

Secondly, I would like to express my deep appreciation to my advisory committee members who have always been supportive. I would like to thank Dr. Lee R. Krumholz for teaching me Geomicrobiology, tirelessly improving my manuscript and dissertation, and helping me on improving my English. I would like to thank Dr. Bradley S. Stevenson who has been my committee member for only a short time but taking great efforts giving me helpful advices on my dissertation. I thank Dr. Heather R. McCarthy for your expertise in plant biology and your constructive comments in this field. I thank Dr. Shaorong Liu for enlightening me both in the perspective of bioanalytical science and for my career.

Then, I would like to thank many of my colleagues at the Institute for Environmental Genomics. I thank Mr. Xuanyu Tao, a Ph.D. candidate, for assisting, encouraging and collaborating with me in almost all of my studies. I thank Drs. Mengting M. Yuan, Kai Xue, Daliang Ning and Jie Deng for introducing me into the

world of microbial ecology. I thank Drs. Linwei Wu, Liyou Wu, Xishu S. Zhou, Joy D. Van Nostrand, Yujia Qin, Feifei Liu, Zhou J. Shi, Zhili He, Xue Guo, Gangsheng Wang, Fenliang Fan, Renmao Tian, Jialiang Kuang, Colin T. Bates and Qun Gao for helping me in various academic issue. Without you and every other helpful colleague, this work could not be finished.

I also must thank many of my collaborators from other institutes. I especially thank Dr. Yunfeng D. Yang for patiently teaching me how to write and do many other things, relevant to academics and life. I want to thank Drs. C. Ryan Penton, Kostas T. Konstantinidis, Marguerite Mauritz, and E.A.G Schuur for insightful communications on the studies I worked on and efforts on providing samples and feedbacks to my manuscripts.

Finally, I dedicate my deepest appreciation to my dear parents, Mr. Wencheng Feng and Prof. Li N. Jiang, who have been physically away from me during this Ph.D. program but supported and encouraged me throughout this journey. You are my greatest treasures forever.

Table of contents

Abstract

As illustrated by accumulating scientific evidence, unconscionable anthropogenic activities since industrialization such as intensive land utilization and accumulation of various greenhouse gases due to fossil fuel combustion have caused global climate warming, which has in turn caused instability of the earth's ecosystems and impacts on human society. Granted that huge efforts through scientific research have been devoted to address the interactions between the biosphere and the warmer climate, there are still numerous understudied scientific areas and questions of this topic due to the complicacy of both the biosphere and the climate system. Microbial communities are the most abundant, diverse and complex assemblages in the biosphere, and play crucial roles in geochemical processes closely related to climate warming. However, due to the difficulties in observing and cultivating the microorganisms, responses and feedbacks of microbial communities to climate warming are difficult to observe and predict, in terms of microbial taxonomic, functional and interactional patterns under warming.

High-throughput genomic technologies have revolutionized microbial ecology. Such technologies are capable to provide detailed characterization and thus great insight into studies of complex and uncultivated microbial communities and the microbially-mediated mechanisms governing the carbon balance under a warmer climate. Using several such high-throughput genomic technologies, this dissertation attempts to assess responses of soil microbial community to warming, based on field experiments and laboratory incubations. The high-latitude permafrost region (tundra) could be a "hot spot" in global carbon balance and the changing climate because it possesses the largest carbon reservoir globally. This dissertation focuses on the tundra regions and the residing microbial communities, while tall-grass prairie (temperate

grassland), an understudied but important ecosystem type among the terrestrial ecosystems, should also be studied and compared to the tundra ecosystem to assess the sensitivities of different types of ecosystems to warming.

As short-term warming has been reported as altering microbial functional potentials instead of taxonomic composition, we first attempt to illustrate the impact of long-term (5 years) experimental warming on the responses of the total soil microbial community in the Alaska tundra soils of 0–15 cm depth and their correlations with environmental factors and ecosystem C balance. We applied an amplicon sequencing approach of both bacterial/archaeal 16S rRNA gene and fungal internal transcribed spacer (ITS) to assess microbial taxonomic profiles, and applied the GeoChip 5.0 microarray to assess microbial functional profiles. We observed that longer-term experimental warming altered the structure of tundra bacterial communities ($p < 0.040$ as revealed by Adonis test) but not fungal communities. Thaw depth was the strongest environmental factor correlating with microbial community assembly and interaction networks, suggesting that warming-accelerated tundra thaw fundamentally restructured the microbial communities. Both carbon decomposition and methanogenesis genes increased in relative abundance under warming, and the functional structures strongly correlated ($R^2 > 0.725$, $p < 0.001$) with ecosystem respiration and CH_4 flux, respectively. These results demonstrate that microbial responses associated with carbon cycling could lead to positive feedbacks that accelerate soil organic carbon decomposition in tundra regions, which is alarming because soil organic carbon loss due to tundra thaw is unlikely to subside owing to changes in microbial community composition.

Soil microbial nitrogen fixation serves as a crucial factor in ecosystem feedbacks to climate warming since it largely determines plant growth and plant carbon fixation

in tundra regions. Therefore, it is crucial to examine the responses of diazotrophic communities to warming across the depths of Alaska tundra soils. We assessed the dynamics of soil diazotrophic communities spanning both the organic and mineral layers under long-term (5 years) experimental warming and their correlations with ecosystem carbon balance through amplicon sequencing of *nifH* genes, the α-subunit of bacterial nitrogenase. As observed, warming significantly (p<0.050) enhanced diazotrophic absolute abundance by 86.3% and aboveground plant biomass by 25.2%. Diazotrophic composition in the organic soil layers was markedly altered with an increase of α-diversity. Changes in diazotrophic abundance and composition significantly correlated to soil thaw duration, soil moisture and plant biomass, as shown by structural equation modeling analyses, indicating similar environmental drivers for total microbial and diazotrophic communities. We conclude that more abundant diazotrophic communities induced by warming may serve as an important mechanism of negative feedback to warming by supplementing biologically available nitrogen in the tundra ecosystem.

After assessing soil total microbial community in the tundra soil, it is necessary to further assess microbial community that is active in degrading soil carbon compounds, which is more responsible and representative in the microbial interactions with ecosystem carbon balance. Compared to biologically labile carbon compounds, studying the dynamics of biologically recalcitrant carbon compounds under warming could be crucial as they are the dominant components of tundra carbon storage. Lignin is a major component among the biologically recalcitrant carbon compounds in tundra soil. After depleting soil labile C through a 975-day laboratory incubation, the identity of microbial decomposers of lignin and their responses to warming were characterized by applying stable isotope probing to the

active layer of Arctic tundra soils. Warming considerably increased both total abundance and functional capacities of all potential lignin decomposers. A *β-Proteobacteria* genus, *Burkholderia*, accounted for 95.1% of total abundance of potential lignin decomposers. Consistently, *Burkholderia* strains isolated from our tundra soils could grow with lignin as the sole carbon source. In addition to *Burkholderia*, *α-Proteobacteria* species capable of lignin decomposition (e.g. *Bradyrhizobium* and *Methylobacterium* genera) was stimulated by 82-fold, indicating that *α-Proteobacteria* species are more stimulated by warming than *Burkholderia* species. Those community changes collectively doubled the priming effect, i.e., decomposition of existing carbon after fresh carbon input to soil. Consequently, warming would cause a higher rate of soil carbon decomposition in the long-term as verified by microbially-enabled climate-carbon modeling. Our alarming findings demonstrate that accelerated carbon decomposition under warming conditions will make tundra soils a larger biospheric carbon source than anticipated.

To allow the comparison of microbial feedbacks to warming in different ecosystems, we further assessed the active bacterial community of carbon degradation and its response to warming in grassland ecosystems. Combining metagenomic technologies with a stable isotope probing incubation using isotopically labelled straw to simulate grass litter, we examined the dynamics of active bacterial communities and carbon dioxide emissions of grassland soil in response to a long-term (7 years) experimental warming treatment. Our study unveiled a comprehensive stimulation of warming on active bacterial communities in terms of abundance and carbon-degrading potentials, which collectively increased the carbon degradation rates of both straw input and old soil organic matter, indicative of an increased positive feedback to climate warming. This stronger positive feedback could be permanent as

warming compositionally changed the active bacterial communities, turning the majority of phylum *Firmicutes* into active (18.5% of total bacterial abundance), which was reported as efficient in degradations of both biologically labile and recalcitrant carbon compounds. Moreover, divergent successions (larger internal dissimilarities) of active bacterial communities were observed under warming, which may cause less predictable dynamics of active bacterial communities. The response of microbial carbon-degrading activities to warming displayed a phylogenetic clustering pattern (*Firmicutes*), indicative of a phylogenetically conserved ecological strategy, which could be related to the alarming positive feedback to the warmer climate.

Overall, this dissertation provided valuable observations based on field experiments and laboratory incubations on responses of microbial communities to climate warming, revealed that both total and active microbial communities could be sensitive to warming, and captured warming-induced environmental drivers of microbial communities such as tundra soil thaw and aboveground plant biomass. These findings collectively accumulate valuable experience for microbially-mediated mechanisms underlying carbon cycle ecosystem models in a warmer world.

Keywords: climate warming, soil microbial community, nitrogen-fixing bacteria, diazotrophs, high-throughput genomic technologies, metagenomics, permafrost regions, tundra soil, tall-grass prairie soil, temperate grassland soil, GeoChip, microarray, stable-isotope probing, active degraders

Chapter 1: **Introduction**

1.1 Impact of global climate warming on the biosphere

Global climate warming, resulted from unconscionable land utilization and accumulation of various greenhouse gases such as CO_2 and CH_4 due to fossil fuel combustion, has become the largest anthropogenic disturbance on natural systems (Deutsch, Tewksbury et al. 2008) and a major scientific and political issue worldwide (Stocker, Qin et al. 2013). Projections of global climate models concluded that by the end of the 21st century, the global surface temperature would rise by 0.3 to 1.7 °C in a moderate scenario, or as much as 2.6 to 4.8 °C in an extreme scenario, depending on the trend of future greenhouse gas emissions and land utilization (Stocker, Qin et al. 2013). These conclusions have been accepted by national academies of the major industrialized nations (National Academies of Sciences and Medicine 2018) and are not disputed by any scientific body of national or international standing (Aeronautics and Administration 2017). In addition to the increasing temperature, other observations such as thawing permafrost, rising sea level, and retreating arctic ice are together verifying the phenomenon that the global climate is changing unprecedentedly (Stocker 2014). Despite the huge temporal variability of the global climate system (Wigley and Raper 1990), these recent variabilities are regarded unusual according to model projections, and cannot be explained by natural causes alone, such as the solar radiation (IPCC 2007). The Fifth Assessment Report of the Intergovernmental Panel on Climate Change (IPCC) concluded that it is considerably likely that human activities have been the major cause of the observed global climate warming since the 1950's (Stocker, Qin et al. 2014). The largest anthropogenic cause of climate warming is the release of greenhouse gases such as carbon dioxide, water vapour, methane, and nitrous oxide. Greenhouse gases are more capable to absorb and

emit infrared radiation than other gases, causing the atmosphere trapping more heat (Abram, McGregor et al. 2016).

Environmental effects of global warming can be broad and far-reaching, with huge impacts on natural ecosystems and human systems (IPCC 2007, Stocker 2014) including rising sea level, retreating glacier, melting ice, degrading permafrost, and larger frequency or strength of extreme weathers. As higher temperature is a primary driver of metabolic rates and biochemical processes (Gillooly, Brown et al. 2001, Brown, Gillooly et al. 2004), impacts on biosphere are also vast and broad, such as species extinction, changes in biological activities and interactions, decreased agricultural production, and altered distributions of pathogen and disease. Finer-scale observations have indicated that climate warming has affected biodiversity at all systematic levels, leading to restructured community (Xue, Yuan et al. 2016), enhanced abundance (Feng, Penton et al. 2019), divergent successional trajectories (Guo, Feng et al. 2018), and shifted geographic distribution (Chen, Hill et al. 2011) of organisms. In addition, based on studies evaluating these impacts, as concluded in several reviews (McMichael 2003, Patz, Campbell-Lendrum et al. 2005, Pecl, Araújo et al. 2017), negative impacts of global climate warming on human society were comprehensively predicted. Climate change may further lead to more severe stresses in food security, drinking water quality, public health and socioeconomic balance if not solved properly.

1.2 Responses of terrestrial ecosystems to climate warming

Deconvolution of the feedbacks of the biosphere carbon (C) cycling to climate warming is crucial for projections given the emission of greenhouse gases to the atmosphere, especially CO_2, is the major anthropogenic cause of climate warming.

The terrestrial C pool, the second largest C pool globally, exchanges C with the atmosphere with the largest flux mainly through respiration and photosynthesis (Stocker 2014). Given that a warmer climate is a powerful driver of metabolic rates and biochemical processes (Gillooly, Brown et al. 2001, Brown, Gillooly et al. 2004), both C fixation by photosynthesis, which serves as the negative feedback to warming, and C release through respiration, which serves as the positive feedback, are likely to be stimulated in a warmer world, resulting in a changed global C balance.

The extent of how these two types of feedbacks would be stimulated determines whether the climate warming would be intensified or mitigated (Luo 2007, Zhou, Xue et al. 2012). Debates based on contradictory experimental results have taken place on whether the overall feedback of global ecosystem to warming would be positive or negative (Luo 2007). Different ecosystem types have exhibited different outcomes based on experimental data, including northern high-latitude regions where the temperature has been increasing at a rate of twice of the global average (Hansen, Sato et al. 2006, Comiso, Parkinson et al. 2008, Kortsch, Primicerio et al. 2012) which lead to the overall positive feedbacks to warming (Friedlingstein, Bopp et al. 2001, Dufresne, Fairhead et al. 2002, Kirschbaum 2004, Scheffer, Brovkin et al. 2006, Walter, Zimov et al. 2006), and temperate terrestrial ecosystems which were more reported as negative or inconspicuous feedback to warming (Lenton, Held et al. 2008). Therefore, such debates focus on an essential question that whether the response of the global ecosystem would offset the global warming, and what underlying biological and ecological mechanisms would determine such responses.

1.3 Responses of soil microbial communities to climate warming

Microbial communities, the most diverse and complex assemblage of the biosphere (Singh, Campbell et al. 2009), could also be stimulated to be a larger source of greenhouse gases such as methane and CO_2 and thus a stronger positive feedback to warming compared to the past (Xue, Yuan et al. 2016). Previous research has assessed phylogenetic, compositional, and functional changes of microbial communities in response to warming (Xue, Yuan et al. 2016, Guo, Feng et al. 2018, Feng, Penton et al. 2019), and uncovered relationships between warming and CO_2 emissions from microbial communities (Luo, Wu et al. 2001, Mahecha, Reichstein et al. 2010, Carey, Tang et al. 2016), but the underlying mechanisms of microbial C degradation change in response to warming remain understudied, which are crucial for predicting future carbon (C) dynamics and thus global climate change (Wang, Jagadamma et al. 2015).

Microbial communities play integral and unique roles in many ecological and biogeochemical processes. They degrade organic materials and cycle elements, which are essential processes affecting the global nutrient element cycling (Bardgett, Freeman et al. 2008). It is critical to understand how microbial communities respond to various types of disturbances driven by climate warming in climate change biology. Development of cutting-edge metagenomic technologies has revolutionized the understanding of environmental microbial diversity. Many publications have assessed and discussed the phylogenetic, compositional, and functional dynamics of soil microbial communities in response to warming (Zhang, Parker et al. 2005, Hartley, Heinemeyer et al. 2007, Bradford 2013, Jassey, Chiapusio et al. 2013, Nie, Pendall et al. 2013, Rousk, Smith et al. 2013, Tucker, Bell et al. 2013, Zhang, Liu et al. 2013, Ziegler, Billings et al. 2013, Pailler, Vennetier et al. 2014, Streit, Hagedorn et al. 2014, Wang, Dong et al. 2014, Deng, Gu et al. 2015, Peltoniemi, Laiho et al. 2015,

Semenova, Morgado et al. 2015, Yoshitake, Tabei et al. 2015). In addition to warming, the responses of soil microbial communities also depend on other environmental factors shaped by warming (Castro, Classen et al. 2010, Docherty, Balser et al. 2012, Walter, Hein et al. 2013, Cavaleri, Reed et al. 2015), such as nutrition availability (Hines, Reyes et al. 2014, Melle, Wallenstein et al. 2015), precipitation (Zhang, Liu et al. 2013, Liu, Allison et al. 2016), soil thaw intensity (Sistla, Moore et al. 2013, Feng, Penton et al. 2019), and disturbances deriving from grazing (Zhang, Parker et al. 2005, Walter, Hein et al. 2013, Crowther, Thomas et al. 2015, Steven, Kuske et al. 2015). These literatures collectively contributed a lot to the understanding of how soil microbial communities respond to warming.

Microbial N fixation is one of the negative feedbacks from global ecosystems to warming due to the promotion of enriched soil N on plant growth and thus photosynthesis (Hobbie 1992). Nitrogen deficiency is universal in terrestrial ecosystems, and the limited soil N constrains production of plants (Hobbie, Eddy et al. 2012), thus strongly affecting the net response of terrestrial ecosystems to warming. Biological N fixation is the major N source for N-limited terrestrial ecosystems (Barsdate and Alexander 1975), which is typically stimulated by elevated temperature and moisture (Liengen and Olsen 1997, Zielke, Solheim et al. 2005, Stewart, Lamb et al. 2011, Stewart, Brummell et al. 2013). Experimental warming has been shown to enhance diazotrophic (i.e., N-fixing) richness (Penton, St Louis et al. 2015) and N fixation rates (Chapin and Bledsoe 1992, Belnap 2002). The metabolic theory of ecology predicts that warming will increase the metabolic rates of organisms, resulting in higher rates of speciation (Brown, Gillooly et al. 2004), which may potentially interpret the increased N fixation rates and diazotrophic richness, but the

responsible diazotrophs, their interactions with plants, and the underlying metabolic mechanisms remain largely elusive in terrestrial ecosystems.

Feedbacks from plants to climate warming highly depend on interactions between plants and soil microbes, which may change under warming. The major components of plant root exudates are organic acids and carbohydrates, which are insufficient for microbial N sources and cannot explain the size of rhizospheric microbial population (Simons, Permentier et al. 1997). Therefore, N should be limited for microbial growth in the rhizosphere, leading to a potential advantage of diazotrophs. Consistently, rhizosphere soil showed higher diazotrophic activities compared with bulk soil (Jones, Farrar et al. 2003). Diazotrophs have also been shown to promote plant growth via other mechanisms, such as competing with plant pathogens or synthesizing phytohormones (Gaskins, Albrecht et al. 1985, Okon, Itzigsohn et al. 1995, Dobbelaere, Vanderleyden et al. 2003). Long-term soil warming strongly enhanced aboveground plant biomass and foliar N content in Alaskan tundra (Salmon, Soucy et al. 2015), and the rate of root exudation was lower under a higher level of soil N fertility (Yin, Li et al. 2013), together implying that promoted root exudation by warming is critical for the activity of soil diazotrophs, which in turn is potentially critical for plant absorption of fixed N. However, the detailed components of root exudates in warmed soils and diazotrophic response to them remain elusive. Root exudates are mainly composed of low-molecular-weight compounds(Cieslinski, Van Rees et al. 1997, Hütsch, Augustin et al. 2002, Farrar, Hawes et al. 2003), which are assigned as fresh C or labile C among the soil C pool(Leake, Ostle et al. 2006). These fresh C compounds may stimulate root-exudate-mediated decomposition of biologically recalcitrant SOM in the rhizosphere(el Zahar Haichar, Marol et al. 2008) (i.e., priming effects), which is a central issue in global change biology. This priming

effect is, on the contrary, a positive feedback to warming compared to the negative feedback derived from enhanced diazotrophic activities, which is closely related to the integrated response of ecosystem to warming.

1.4 Microbial responses to warming in permafrost regions

The northern circumpolar permafrost regions contain approximately 1,672 Pg of C, accounting for nearly half of the global soil carbon (C) storage, although this zone accounts for only 16% of the global terrestrial area (Schuur, Bockheim et al. 2008, Tarnocai, Canadell et al. 2009). This large C reservoir has become increasingly vulnerable to microbial decomposition as permafrost thaw depth increases due to global warming (Tarnocai, Canadell et al. 2009), which may release greenhouse gases (CO_2 and CH_4) (Osterkamp 2007). In tundra regions, ~90% of total C is stored in the recalcitrant C pool, consisting of old soil organic matter (SOM) such as lignin, chitin, and terpenes (Bracho, Natali et al. 2016). Since the global climate is getting warmer, the labile C pool tends to be depleted soon (Schädel, Schuur et al. 2014, Bracho, Natali et al. 2016), causing soil organic matter in the recalcitrant C pool more accessible to decomposition (Pold, Melillo et al. 2015). Therefore, the recalcitrant C pool in tundra soil may act as a major source for the accumulation of atmospheric greenhouse gases.

As soil microbial communities play significant roles in the terrestrial carbon cycle, assessing their responses to warming is vital for projecting future carbon balance in permafrost regions. So far, a few laboratory incubation studies (Mackelprang, Waldrop et al. 2011, Coolen and Orsi 2015) and a few field studies (Taş, Prestat et al. 2014, Lipson, Raab et al. 2015) have assessed the microbial response to permafrost region geochemical events such as hydrology reformation, soil thaw, and wild fire.

However, field experiments using warming as a treatment are few, and long-term dynamics of microbial responses to permafrost warming remain understudied. Only a few studies of permafrost ecosystems have examined microbial responses to climate warming (Deng, Gu et al. 2015, Schuur, McGuire et al. 2015, Xue, Yuan et al. 2016). For example, a substantial fraction of soil C in permafrost was available for microbially-mediated decomposition during a lab incubation simulating warming (Elberling, Michelsen et al. 2013). Consistently, a field study in a permafrost-based tundra revealed that the microbial community functional potential was highly sensitive to a 1.5-year experimental warming, despite the taxonomic composition remaining unaltered (Xue, Yuan et al. 2016). As a result, soil C was more vulnerable to microbial decomposition. However, it remains unclear whether microbial community responses to short-term warming persist in the longer term.

1.5 Foci of this dissertation

This dissertation will address how climate warming and how warming-induced changes of environmental factors would affect soil microbial communities, and what feedbacks soil microbial communities would have on climate warming. Experimentally warmed soil samples were collected from field sites and analyzed using cutting-edge metagenomic approaches to uncover compositional, phylogenetic, functional and interactional profiles of microbial communities. Environmental factors were monitored and the data was collected for the analyses on their correlations with microbial communities. This dissertation mainly focuses on the high-latitude permafrost regions (tundra) microbial communities, the “hot spot” in the changing climate, while tall-grass prairie, an understudied but important ecosystem type among

the terrestrial ecosystems, would also be studied and compared to the tundra ecosystem.

Chapter 2 attempts to assess the total soil microbial community in tundra regions under warming, including soil bacterial community, soil archaeal community and soil fungal community, and correlations between their profiles with environmental factors and ecosystem C balance. We expected three mutually exclusive outcomes after longer-term warming: (i) the microbial functional structure would be altered, while the taxonomic composition would remain similar to that of the control group, which would in turn be similar to that observed after the 1.5-year warming period (resistance); (ii) the microbial communities that are acclimated to experimental warming would manifest a functional structure and taxonomic composition that approximates that of the control group (resilience); or (iii) microbial communities would continue to evolve into new states and both functional structure and taxonomic composition would be altered by warming (sensitivity). Using amplicon sequencing technology of 16S rRNA gene and fungal internal transcribed spacer (ITS) to assess microbial taxonomic profiles, and using GeoChip 5.0 to analyze microbial functional profiles, the study in this chapter aims to provide both general and detailed microbial responses to warming and C balance in the tundra regions.

As soil microbial N fixation provides the N source for plants and thus largely determines plant growth and C fixation, in Chapter 3 we assessed the dynamics of soil diazotrophic communities under warming and their correlations with ecosystem C balance. We hypothesize that the warming would significantly increase soil diazotrophic community abundance by stimulating microbial growth, and also stimulate plant primary production by supplementing biologically available N. Using

amplicon sequencing of *nifH* genes, the α-subunit of bacterial nitrogenase, we assessed the taxonomic profiles of diazotrophic communities in tundra regions.

Granted that the total soil microbial community is assessed, the ubiquity of microbial dormancy (Jones and Lennon 2010) may weaken the representativeness of total microbial communities in such relationships (Wang, Jagadamma et al. 2015). Therefore, investigations into active microbial communities, which are actually responsible for soil C degradation, and their mechanistic linkages with C degradation under warming is necessary for predicting the future C balance of grassland ecosystems. Chapter 4 aims to evaluate the active bacterial communities in degrading lignin, one of the major components of tundra soil biologically recalcitrant compounds. Using stable isotope probing (SIP), we assessed the active degraders of lignin and their response to warming, which would provide valuable insights into the microbially-mediated mechanisms in tundra C degradation. To compare with the tundra ecosystem, in Chapter 5, we further assessed the active bacterial community and its response to warming in a grassland ecosystem. We primarily focus on the warming effects on microbial community succession by determining: (i) whether and how warming will alter temporal succession rates of the grassland soil microbial communities across different organismal groups (e.g. bacteria and fungi); (ii) if warming will lead to divergent or convergent succession of soil microbial communities; and (iii) what are the relative roles of deterministic and stochastic processes in shaping temporal succession of soil microbial communities in response to climate warming.

The summary chapter (Chapter 6) summarized the major conclusions related to the main message of this dissertation from each chapter, highlighted their intellectual merits in filling gaps of our current understandings, and illustrated their importance

for future research and contributions to our society. Overall, this dissertation accumulates experimental evidence on responses of soil microbial community to climate warming, and provides updated hypotheses formulated for testing mechanistic understandings of these responses. We may expect better projections of future climate dynamics through the discoveries of this work.

Chapter 2: Warming-accelerated thaw of permafrost-based tundra exacerbates soil carbon loss by restructuring the microbial community

2.1 Abstract

The sensitivity of high-latitude tundra underlain with permafrost to global warming has been well documented. This leads to a serious concern that decomposition of soil organic carbon (SOC) previously stored in this region, which accounts for about 50% of the world's SOC storage, will cause stronger positive feedbacks that further accelerate climate warming. We previously showed that short-term warming (1.5 years) stimulated rapid, microbially-mediated decomposition of tundra soil carbon without affecting the composition of the soil microbial community. Here, we show that longer-term (5 years) experimental winter warming at the same site, altered tundra microbial communities ($p < 0.040$). Thaw depth correlated strongest with community assembly and interaction networks, suggesting that warming-accelerated tundra thaw fundamentally restructured the microbial communities. Both carbon decomposition and methanogenesis genes increased in relative abundance under warming, and the functional structures strongly correlated ($R^2 > 0.725$, $p < 0.001$) with ecosystem respiration and CH_4 flux, respectively. These results demonstrate that microbial responses associated with carbon cycling could lead to positive feedbacks that accelerate SOC decomposition in tundra regions, which is alarming because SOC loss due to tundra thaw is unlikely to subside owing to changes in microbial community composition.

2.2 Introduction

High-latitude permafrost-underlain tundra ecosystems have been a hotspot for climate change research, owing to their substantial carbon (C) pool and high vulnerability to climate warming (Schuur, Bockheim et al. 2008, Schuur, Vogel et al. 2009, Schuur, Abbott et al. 2011, Xue, Yuan et al. 2016). Old C from plant and animal remnants has been sequestered in permafrost soils for thousands of years under frozen soil conditions (Pries, Schuur et al. 2012). Although accounting for only 15% of the total global land mass, the northern hemisphere permafrost regions at a depth of 0–3 m contain 1 672 Pg C, roughly half of the global soil C pool (Schuur, Bockheim et al. 2008, Tarnocai, Canadell et al. 2009). Since permafrost regions have the potential to release a large amount of previously stored soil C to the atmosphere in a warmer world (Schuur, Abbott et al. 2011, Xue, Yuan et al. 2016), it is a significant variable that affects the future trajectory of climate change (Schuur, McGuire et al. 2015).

Over the past 30 years, annual average temperatures in high latitude regions have increased by 0.6 °C per decade, twice as fast as the global average (Stocker, Qin et al. 2014), resulting in substantial thaw of permafrost regions. It has been estimated that climate warming will cause a reduction of 30–70% of the total permafrost region by the end of the 21st century (Lawrence, Slater et al. 2012). As a consequence, previously protected soil C becomes available for microbial decomposition (Schuur, Bockheim et al. 2008). A number of studies have shown that tundra soil C is highly vulnerable and responds rapidly to warming-accelerated thaw of permafrost regions (Schuur, Bockheim et al. 2008, Grosse, Harden et al. 2011, Xue, Yuan et al. 2016). Although the increase in plant productivity across the tundra regions may partially offset soil C loss (Natali, Schuur et al. 2012, Deane-Coe, Mauritz et al. 2015, Salmon, Soucy et al. 2016), there remains a lack of a mechanistic understanding of microbial

responses to climate warming, which makes it challenging to assess the future C balance.

Only a few studies of permafrost ecosystems have examined microbial responses to climate warming (Deng, Gu et al. 2015, Schuur, McGuire et al. 2015, Xue, Yuan et al. 2016). For example, a substantial fraction of soil C in permafrost was available for microbially-mediated decomposition during a lab incubation simulating warming (Elberling, Michelsen et al. 2013). Consistently, a field study in a permafrost-based tundra (the same site as this study) revealed that the microbial community functional potential was highly sensitive to a 1.5-year experimental warming, despite the taxonomic composition remaining unaltered (Xue, Yuan et al. 2016). As a result, soil C was more vulnerable to microbial decomposition. However, it remains unclear whether microbial community responses to short-term warming persist in the longer term.

Here, we examined soil microbial communities subjected to a 5-year warming at the Carbon in Permafrost Experimental Heating Research (CiPEHR) site. This site has been extensively used to analyze the effects of climate warming on plants, soil nitrogen (N) availability, and soil microbial communities within a permafrost region (Bracho, Natali et al. 2016, Pries, Schuur et al. 2016, Webb, Schuur et al. 2016, Xue, Yuan et al. 2016). Since a 1.5-year warming altered the microbial functional structure but not the taxonomic composition of the soil microbial communities in permafrost-based tundra (Xue, Yuan et al. 2016), we expected three mutually exclusive outcomes after longer-term warming: (i) the microbial functional structure would be altered, while the taxonomic composition would remain similar to that of the control group, which would in turn be similar to that observed after the 1.5-year warming period (resistance); (ii) the microbial communities that are acclimated to experimental

warming would manifest a functional structure and taxonomic composition that approximates that of the control group (resilience); or (iii) microbial communities would continue to evolve into new states and both functional structure and taxonomic composition would be altered by warming (sensitivity). Therefore, we investigated both the taxonomic composition and functional structure of microbial communities under warming, in addition to potential drivers and ecological consequences of community changes.

2.3 Materials and methods

2.3.1 Field site description and soil sampling

Established in 2008, the CiPEHR project is located within a discontinuous permafrost region in the northern foothills of the Alaska Range (~670 m elevation) at the Eight Mile study site, AK, USA (63°52'59"N, 149°13'32"W) (Natali, Schuur et al. 2011, Natali, Schuur et al. 2012). Soils in the experimental site are gelisols and comprise a 45–65 cm thick organic horizon above a cryoturbated mineral mixture of glacial till and loess. The active layer, which thaws annually, is 50–60 cm thick. The site had a mean annual air temperature of -1.45 ± 0.25 °C from 1977 to 2013 and a mean growing season precipitation of 216 ± 24 mm from 2004 to 2013. The dominant vegetation is a tussock-forming sedge, *Eriophorum vaginatum*. More detailed information on this site is available elsewhere (Natali, Schuur et al. 2011).

Soils have been warmed since 2008 via snow fences (1.5 m tall, 8 m long), which act as insulators to increase the depth of the snow layer. Six snow fences are arranged in 3 blocks of 2 each, with each fence representing a warming-control plot pair. Each block is approximately 100 m apart and fences within a block are 5 m apart. Snow removal is conducted in the early spring (March 8^{th}–15^{th}) to avoid

moisture and meltdown effects of the additional snow. In May 2013, surface soil samples at a depth of 0–15 cm were collected from both warming and control plots (6 replicates each), and then used for microbial community and environmental factor analyses.

2.3.2 Measurement of environmental factors

Soil temperature at depths of 5 and 10 cm was measured every half an hour in each plot using constantan-copper thermocouples and recorded using CR1000 data loggers (Campbell Scientific, Logan, UT, USA). Site-calibrated CS616 water content reflectometer probes (Campbell Scientific, Logan, UT, USA) were used to measure volumetric water content (moisture) at a depth of 0–15 cm. CS450 pressure transducers (Campbell Scientific, Logan, UT, USA) located in wells were used to continuously measure water table depth. The thaw depth was measured weekly during the growing season using a metal probe. Aboveground biomass was determined by a non-destructive point-frame method using a 60×60 cm frame with 8×8 cm grids, and species identity and tissue type (leaf, stem or fruit) for plants touching the rod ("hits") were recorded as previously described (Natali, Schuur et al. 2012). Soil C and N content was measured using an ECS 4010 Elemental Analyzer (Costech Analytical Technologies, Valencia, CA, USA). CH_4 fluxes from each plot were measured as previously described (Natali, Schuur et al. 2015), using a HP 5890 gas chromatograph (Hewlett-Packard, Palo Alto, CA, USA) equipped with a flame ionization detector and a molecular sieve 13X packed column. Ecosystem respiration, the sum of autotrophic and heterotrophic respiration, was measured using an LI-820 infrared gas analyzer (LI-COR Biosciences, Lincoln, NE, USA) connected to a chamber placed on the plot base and covered by a dark tarp to exclude photosynthesis. Growing season soil

temperature, soil moisture, water table depth, thaw depth, ecosystem respiration, and CH_4 flux data from the 2012 growing season were time-averaged within each plot for use in this study. Winter soil temperature for 2012–2013 was time-averaged within each plot.

2.3.3 Soil DNA extraction

Soil DNA was extracted from 3 g of each soil sample by freeze-grinding mechanical cell lysis as described previously (Zhou, Bruns et al. 1996) and then purified with a PowerMax Soil DNA Isolation Kit (MO BIO, San Francisco, CA, USA). A NanoDrop ND-1000 spectrophotometer (NanoDrop Technologies Inc., Wilmington, DE, USA) was used to assess DNA quality using absorbance ratios of 260/280 and 260/230 nm. Final DNA concentrations were quantified using a Quant-iT PicoGreen dsDNA Assay kit (Invitrogen, Carlsbad, CA) with a FLUOstar OPTIMA fluorescence plate reader (BMG LabTech, Jena, Germany).

2.3.4 High-throughput amplicon sequencing and raw data processing

The V4 hypervariable region of 16S rRNA gene was amplified with the primer pair 515F (5'-GTGCCAGCMGCCGCGGTAA-3') and 806R (5'-GGACTACHVGGGTWTCTAAT-3'). The fungal internal transcribed spacer (ITS) was amplified with the primer pair ITS7F (5'-GTGARTCATCGARTCTTTG-3') and ITS4R (5'-TCCTCCGCTTATTGATATGC-3'). A 2-step PCR protocol was used to avoid bias introduced by the additional components in the long sequencing primers (Wu, Wen et al. 2015). Cycling conditions were an initial denaturation at 94 ° C for 1 min, then 10 cycles (first step) or 20 cycles (second step) of 94 ℃ for 20 s, 53 ℃ (16S rRNA) or 52 ℃ (ITS) for 25 s, 68 ℃ for 45 s, followed by a final 10-min

extension at 68 °C. The amplicons were paired-end sequenced (2×150) on a MiSeq sequencer (Illumina, San Diego, CA, USA). Sequences were processed on IEG Sequencing Analysis Pipeline (http://www.ou.edu/ieg/tools/data-analysis-pipeline). Specifically, sequences were trimmed using BTRIM with a threshold quality score greater than 20 within a 5 bp window size and a minimum length of 100 bp. Forward and reverse reads with at least a 50 bp overlap and no more than 5% mismatches were joined using FLASH (Magoč and Salzberg 2011). After removing sequences with ambiguous N bases, joined sequences with lengths between 245 and 260 bp for 16S rRNA, and between 100 and 450 bp for ITS were subjected to chimera removal by U-Chime (Edgar, Haas et al. 2011). OTUs were clustered through Uclust at a 97% similarity level (Edgar, Haas et al. 2011). Taxonomic assignment was conducted through the RDP classifier (Wang, Garrity et al. 2007) with a confidence cutoff of 0.5, and singletons were removed. The remaining sequences were randomly resampled to a depth of 34 673 reads per sample for 16S rRNA gene sequences, and 19 242 reads per sample for fungal ITS.

2.3.5 GeoChip 5.0 analyses and raw data processing

Microbial functional genes were analyzed using the GeoChip 5.0M (Agilent Technologies Inc., Santa Clara, CA, USA), which contains 161 961 probes targeting 1 447 gene families involved in 12 major functional categories, such as C, N, P and S cycling (Wu, Yang et al. 2017). For each sample, 1 μg of soil DNA was labeled with Cy3 using random primers, dNTP solution and Klenow, purified with the Qiagen QIAquick Kit (Qiagen, Germantown, MD, USA) and dried using a SpeedVac (Thermo Fisher Scientific Inc., Waltham, MA, USA). Labeled samples were hybridized onto GeoChip at 67 °C in the presence of 10% formamide for 24 hours.

After hybridization, the arrays were washed, dried and scanned at 100% laser power and photomultiplier tube on an MS200 Nimblegen microarray scanner (Roche Nimblegen, Madison, WI, USA). Scanned images were processed and transformed into signal intensities with Agilent's Data Extraction software. Raw signal intensity files were uploaded onto a microarray data manager pipeline (www.ou.edu/ieg/tools/data-analysis-pipeline) for further data quality filtering, normalization and analysis. We normalized the signal intensity of each spot by relative abundance among all samples, removed spots with a signal-to-noise ratio (SNR) < 2 or a signal intensity < 1.3 of background, and removed outliers based on standard deviation as described previously (Yue, Wang et al. 2015).

2.3.6 Molecular ecological network analysis

Phylogenetic molecular ecological networks (pMENs) were constructed from both the 16S rRNA gene and ITS sequences, using a random matrix theory (RMT)-based network approach (Yang, Harris et al. 2009). To ensure reliability, only OTUs detected in all six replicates were used for network construction. In brief, a matrix containing Spearman's rho correlation between any pair of OTUs was generated. The threshold for network construction was automatically determined when the nearest-neighbor spacing distribution of eigenvalues transitioned from Gaussian orthogonal ensemble to Poisson distributions. Consequently, a threshold of 0.980 was used for the warming and control sample bacterial networks, 0.915 was used for the control sample fungal network, and 0.920 was used for the warming sample fungal network. To identify environmental factors important for network topology, environmental factors were also incorporated into networks, as RMT-based networks were designed to use multiple data types (Deng, Jiang et al. 2012). Random networks corresponding

to all pMENs were constructed using the Maslov-Sneppen procedure with the same network size and average number of links to verify the system-specificity, sensitivity and robustness of the empirical networks (Maslov and Sneppen 2002). Network graphs were visualized with Cytoscape 3.5.1 software.

2.3.7 Statistical analyses

Various statistical analyses were conducted with the package vegan (v2.3-2) in R software version 3.2.2. Two-tailed Monte-Carlo permutation *t*-tests and permutation analysis of variance (PERMANOVA) were used to examine the statistical significance of differences between microbial taxa, functional gene abundance or environmental factors (10 000 permutations were generated for each test). Three complementary dissimilarity tests (multi-response permutation procedure (Van Sickle 1997), analysis of similarity (CLARKE 1993), and non-parametric multivariate analysis of variance (Zapala and Schork 2006)) and detrended correspondence analysis (Oksanen and Minchin 1997) (DCA) were used to examine community differences. Canonical correspondence analysis (CCA) was used to detect linkages between microbial communities and environmental factors, with a threshold variance inflation factor of less than 20 to select independent environmental factors. To evaluate community assembly mechanisms, stochastic ratios were calculated with a modified stochastic ratio method (Zhou, Deng et al. 2014) on IEG Statistical Analysis Pipeline (www.ou.edu/ieg/tools/data-analysis-pipeline) based on phylogenetic (Beta-Mean Nearest Taxon Distance, βMNTD) metrics. Linear models were constructed to detect correlations among microbial communities and C fluxes with the package stats (v3.5.2) in R, and tested for significance by permutation tests with the package lmPerm (v2.1.0).

2.4 Results

2.4.1 Edaphic factors, plant biomass and ecosystem C fluxes

As shown in Table S1, the average winter soil temperature increased by 0.63 ℃ (p = 0.037) under warming and the maximum thaw depth increased by 11.37 cm (p = 0.006), which was more substantial than the 4.78 cm increase after the 1.5-year warming (Xue, Yuan et al. 2016). Aboveground plant biomass increased by 25.2% (p = 0.049) under warming, similar to other observations in tundra regions (Natali, Schuur et al. 2012, Deane-Coe, Mauritz et al. 2015, Salmon, Soucy et al. 2016). Ecosystem respiration increased by 72.8% ($p < 0.001$) under warming, and CH_4 flux increased by 218.8% (p = 0.004) .

2.4.2 Microbial community composition

We examined the taxonomic composition of microbial communities via high-throughput amplicon sequencing of 16S rRNA genes and the internal transcribed spacer (ITS) region. After resampling at 34 673 reads per sample, 5 117 OTUs were generated by 16S rRNA gene amplicon sequencing. Almost all of the OTUs (99.86%) and gene abundance (99.88%) belonged to bacteria, with 2 740 OTUs mapping to 214 known genera, and only 0.12% of the abundance belonging to archaea. *Proteobacteria* was the most abundant phylum (31.00% in relative abundance), followed by *Acidobacteria* (30.61%), *Actinobacteria* (12.08%), and *Verrucomicrobia* (8.34%) (Figure S1a). For fungi, 1 465 OTUs were generated by ITS amplicon sequencing after resampling at 19 242 reads per sample. *Leotiomycetes* was the most abundant class (47.35% in relative abundance), followed by *Eurotiomycetes*

(18.85%), unidentified *Ascomycota* (16.06%), and *Agaricomycetes* (10.05%) (Figure S1b).

Warming slightly and significantly increased the phylogenetic α-diversity of the bacterial communities (Faith's *PD*, $p = 0.032$, Figure 1a), but did not significantly increase the phylogenetic α-diversity of the fungal communities ($p = 0.406$, Figure 1b). Bacterial within-group β-diversity, i.e., the difference within biological replicates, was also increased in warmed samples ($p < 0.001$, Figure 1c), indicating that warming led to more divergent bacterial communities. In contrast, fungal within-group β-diversity remained unchanged ($p = 0.143$, Figure 1d). Three nonparametric multivariate statistical tests of dissimilarity (MRPP, ANOSIM and Adonis) showed that warming altered the composition of the bacterial communities but not the fungal communities ($p < 0.040$, Table 1).

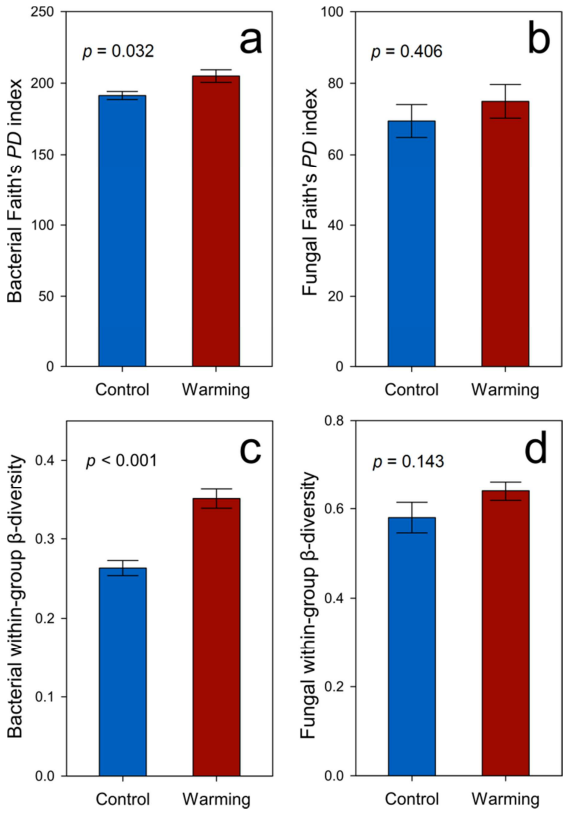

Figure 1. Diversity indices of bacterial/fungal communities, including (a) bacterial Faith's *PD* index (phylogenetic α-diversity index), (b) fungal Faith's *PD* index, (c) bacterial within-group β-diversity (Bray-Curtis distance), and (d) fungal within-group β-diversity (Bray-Curtis distance). Statistical significances were determined by permutation *t*-tests. Error bars represent standard error of the mean for n = 6 biological replicates.

2.4.3 Microbial community functional structure

A total of 38 484 probes on the GeoChip showed positive signals. Three nonparametric multivariate statistical tests of dissimilarity (MRPP, ANOSIM and Adonis) showed that the overall functional structure of soil microbial communities was altered by warming ($p < 0.012$, Table 1), and positively correlated with bacterial and fungal community composition ($p < 0.015$, Figure S2).

C cycling. We detected 50 genes associated with decomposition of labile or recalcitrant C. Among them, 42 genes exhibited higher abundances in warmed samples than control samples ($p < 0.038$, Figure 2a), including *amyA* encoding amylase, *xylA* encoding xylose isomerase, exoglucanase, cellobiase, pectate lyase, phenol oxidase, *vdh* encoding vanillin dehydrogenase, and ligninase.

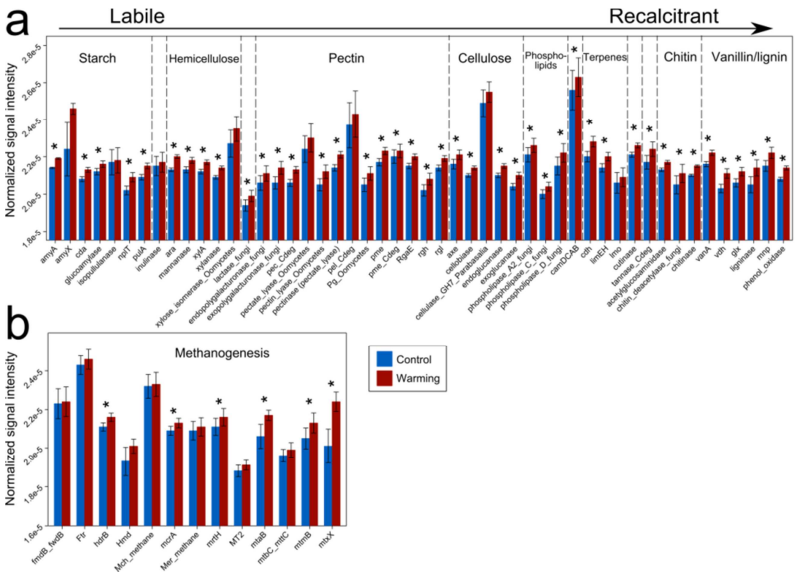

Figure 2. Normalized signal intensities of representative genes involved in (a) C decomposition and (b) methanogenesis, as revealed by GeoChip 5.0 analysis. Error

bars represent standard error of the mean for n = 6 biological replicates. The differences of the functional gene abundances between warming and control samples were tested using PERMANOVA, indicated by * when $p < 0.050$.

A total of 13 methanogenesis genes were detected (Figure 2b). Among them, *mcrA* encoding methyl coenzyme M reductase, *mrtH* encoding tetrahydromethanopterin S-methyltransferase, *mtaB* encoding methanol-cobalamin methyltransferase, *mtmB* encoding monomethylamine methyltransferase, *mtxX* encoding methyltransferase, and *hdrB* encoding CoB/CoM heterodisulfide reductase exhibited higher abundances in warmed samples ($p < 0.007$), suggesting a higher functional potential of methanogenesis.

N cycling. As a limiting nutrient in tundra ecosystems, N plays an essential role in ecosystem productivity. All the detected genes associated with N cycling exhibited higher abundances in warmed samples ($p < 0.025$, Figure S3a), suggesting that warming enhanced microbial functional capacity for N cycling. These genes included the N fixation gene (*nifH* encoding nitrogenase reductase), nitrification gene (*hao* encoding hydroxylamine oxidoreductase), denitrification genes (*narG* encoding nitrate reductase, *nirS*/*nirK* encoding nitrite reductase, *norB* encoding nitric oxide reductase, and *nosZ* encoding nitrous-oxide reductase), dissimilatory nitrate reduction genes (*napA* encoding periplasmic nitrate reductase and *nrfA* encoding periplasmic nitrite reductase), assimilatory nitrate reduction genes (*nasA* encoding assimilatory nitrate reductase, and *nir* encoding nitrite reductase), N mineralization gene (*ureC* encoding urease), and ammonia assimilation gene (*gdh* encoding glutamate dehydrogenase).

Phosphorus (P) and sulfur (S) cycling. P deficiency is common in global soil ecosystems. We found that P cycling genes including phytase and *ppx* encoding exopolyphosphatase (*ppx*) were in higher abundance in the warmed samples ($p <$

0.001, Figure S3b), suggesting that warming could potentially increase microbial functional capacity of P cycling. Similarly, 27 genes associated with S cycling were detected, of which 21 showed higher abundance in warmed samples ($p < 0.027$, Figure S3c). These genes included *dsrA*/*B* encoding dissimilatory sulfite reductase, *SiR* and *cysI*/*J* encoding sulfate reductase, and *soxY* encoding sulfur oxidation protein.

2.4.4 Microbial community assembly mechanisms and the importance of thaw depth

To assess the importance of deterministic and stochastic processes in shaping soil community composition, stochastic ratios were calculated. Stochastic processes of bacterial communities were reduced by warming from 91.5% to 65.9% ($p < 0.001$, Figure S4a), suggesting that environmental filtering was elicited by warming. In contrast, stochastic ratios of fungal communities were similar between warming and control samples ($p = 0.370$, Figure S4b).

To identify environmental factors that may have a strong effect on the microbial communities, we performed correlation tests between the beta-nearest taxon index (βNTI, also known as phylogenetic β-diversity) (Webb, Ackerly et al. 2002) and pairwise differences in environmental factors. Correlations were performed on all environmental factors (14 factors were examined), but only factors with significant correlations are discussed. Bacterial βNTI correlated with the thaw depth ($R^2 = 0.503$, $p < 0.001$, Figure 3a), and to a lesser extent with soil moisture ($R^2 = 0.128$, $p < 0.001$, Figure 3b) and aboveground plant biomass ($R^2 = 0.158$, $p < 0.001$, Figure 3c). Fungal βNTI had weaker correlations with those factors than bacterial βNTI, but correlated with thaw depth ($R^2 = 0.067$, $p = 0.038$, Figure 3d) and soil moisture ($R^2 = 0.085$, $p = 0.013$, Figure 3e) while not with aboveground plant biomass ($R^2 = 0.001$, $p = 1.000$, Figure 3f).

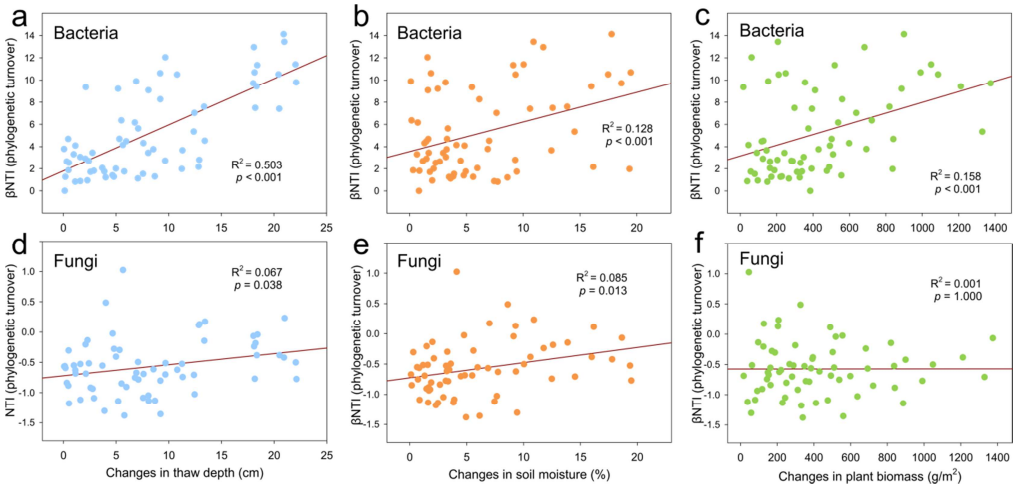

Figure 3. Linear regressions between pairwise microbial community phylogenetic turnovers (Beta Nearest Taxon Index, βNTI) and pairwise differences of plant and soil factors. Phylogenetic turnover metrics are related to changes in (a) soil thaw depth, (b) soil moisture and (c) aboveground plant biomass for bacterial communities, and changes in (d) soil thaw depth, (e) soil moisture and (f) aboveground plant biomass for fungal communities. The 66 points in each sub-figure represent the 66 pairwise differences generated from the 6 warmed samples and 6 control samples.

We performed CCA to verify the importance of the thaw depth in microbial community assembly. The bacterial community composition correlated with thaw depth, aboveground plant biomass, soil moisture and winter soil temperature, with thaw depth, aboveground plant biomass, and moisture being the most important variables (p = 0.007, Figure S5a). Similarly, thaw depth, aboveground plant biomass, soil moisture, winter soil temperature and soil C/N ratio correlated with the fungal community composition (p = 0.012, Figure S5b) and with the microbial functional structure ($p < 0.001$, Figure S5c).

Higher functional capacities of microbial C degradation and methanogenesis in warmed samples could lead to *in situ* C loss. As expected, strong correlations were detected between functional structure of C decomposition genes and *in situ* ecosystem respiration (R^2 = 0.725, $p < 0.001$, Figure 4a), and between functional structure of methanogenesis genes and *in situ* CH_4 flux (R^2 = 0.772, $p < 0.001$, Figure 4b).

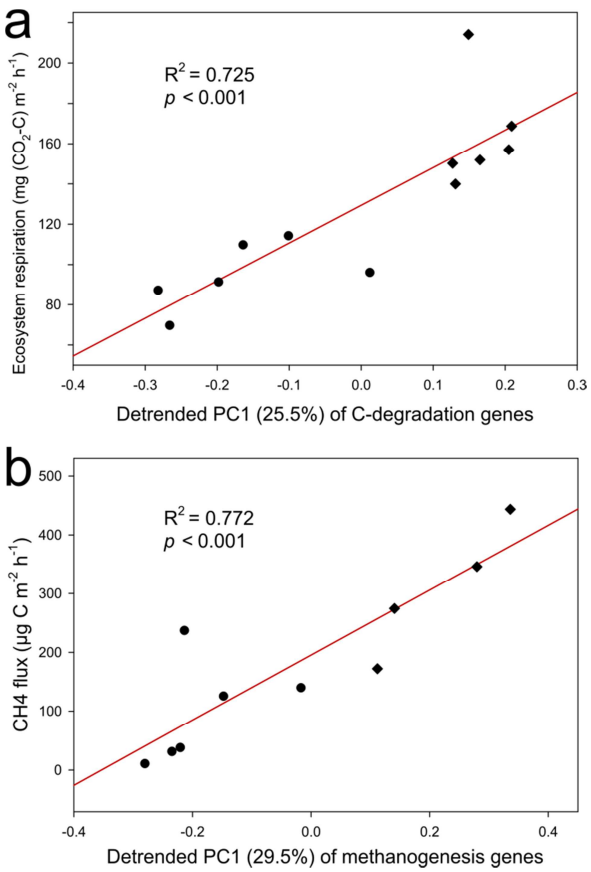

Figure 4. Linear regressions between (a) *in situ* ecosystem respiration and the 1st detrended principle component (PC1) of C decomposition genes, and (b) *in situ* methane flux and detrended PC 1 of methanogenesis genes. Each point represents a biological replicate of warming (diamonds) or control (circles) samples.

2.4.5 Microbial correlation networks

All bacterial and fungal networks generated from control or warmed samples showed topological properties of small world, scale-free, and modularity, and were significantly different from randomly generated networks (Table S1). Average connectivity of the bacterial network in warmed samples was higher ($p < 0.001$), but the average geodesic distance was lower ($p < 0.001$) than those in the control samples, suggesting that nodes were more connected in warmed samples. In contrast, the average connectivity and the average geodesic distance of fungal networks were

reduced by warming ($p < 0.001$), owing to an increased network modularity (Table S1).

To explore the relationship between network topology and environmental factors, we included environmental factors as nodes in the networks. Thaw depth had the highest node connectivity in the bacterial network of the warmed samples (Figure 5a), while water table depth had the highest node connectivity in the control sample bacterial network (Figure 5b). In contrast, the thaw depth, bulk density and soil N had the highest node connectivity in the fungal network of the warmed samples (Figure 5c), while bulk density and soil N showed the highest node connectivity in the bacterial network of the control samples (Figure 5d).

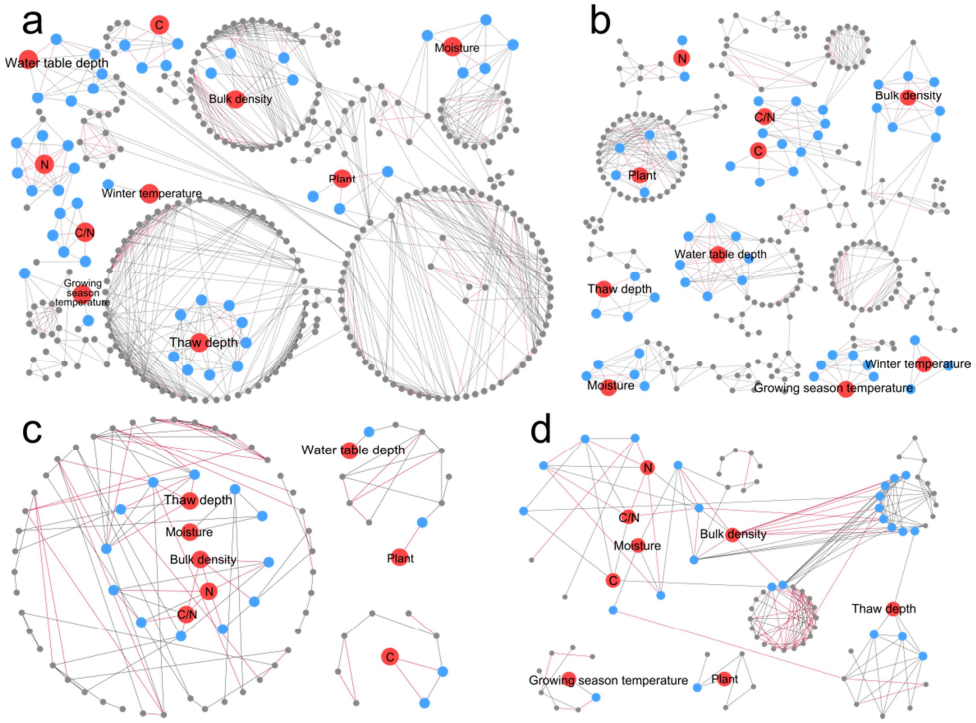

Figure 5. Networks among environmental factors and microbial communities. Bacterial communities from warming (a) and control plots (b), fungal communities from warming (c), and control plots (d). Red nodes represent environmental factors, blue nodes represent OTUs directly connected to environmental factors, grey nodes represent OTUs indirectly connected to environmental factors. Grey edges represent positive correlations, red edges represent negative correlations. Abbreviations: Plant,

aboveground plant biomass; Moisture, soil moisture; Bulk density, bulk soil density; C, soil total carbon; N, soil total nitrogen, and C/N, soil carbon/nitrogen ratio.

2.5 Discussion

Considering the tremendous amount of soil C stored within permafrost regions and its high vulnerability to climate warming, microorganisms have been recognized as the key to mediate the impact of climate warming on permafrost region soil C in both C decomposition and fixation (Graham, Wallenstein et al. 2012). In contrast to the previous observation that bacterial community taxonomic composition was unaltered by 1.5-year warming (Xue, Yuan et al. 2016), we showed that 5-year warming caused significant changes in the bacterial community composition, functional structure, and correlation networks (Table 1 & Table S1). Our findings support the hypothesis that bacterial communities continue to evolve and diverge into new states (sensitivity) after long-term warming. Consequently, the higher functional capacity of soil C microbial decomposition under warming correlates to higher soil respiration and CH_4 flux, which in turn accelerates tundra C loss.

The thawing of permafrost regions has long been considered to have profound effects on local hydrological, thermal, and C dynamics (Schuur, Abbott et al. 2011, O'Donnell, Jorgenson et al. 2012, Pries, Schuur et al. 2013, Pries, Schuur et al. 2016). We found that warming increased the thaw depth (Natali, Schuur et al. 2015), which was the strongest factor linking to bacterial phylogenetic assembly (Figure 3a), community composition (Figure S5a) and network topology (Figure 5). Soil moisture (Figure 3b) and aboveground plant biomass (Figure 3c) also significantly correlated with bacterial phylogenetic assembly. Consistently, deterministic processes (e.g. selection) played a more crucial role in shaping bacterial communities under warming

(Figure S4a). These results were consistent with a recent study of permafrost regions showing that changes in thaw depth induced changes in soil diazotrophic communities (Penton, Yang et al. 2016). Moreover, the divergence of bacterial communities observed in this study under experimental warming, manifested as increases of within-group β-diversity (Figure 1c), might be a phenomenon generalizable to other ecosystems, since bacterial communities in a tallgrass prairie site were also divergent within warming replicates (Guo, Feng et al. 2018). In sharp contrast, fungal communities remained unaltered by warming (Table 1). This could arise from the large variability of fungal communities notable in Figure 1.

The bacterial network of warmed samples exhibited a higher average connectivity and shorter average geodesic distance than that of control samples (Table S1), suggestive of a more complex network and denser interactions within the network. The dense network is likely associated with deterministic processes (e.g., environmental filtering) (Cornwell, Schwilk et al. 2006). Accordingly, we detected a higher contribution of deterministic processes under warming condition (Figure S4a).

Similar to the results of the 1.5-year warming at our study site (Xue, Yuan et al. 2016), relative abundances of functional genes associated with both aerobic and anaerobic C decomposition were increased by 5-year warming. These results could be crucial in assessing C dynamics in permafrost regions, since warming-accelerated thaw of permafrost regions exposes previously protected C stock to microbial activity. These findings also provide a mechanistic explanation for the recent observation that warming at our study site increased the annual cellulose decomposition rate at a soil depth of 0–10 cm by a factor of two (Natali, Schuur et al. 2015). In addition, functional genes associated with recalcitrant C decomposition (e.g., aromatics and lignin, Figure 2a) were increased by warming, which is in accordance with our

finding that the abundance of the genus *Chitinophaga*, a strong chitinolytic taxon (Sangkhobol and Skerman 1981), was also increased by warming. Therefore, a potential increase in decomposition of recalcitrant C is expected.

Field warming experiments have demonstrated that an initial increase of CO_2 flux gradually subsides over time, returning to pre-warming values (Oechel, Vourlitis et al. 2000, Luo, Wan et al. 2001, Rustad, Campbell et al. 2001, Melillo, Steudler et al. 2002, Eliasson, McMurtrie et al. 2005, Knorr, Prentice et al. 2005). However, we observed a persistent, enhanced ecosystem respiration after 5-year warming, which could have resulted from a stimulated microbial decomposition of soil organic C over that same period (Table S1). Those phenomena may arise from three mechanisms: (1) continuous warming increases the thaw depth, a crucial difference in the soil environment between warming and control plots, so acclimatization of microbial communities to warming is unlikely to occur; (2) since the temperature sensitivity of recalcitrant SOC is higher than labile SOC (Knorr, Prentice et al. 2005, Bracho, Natali et al. 2016), a higher microbial functional capacity of recalcitrant C decomposition under warming can aggravate soil C instability related to ecosystem respiration; and (3) the warming effect in permafrost regions is often more substantial for deeper soils (Feng, Penton et al. 2019), which contributes to ecosystem respiration. Therefore, we project that the soil microbial community would continue to provide a positive feedback to climate warming.

All N cycling-associated genes exhibited higher abundance in warmed samples (Figure S3a), which was consistent with the observations that both inorganic N availability and foliar N pools were increased by warming at our study site (Salmon, Soucy et al. 2016), and that soil nutrient contents were generally stimulated by warming in the tundra ecosystem (Deane-Coe, Mauritz et al. 2015, Salmon, Soucy et

al. 2016). The larger nutrient pool available to plants could increase aboveground plant biomass (Table S1). However, this higher plant productivity may only partially offset C loss, as a previous study of the Alaskan tundra observed a negative net ecosystem exchange due to a larger loss of C in deep soils than was increased by plant production (Mack, Schuur et al. 2004). Similarly, addition of organic N to the active layer above the permafrost increased SOM decomposition 2–3 fold (Wild, Schnecker et al. 2014). Therefore, an increased soil nutrient availability associated with warming may further amplify C loss and consequently impose a positive feedback to climate warming.

Collectively, our results show that 5-year warming significantly altered the bacterial composition and functional structure of microbial communities in permafrost-based tundra soil, revealing an evolving sensitivity to warming. For the first time, this work shows that soil thaw depth was the strongest factor directly shaping bacterial taxonomic composition, C decomposition potential and network topological properties, demonstrating that the warming-accelerated thaw of permafrost regions fundamentally restructures the associated bacterial communities. The network analysis section which shows warming-induced differences in the fungal community not detected by diversity statistics is particularly noteworthy. Together, microbial responses to long-term warming may lead to a positive feedback enhancing C decomposition in tundra regions.

2.6 Author contributions

J.Z., E.A.G.S., Y.L., J.M.T., J.R.C., Y.Y., C.R.P and K.T.K. developed the original concepts. R.G.B. and K.T.K collected soil samples. J.F., X.T. and C.W. extracted DNA. C.W. carried out 16S rRNA gene and ITS amplicon sequencing experiments.

J.F., C.W., Y.Q. and Z.J.S. processed the data of amplicon sequences. Q.Y. and X.Z. performed GeoChip microarray experiments. J.F., C.W. and D.N. performed molecular ecological network analysis and statistical analyses. J.F., C.W., Y.Y. and J.Z. wrote the paper. J.L., M.M.Y., X.G., D.N., Z.H., J.D.V.N., L.W. and C.R.P. edited the manuscript. All authors were given the opportunity to review the results and comment the manuscript.

Chapter 3: **Long-term warming in Alaska enlarges the diazotrophic community in deep soils**

3.1 Abstract

Tundra ecosystems are typically carbon (C) rich, but nitrogen (N) limited. Since biological N_2-fixation is the major source of biologically available N, the soil N_2-fixing (i.e., diazotrophic) community serves as an essential N supplier to the tundra ecosystem. Recent climate warming has induced deeper permafrost thaw and adversely affected C sequestration, which is modulated by N availability. Therefore, it is crucial to examine the responses of diazotrophic communities to warming across the depths of tundra soils. Herein, we carried out one of the deepest sequencing efforts of nitrogenase (*nifH*) genes to date in order to investigate how 5 years of experimental winter warming affects the Alaskan soil diazotrophic community composition and abundance spanning both the organic and mineral layers. Warming significantly (P<0.05) enhanced diazotrophic abundance by 86.3% and aboveground plant biomass by 25.2%. Diazotrophic composition in the middle and lower organic layers, detected by *nifH* sequencing and a microarray-based tool (GeoChip), was markedly altered with an increase of α-diversity. Changes in diazotrophic abundance and composition significantly correlated to soil moisture, soil thaw duration, and plant biomass, as shown by structural equation modeling analyses. Therefore, more abundant diazotrophic communities induced by warming may potentially serve as an important mechanism for supplementing biologically available N in this tundra ecosystem.

3.2 Introduction

The northern circumpolar permafrost zone contains approximately 1,672 Pg of C, accounting for nearly half of the global soil C storage (Schuur, Bockheim et al. 2008, Tarnocai, Canadell et al. 2009). As the extent of permafrost thaw increases due to global warming, this large soil C reservoir has become increasingly vulnerable to microbial decomposition (Tarnocai, Canadell et al. 2009), resulting in a positive feedback to greenhouse gas emissions (Osterkamp 2007). However, the responses of tundra ecosystems to climate warming vary across ecosystem types and the duration of field experiments, which leads to uncertainty in predicting future C storage. For example, soils of the Alaskan tundra near Eight Mile Lake (EML) have been documented as a C sink during the first 2 years of experimental warming but became a C source after the third year (Natali, Schuur et al. 2014, Salmon, Soucy et al. 2015, Xue, Yuan et al. 2016). In contrast, soil C storage under warming in Alaskan tundra soils near Toolik Lake remained unchanged (Sistla, Moore et al. 2013).

The limited soil nitrogen (N) in tundra soils constrains both plant production (Hobbie 1992) and microbial decomposition (Hobbie, Eddy et al. 2012), thus strongly affecting the net response of tundra ecosystems to climate warming. Plants and soil microbes compete for essentially the same soil N pool since they utilize similar N sources (e.g. amino acids, NH_4^+ and NO_3^-) (Nordin, Schmidt et al. 2004). This is true for tundra ecosystems as well (Lipson and Monson 1998), wherein factors such as the spatiotemporal dynamics of N components, roots, and microbes collectively determine the fate of soil N (Hodge, Robinson et al. 2000). Enlarging the available N pool has a significantly positive impact on tundra plant growth (Bassin, Volk et al. 2007). However, the impact of N addition on soil microbes is highly dissimilar between tundra and other ecosystems. For example, addition of N fertilizer inhibited

microbial respiration and biomass in forest and grassland soils (Barsdate and Alexander 1975), but enhanced microbial decomposition rates in tundra soils due to the alleviation of N limitation (Mack, Schuur et al. 2004). Consequently, the concomitant increase in tundra plant productivity may or may not offset C losses owing to accelerated decomposition associated with a larger soil N pool, which in turn provides an important feedback to global warming.

Free-living and plant-associated N_2-fixation is a major biological N source for the N-limited tundra (Barsdate and Alexander 1975), which is regulated by plant-diazotroph symbiotic interaction (Mus, Crook et al. 2016) and abiotic factors such as temperature and moisture (Reed, Cleveland et al. 2011). Although plant-associated N_2-fixers (i.e., diazotrophs) exhibit higher activities compared to the bulk soil, thus supplying more N to plants (Jones, Farrar et al. 2003), N fixed by free-living soil diazotrophs is also crucial to the productivity of the soil ecosystem. Microbial *nifH* genes encode an ATP-hydrolyzing subunit of the nitrogenase complex necessary for biological N_2-fixation. These genes can serve as a proxy to assess the composition of microbial diazotrophic communities based on *nifH* gene sequences. *NifH* genes have also been used to estimate N_2-fixing rates based on significant correlations between *nifH* gene abundances and N_2-fixing rates (Hadri, Spaink et al. 1998, Reed, Townsend et al. 2010, Huang, Tang et al. 2011). However, these previous correlations do not necessarily indicate that *nifH* gene abundances always correlate with N_2-fixation rates, since soil edaphic factors, nutrient availability, and other soil properties likely influence the strength of these correlations. It was recently shown that long-term (10-year) warming significantly increased *nifH* gene richness and evenness in Oklahoma tallgrass prairie bulk soils (0–15 cm depth), suggesting that diazotrophic communities were sensitive to warming (Penton, St Louis et al. 2015). However, the composition

of the diazotrophic community in a tundra soil near EML, Alaska exhibited no change after short-term (1.5-year) winter warming (Xue, Yuan et al. 2016). Therefore, it is important to examine whether the lack of diazotrophic community responses to warming is persistent over a longer time period, a possibly important mechanism in determining tundra soil C stability.

Using deep sequencing of *nifH* gene amplicons, quantitative PCR (qPCR), and GeoChip 5.0 technologies, we launched an integrated study to examine diazotrophs across four depths of a tundra soil at the EML study site, where soils were subjected to a 5-year winter (October–April) warming treatment (Natali, Schuur et al. 2014). Longer warming led to a deeper thaw depth and greater soil moisture (Schuur, Bockheim et al. 2008, Salmon, Soucy et al. 2015), which in turn affected diazotrophic abundance (Eaton, Roed et al. 2012). Therefore, we hypothesize that the longer 5-year warming would significantly increase soil diazotrophic community abundance by stimulating microbial growth, and also stimulate plant primary production by supplementing biologically available N.

3.3 Materials and Methods

3.3.1 Site descriptions

The Carbon in Permafrost Experimental Heating Research project (CiPEHR), established in 2008 (Natali, Schuur et al. 2014), is located in the EML site on a gentle northeast-facing slope in the northern foothills of the Alaska Range (63°52'59"N, 149°13'32"W) (Schuur, Crummer et al. 2007). Situated within a moist acidic tundra biome, the mean monthly temperature of the site ranges from -16 ^{o}C in December to +15 ^{o}C in July. The mean annual temperature was -1.45 ± 0.25 ^{o}C from 1977 to 2013. The average annual precipitation is 378 mm. The site lies within the southernmost

discontinuous permafrost zone, where thawing and thermokarst formation has been occurring over past decades (Natali, Schuur et al. 2014). The soil is classified as a Gelisol, with a 45–65 cm thick organic horizon above a mineral horizon that is a cryoturbated mixture of loess and glacial till. The average active layer depth is approximately 50 cm. Vegetation is dominated by the deciduous shrub *Vaccinium uliginosum*, and the tussock-forming sedge *Eriophorum vaginatum*. The tundra soil temperature in the EML site has been monitored since 1985 (Osterkamp, Jorgenson et al. 2009) and ecosystem C fluxes and isotopes have been monitored since 2004 (Schuur, Crummer et al. 2007).

3.3.2 Warming experimental design and sample collection

The winter soil warming treatment at the CiPEHR site was achieved by installing 1.5-m tall × 8-m long snow fences between the winter warming and control treatments, perpendicular to the south-easterly dominant winter winds (Natali, Schuur et al. 2014). Warming plots were on the leeward side of the snow fences, and the control plots were on the windward side. The snow fences trapped and accumulated an insulating snow layer on the warming plots. Snow was removed before snowmelt in spring (March 8th–15th) to keep the hydrological conditions similar to the control treatment. Snow fences were removed simultaneously to avoid shading the experimental plots during the growing season (May–September). Six snow fences were used for 6 warming-control plot pairs, which were arranged in 3 blocks with fences within a block 5 m apart and the blocks separated by approximately 100 m.

Six soil cores were taken from each treatment in May 2013, after 5 years of winter warming. Soil fractions within the active layer at depths of 0–5 cm, 5–15 cm, 15–25

cm, and 45–55 cm were analyzed. The first 3 depths, hereafter referred to as the upper organic layer, the middle organic layer, and the lower organic layer, belonged to the organic layer and included the depth range in which most plant roots resided. The last depth is referred to as the upper mineral layer.

3.3.3 Environmental factor monitoring

Soil moisture was measured using CS616 water content reflectometers (Campbell Scientific, Logan, UT, USA). Soil thaw depths were measured on a weekly basis using a metal thaw depth probe pushed through the unfrozen soil until it hit ice, from which the soil thaw durations were calculated. In the peak growing season, aboveground plant biomass was measured with a non-destructive point-frame method, i.e., using a ~60×~60 cm point frame with a grid size of 8×8 cm to generate 49 intersecting grid points (Walker 1996). A 1-mm-diameter rod was placed vertically through the grid to touch the plants at each grid point. Plant species identities and tissue types (fruit, stem, flower or leaf) were recorded. Then the aboveground biomass was calculated using allometric equations previously developed for this site (Schuur, Crummer et al. 2007). Soil temperature was measured using type-T thermocouples (Campbell Scientific, Logan, UT, USA). Soil C and N contents were measured using an ECS 4010 Elemental Analyzer (Costech Analytical Technologies, Valencia, CA, USA).

3.3.4 Soil DNA extraction

Soil DNA was extracted via liquid N grinding followed by the PowerMax Soil DNA Isolation Kit (MO BIO Laboratories, Inc., Carlsbad, CA, USA) (Zhou, Bruns et al.

1996). DNA was quantified by Pico Green with a FLUOstar OPTIMA fluorescence plate reader (BMG LabTech, Jena, Germany). DNA quality was assessed by a NanoDrop ND-1000 Spectrophotometer (Thermo Fisher Scientific, Waltham, MA, USA) based on spectrometry absorbance at wavelengths of 230 nm, 260 nm and 280 nm. The absorbance ratios of 260/280 nm were larger than 1.8, and the 260/230 nm ratios were around 1.7.

3.3.5 nifH gene amplification and sequence analysis

Extracted DNA was diluted to 5 ng/µl for amplification. Primers PolF/PolR (TGCGAYCCSAARGCBGACTC / ATSGCCATCATYTCRCCGGA) were used for *nifH* PCR amplification for their reliability amplifying DNA extracted from soil (Poly, Monrozier et al. 2001). Both forward and reverse primers were tagged with an Illumina adapter sequence, a primer pad and a linker sequence. Triplicate PCR reactions were performed per sample within a reaction volume of 25 µl. To decrease the inaccuracy of quantitation due to unexpected PCR products (smeared bands), PCR products from each sample were separated on a 1.5% agarose gel at 90 V for 50 min. Bands were excised from the gel and then purified with a QIAquick Gel Extraction Kit (QIAGEN Inc., Valencia, CA, USA). Purified DNA was quantified with Pico Green and 100 ng DNA from each reaction was pooled together. The pooled DNA was diluted to 2 nM and loaded onto the reagent cartridge and run on a MiSeq benchtop sequencer (Illumina, Inc., San Diego, CA, USA) at the Institute for Environmental Genomics, University of Oklahoma, following manufacturer's instructions.

Poor quality reads were removed using the Btrim tool (Kong 2011). Chimeras were removed by Uchime (Edgar, Haas et al. 2011) using a manually curated database

of *nifH* DNA sequences (Heller, Tripp et al. 2014). Frameshifts were screened and corrected by Framebot software (Wang, Quensen et al. 2013), again with a manually curated database of NifH protein sequences (Heller, Tripp et al. 2014). Remaining sequences were then clustered into OTUs with complete linkage clustering on a Galaxy platform (http://zhoulab5.rccc.ou.edu:8080/) pipeline at the 95% amino acid similarity (Loewenstein, Portugaly et al. 2008). Phylogenetic trees were constructed and analyzed using PyNAST alignment (v.1.0.0), FastTree (v.1.0.0), MEGA (v.5.10, BETA2), and visualized using the Interactive Tree of Life (iTOL, v.3.2.2) (Life 2011).

3.3.6 Quantitative PCR

Quantitative PCR of *nifH* genes was performed with both "universal" (PolF/PolR) primers and 11 pairs of specific primers (Table S6). The specific primers were designed according to DNA sequences of the 11 top abundant (>0.02% of the total abundance) *nifH* genes obtained from our sequencing data. Reactions were performed in 25 µl volumes with the iQ SYBR green Supermix (Bio-Rad Laboratories, Hercules, CA, USA) on a Rotor-Gene 3000 apparatus (Corbett Life Science, Sydney, NSW, Australia). Standards were made from 10-fold series dilutions of plasmids in the TOPO TA Cloning kit (Thermo Fisher Scientific, Waltham, MA, USA) containing 11 *nifH* genes used in the quantitative PCR analyses. Quantitation of the products could be accurate because primer dimers were little in the products, as visualized by a gel plot (Figure S6).

3.3.7 GeoChip 5.0 analyses

Diazotrophic community was analyzed with a microarray-based tool (GeoChip 5.0), which is the latest version of GeoChip. This microarray contains 161,961 probes belonging to 1,447 gene families, including genes involved in crucial biogeochemical processes (e.g., C, N, P, and S cycling) (Wu, Yang et al. 2017), among which there are 1,331 probes of the *nifH* gene. For each sample, 1 μg of template DNA was labeled with Cy3 dye, purified with the QIAquick Purification Kit (Qiagen, Germantown, MD, USA) as previously described (Yue, Wang et al. 2015), and hybridized with GeoChip 5.0 M microarrays at 67 ^{o}C with 10% formamide for 24 h. Subsequently, the microarrays were washed, dried and scanned on an MS 200 microarray scanner (Roche, South San Francisco, CA, USA). Images were quantified into signal intensities with Agilent's Data Extraction software. Raw signal intensities were uploaded to the Microarray Data Manager of the Institute for Environmental Genomics at the University of Oklahoma (http://ieg.ou.edu/microarray/) for quality control, normalization and analysis. We normalized the signal intensity of each spot by mean ratio, removed spots with <2 signal-to-noise ratio (Ding, Zhang et al. 2015), and removed outliers based on standard deviations, as described previously (Liu, Wang et al. 2015).

3.3.8 Statistical analyses

Various statistical analyses were performed with the package vegan (v.2.3-2) in R software version 3.2.2 (The R Foundation for Statistical Computing), including diazotrophic α- and β-diversity indices calculated with the package vegan (v.2.3-2) and agricolae, de-trended correspondence analysis (DCA) calculated with the package vegan (v.2.3-2) for displaying diazotrophic community structures, non-parametric

multivariate analysis of variance (Adonis) calculated with the package vegan (v.2.3-2) for determining differences among diazotrophic community structures, analysis of variance (ANOVA) and post-hoc Fisher's Least Significant Difference (LSD) test calculated with the package vegan (v.2.3-2) and agricolae for determining differences among diazotrophic α- and β-diversity indices, canonical correspondence analysis (CCA) calculated with the package vegan (v.2.3-2) for modeling major environmental factors shaping microbial structure, and Pearson correlation analysis calculated with the package Hmisc between environmental factors and diazotrophic abundance. Two-tailed *t* tests were performed using Microsoft Excel 2010 (Microsoft Inc., Seattle, WA, USA). Unless otherwise stated, mean values are given ± standard error of the mean, and values of $P \leq 0.05$ are considered statistically significant.

Structural equation modeling (SEM) analysis was performed with the Amos 24.0 software package (Small Waters Corp., Chicago, IL, USA) to establish the structural relationships among the environmental factors and diazotrophic abundance. A chi-square test of model fit was adopted to determine whether the proposed model was supported by the data. Additionally, We also used three other widely used indices of model fit including comparative fit index (CFI), Tucker Lewis index (TLI), and root mean square error of approximation (RMSEA) (Kline 2015), wherein the good models have a CFI and TLI>0.95 and a RMSEA<0.05 (Byrne 2016).

3.4 Results

3.4.1 Environmental factors

Warming significantly increased winter soil temperature throughout all of the four depths, but the effect was weaker for the deeper soils (increase of 0.76±0.22 °C in the upper organic layer, P=0.026; 0.60±0.11 °C in the middle organic layer, P=0.005;

0.49±0.11 °C in the lower organic layer, P=0.008; 0.44±0.12 °C in the upper mineral layer, P=0.018; Table S2). The effect of warming lingered into the growing season in deeper soils, evidenced by temperature increases in the upper mineral layer (1.11±0.33 °C, P=0.026) and the lower organic layer (1.02±0.30 °C, P=0.029), as compared to shallower soils (0.40±0.37 °C in the middle organic layer and 0.02±0.43 °C in the upper organic layer, P>0.050). Warming significantly increased the duration of annual soil thaw in all layers, where differences between the warming and control plots were much longer in the upper mineral layer (33.8±6.8 days, P=0.006) than in other layers (7.3±1.4 days in the upper organic layer, P=0.005; 8.2±3.6 days in the middle organic layer, P=0.096; 8.0±2.5 days in the lower organic layer, P=0.031; Table S2 shows the absolute lengths of the durations). Warming also significantly increased soil thaw depth from 18.3±0.4 cm to 23.0±1.5 cm (P=0.011), and aboveground plant biomass from 1617±23 g/m^2 to 2025±59 g/m^2 (P=0.035) (Table S2). Other environmental factors remained similar between warming and control plots.

Soil depth played an important role in determining many soil factors (Table S2). Soil temperature increased with depth in the winter, while it decreased with depth during the growing season. Soil thaw durations decreased from 146 days/year to 62 days/year with increasing depth. Total C content, measured in dry soil, decreased from 43.1% to 16.0% with depth, as did total N content, decreasing from 1.3% to 0.7% in the deeper soils. Soil bulk density increased from 0.09 g·cm^{-3} to 0.25 g·cm^{-3} with depth in the organic layer and was substantially higher in the upper mineral layer (0.74 g·cm^{-3}).

3.4.2 Total abundance of nifH genes

In the control plots, the abundance of *nifH* genes was 2.3×10^7 copies / g soil in the upper organic layer (qPCR, Figure 6) with a significant increase to 2.9×10^8 copies / g soil in the middle organic layer, and to 8.9×10^8 copies / g soil in the lower organic layer. In the upper mineral layer abundance was 2.3×10^8 copies / g soil. These results were supported by qPCR using OTU-specific primers that among them, 6 of all 11 OTUs exhibited their highest abundance in the lower organic layer (Figure S7A).

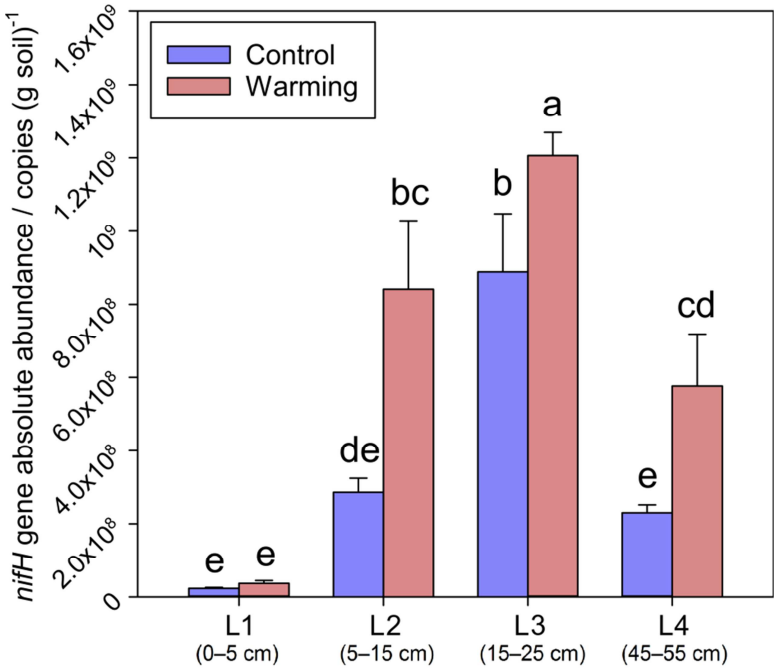

Figure 6. Absolute abundance of *nifH* genes determined by qPCR. Letters (i.e., a, b, bc, cd, de, and e) above the error bars show the results of ANOVA and LSD tests to examine the significant differences. Abbreviations: L1, the upper organic layer; L2, the middle organic layer; L3, the lower organic layer; L4, the upper mineral layer.

Warming significantly increased *nifH* gene abundance in all layers except the upper organic layer (Figure 6). Together, warming increased *nifH* gene abundance by 86.3% ($P<0.001$). A closer examination showed that warming significantly increased individual OTU abundance in 39% of all cases (11 OTUs × 4 layers), while no

decrease of individual OTUs was observed across all of 4 soil depths (Figure S7A). In agreement with qPCR, GeoChip analysis of *nifH* genes also detected significant increases in relative abundances under warming in all layers, with the exception of the upper organic layer (Figure S7B).

3.4.3 Community composition of diazotrophic bacteria

A total of 691,093 raw *nifH* sequences were obtained. After re-sampling to 5,905 sequences per sample, a total of 4,663 *nifH* OTUs were generated at 95% amino acid similarity. The relative abundance distribution of OTUs showed a long-tail pattern (Figure S8), with the top 28 abundant OTUs accounting for 50.4% of the total sequences. Only 196 (4.2%) OTUs closely (≥95% amino acid similarity) matched to cultured taxa, suggesting that our current database coverage of *nifH* genes remains very limited, at least in tundra soil environment (Penton, Yang et al. 2016). The most abundant OTU was most closely related to *Rubrivivax gelatinosus*, which accounted for 9.4% of total sequences. The next 4 abundant OTUs accounted for 5.5%, 4.1%, 3.6% and 3.0% of total sequences, respectively.

A neighbor-joining tree for the 200 top abundant *nifH* OTUs shows that closely clustered *nifH* OTUs usually have their closest affiliation to different phylogenetic clades as determined by 16S rRNA genes, implying frequent horizontal gene transfer (HGT) events for these *nifH* genes (Figure 7) (Zehr, Jenkins et al. 2003). The 3 clusters in the tree match to the 3 previously reported clades of *nifH* genes (Raymond, Siefert et al. 2004): Cluster 1 corresponds to Group I, Cluster 2 corresponds to Group II, and Cluster 3 consists of only one OTU of Group III. The relative abundances of *nifH* OTUs in Cluster 1 showed a decreasing trend with soil depth (23.9%, 41.8%, 31.5%, and 2.7% sequences in the 4 layers, respectively), while Cluster 2 increased

with depth (0.7%, 9.1%, 32.2%, and 58.0% sequences in the 4 layers, respectively). Many abundant OTUs were layer-specific (e.g., OTU 35, OTU 36, and OTU 130) or treatment-specific (e.g., OTU 58 and OTU 753).

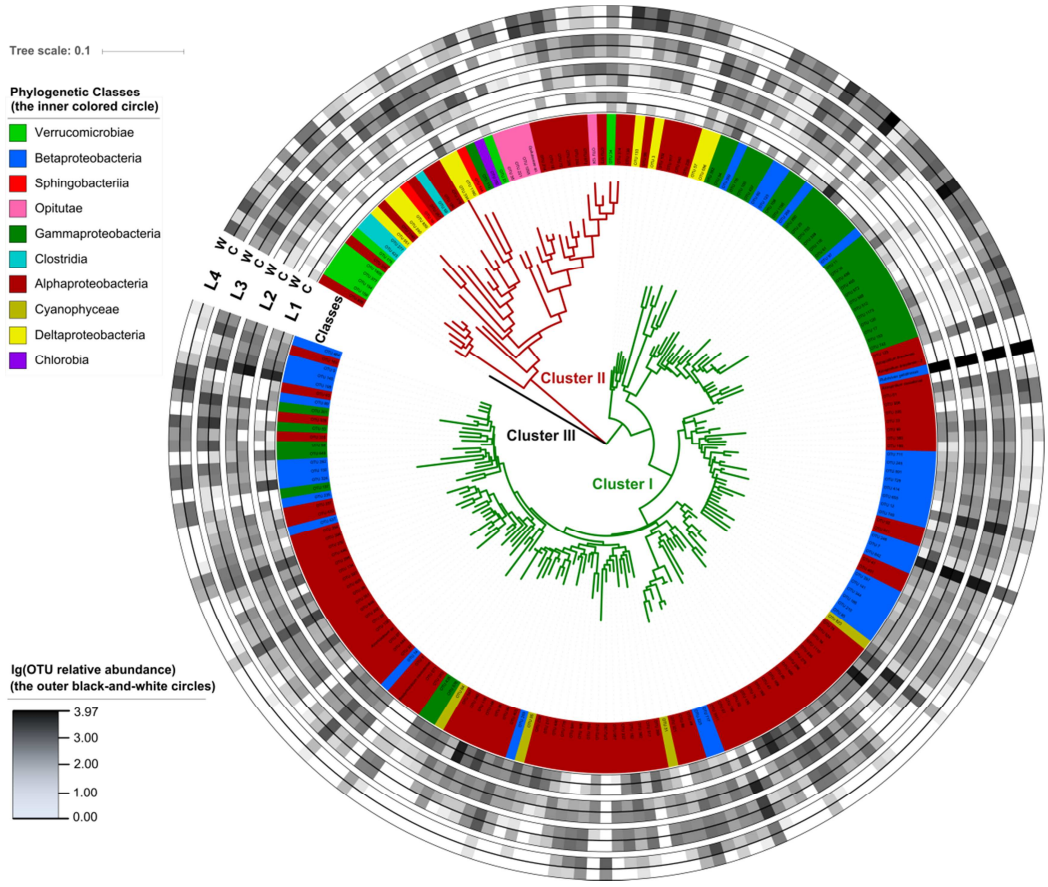

Figure 7. The circular maximum likelihood phylogenetic tree of the top 200 abundant *nifH* OTUs. Tree leaves on the inner circle highlighted by colors show the affiliation of different phylogenetic clades. The outer black-and-white circles show the logarithmic value of OTU relative abundances in percentage in different soil layers and treatments, where tree leaves without abundance are anchored reference taxa. Abbreviations: L1, the upper organic layer; L2, the middle organic layer; L3, the lower organic layer; L4, the upper mineral layer. W, warming; C, control.

The dissimilarities in the composition of bacterial communities in different soil depths is generally large, with even greater differences than communities kilometers apart (Chu, Sun et al. 2016). Consistently, we found that soil depth was a considerably stronger factor than warming on influencing diazotrophic community composition (Table 1). Detrended correspondence analysis (DCA) showed that *nifH* sequences

clustered by soil depth rather than by treatment (Figure S9). Diazotrophic community composition exhibited significant differences between all layers (P<0.001, adonis test), but not between warming and control (Table S3). Diazotrophic α-diversity indices (richness, Chao1 index and Shannon index) among any pair of adjacent layers were also significantly different (paired *t*-test). These index values increased with depth within the organic layer followed by a decrease in the mineral layer (Table S4) with abundances illustrating the same pattern.

TABLE 1 Adonis test to examine the importance of the effects of warming and depth in shaping diazotrophic community composition (*nifH* gene amplicon sequencing or GeoChip data of *nifH* gene). Abbreviations: Df, degrees of freedom. Significance: bold values, $P \leq 0.05$; bold and italic values, $0.05 < P < 0.1$.

		nifH gene sequencing		GeoChip (*nifH*)	
	Df	R^2	*P*	R^2	*P*
Warming	1	0.015	0.217	0.029	***0.056***
Depth	3	0.469	**0.001**	0.386	**0.001**
Warming:Depth	3	0.040	0.278	0.056	0.155
Residuals	40	0.476		0.530	

Warming significantly altered the composition (Table S3) and enhanced the α-diversity (Table S4) of the diazotrophic community in the middle organic layer. Seven out of 16 phyla affiliations were significantly altered in sequencing-derived relative abundance by warming (Table S4). The GeoChip data, an often more sensitive tool than sequencing (Xue, Yuan et al. 2016), showed a general but weak consistency with the relative abundances derived from the sequencing data (P<0.001, R^2=0.171; Figure S10A). Warming altered diazotrophic communities in the middle and lower organic layers (Table S3). In agreement with a previous study (Zhou, Deng et al. 2016), the value of ln(N_2-fixer Chao1 index) showed a negative correlation with the reciprocal of

absolute soil temperature (R^2=0.389, P<0.001; Figure S11), suggesting that soil temperature may increase the α-diversity of the diazotrophic community. Warming significantly increased the within-treatment *nifH* β-diversity in the middle and lower organic layers (Table S4), suggesting that warming also increased community dissimilarity within biological replicates.

3.4.4 Drivers shaping diazotrophic community composition

Diazotrophic community composition significantly correlated with the measured environmental factors (Figure S10B & Figure S10C). Six top environmental factors (soil thaw duration, growing season temperature, winter temperature, moisture, C content, and N content) explained 88.3% of the variation in the diazotrophic community composition, as determined by a significant (P<0.001) CCA model (Figure 8). Differences between control and warming samples revealed by CCA were not apparent except in the middle organic layer, which was consistent with the dissimilarity test (Table S3). Some factors among them were dependent on specific soil layers. For instance, water saturated time and winter temperature were major factors linking to the microbial community structure within the upper mineral layers. Diazotrophic abundance positively correlated with soil moisture (P=0.037), which was tested as driven by the upper mineral layer only through Pearson correlation (Table S5). For other individual layers other than the upper mineral layer, diazotrophic abundances in the middle organic layer positively correlated with soil thaw duration (P=0.053) and plant biomass (P=0.015). In addition, diazotrophic abundances in the upper mineral layer positively correlated with soil thaw duration (P=0.016).

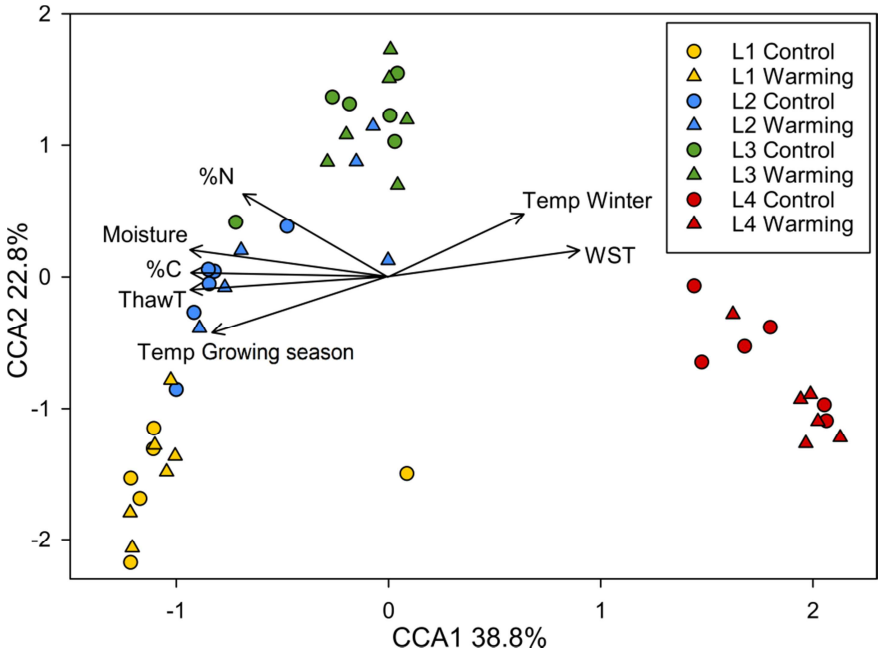

Figure 8. Canonical correspondence analysis (CCA) of *nifH* genes based on sequencing data (circle and triangle symbols) and major environmental factors (arrows). The values in Axis 1 and 2 labels are percentages of variations in the diazotrophic community that the axis can explain. Abbreviations: L1, the upper organic layer; L2, the middle organic layer; L3, the lower organic layer; L4, the upper mineral layer; %N or %C, soil N or C content; Moisture, soil volumetric water content; ThawT, the duration of soil's thawed period in growing season; Temp Growing season, growing season soil temperature; Temp Winter, winter soil temperature; WST, the duration of soil being water saturated during growing season.

Structural equation modeling was applied to identify the impacts of environmental factors on diazotrophic abundance (Figure 9). The interactive model of environmental factors and diazotrophic abundance was well fitted (χ^2=2.524, df=2, *P*=0.283). Diazotrophic abundance positively and significantly correlated to aboveground plant biomass, unveiling a possible interaction between increased diazotrophic abundance and higher plant biomass. Diazotrophic abundance also positively and significantly correlated to soil moisture, which was also supported by the result of the Pearson correlation analysis (Table S5).

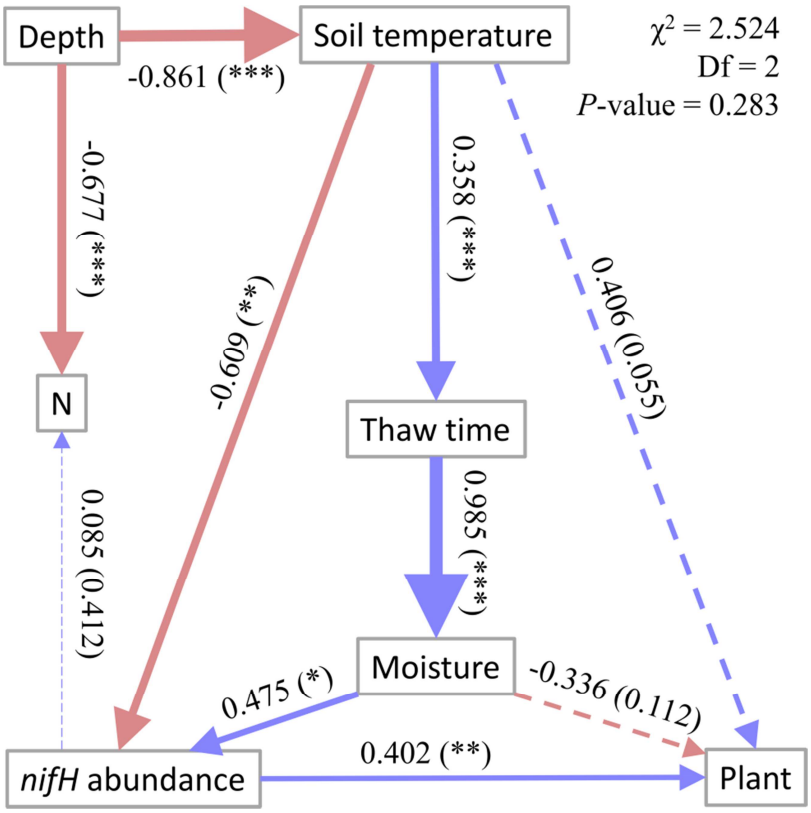

Figure 9. Structural equation modeling (SEM) of *nifH* gene abundance and key environmental factors. Chi-square = 2.524; Degrees of freedom = 2; probability level = 0.283. Blue arrows indicate positive relationships, and red arrows indicate negative relationships. Solid lines represent significant correlations, and dashed lines indicate insignificant correlations. Numbers adjacent to arrows are standardized path coefficients (co-variation coefficients) which are proportional to the thickness of the lines, with *P*-values in the brackets. Significance: *, $0.01<P\leq0.05$; **, $0.001<P\leq0.01$; ***, $P\leq0.001$. Abbreviations: N, soil N content; Moisture, soil volumetric water content; Thaw time, the duration of soil's thawed period in growing season; Soil temperature, growing season soil temperature; Plant, aboveground plant biomass; χ^2, Chi-square; Df, degrees of freedom.

3.5 Discussion

The experimental warming of tundra soils has been shown to increase soil inorganic N (Natali, Schuur et al. 2011). This has been previously attributed to N transport from the mineral soils into the upper thawed soil layers when water in the extended thawing layer flows through the deeper soil (Keuper, vanBodegom et al. 2012). However, deeper thawing could also export inorganic N from the soil to groundwater and/or

surface water (Harms and Jones 2012), thus reducing inorganic N. Here, by detecting higher diazotrophic abundance in deep tundra soils (Figure 6), we unveiled a potential alternative mechanism that enriches inorganic N.

N availability has a strong influence in tundra ecosystems, especially through altering plant species composition and enhancing plant growth (Walker, Wahren et al. 2006). Since soil warming has been shown to stimulate plant root exudation (Yin, Li et al. 2013), increased C substrates and decreased soluble N may further stimulate the activity of soil diazotrophs. Long-term soil warming enhanced aboveground plant biomass and foliar N content in Alaskan soil (Salmon, Soucy et al. 2015), which resulted in enhanced plant competition with soil microbes for N acquisition. As a consequence, the diazotrophic community would be expected to respond to meet the increased N demand when there were favorable environmental conditions. We found that diazotrophic abundance strongly and positively correlated to aboveground plant biomass (SEM, Figure 9), which was significantly enhanced by warming (Figure 6 & Table S2). It was shown that warming can also affect diazotrophic abundance indirectly via increased soil moisture (Eaton, Roed et al. 2012) and water-filled pore space (Teepe, Vor et al. 2004) owing to extended thawing, which is consistent with our results (Figure 9 & Table S5). Whether the tundra ecosystem acts as a C sink or C source depends on both the microbial and plant responses (Xue, Yuan et al. 2016), as net ecosystem CO_2 exchange was reported as increased from -105 to -61 g (CO_2-C)$\cdot m^{-2}$ (negative values indicate a net C source) by climate warming in the site our samples were taken by May 2013 (Mauritz, Bracho et al. 2017).

The effect of warming on diazotrophic communities varies with soil depth. The temperature sensitivity (Q_{10}) of soil C decomposition in a temperate forest organic layer has been previously shown to be higher than the mineral layer, since the organic

layer contained more C (Xu, Li et al. 2014). Similarly, we found that warming affected the diazotrophic composition and abundance more substantially in the tundra organic layer than in the mineral layer (Table S4 & Figure 6). In the upper mineral layer (45–55 cm), warming enhanced only diazotrophic abundance (Figure 6). Transplanting soils to a warmer region has been shown to increase within-treatment β-diversity of microbial taxonomic composition (Liang, Jiang et al. 2015). Similarly, warming significantly enhanced the within-treatment diazotrophic β-diversity in the middle and lower organic layers (5–25 cm) for both Bray-Curtis and UniFrac distances (Table S4), suggesting that warming enhanced the diversity of the diazotrophic communities. Therefore, it would be challenging to predict diazotrophic composition under a warmer climate due to the higher temporal turnover rates, which is caused by intensified competition or increased niche differentiation as more resources become accessible (Rousk, Frey et al. 2012).

Nitrogenase is sensitive to oxygen (White, Prell et al. 2007). The arctic tundra soil becomes increasingly saturated by water with depth, leading to oxygen depletion (Gebauer, Reynolds et al. 1995). Soil moisture also positively regulates N_2-fixing rates and diazotrophic community biomass, which could be partly explained by the more anaerobic conditions created by water saturation (Liengen and Olsen 1997, Zielke, Solheim et al. 2005, Stewart, Lamb et al. 2011, Eaton, Roed et al. 2012, Stewart, Brummell et al. 2013). In addition, the lack of photosynthesis in deep soils could further deplete oxygen (Liebner, Zeyer et al. 2011). Therefore, N_2-fixation rates would be expected to be influenced by depth with concomitant changes in the abundance of the diazotrophs as correlations between abundance and rate have been previously identified (Hadri, Spaink et al. 1998, Reed, Townsend et al. 2010, Huang, Tang et al. 2011). However, it is important to note that differences in soil edaphic

properties, nutrients, and the soil environment as a whole may influence the strength of these correlations. In addition, the composition of the diazotrophic community may be altered, resulting in varying cell-specific N_2-fixation rates that can impact this correlation. Our results show that diazotrophic abundance within the organic layer (0–25 cm) increased with depth, likely due to increasing anaerobiosis and the absence of light in deeper soils. Likely due to the higher O_2 availability, diazotrophic abundance was very low in the upper organic layer (0–5 cm). Diazotrophic richness within the organic layer (0–25 cm) also increased with depth, which might be attributed to more varied metabolic pathways associated with respiration along the anaerobic continuum. Many plant species living with stress of anaerobic soil conditions have developed aerenchyma, the enlarged and interconnected intercellular gas spaces in roots and stems to facilitate oxygen utilization (Vartapetian and Jackson 1997). Those plant species include *Eriophorum vaginatum* (Iversen, Sloan et al. 2015), the most abundant plant species in our site (43.4% of total aboveground plant biomass). It remains unclear how diazotrophic communities, which prefer to anaerobic condition, supply N nutrient to plants. One possibility is through water flow, which provides an explanation to the observation that permafrost thawing increases plant-available N (Keuper, vanBodegom et al. 2012). Diazotrophic abundance and richness were low in the mineral layer (45–55 cm) (Figure 6 and Table S4), most likely due to limited C substrates essential for diazotrophic communities (Yin, Li et al. 2013), given that plant roots reside in the organic layer (Iversen, Sloan et al. 2015).

Extensive sequence reads were obtained in this study, with the majority of the diazotrophic community not taxonomically identified. In Zehr laboratory's *nifH* gene database (2014 version), only 16.6% at the genus level and 29.8% at the phylum level of all 41,229 *nifH* gene sequences have taxonomic information. The relative

abundances of *nifH* OTUs in Cluster I, predominantly composed of aerobic taxa, decreased with soil depth while those of Cluster II, composed of obligate anaerobes, increased with depth (Figure 7) (Raymond, Siefert et al. 2004). In addition, closely clustered *nifH* OTUs often belong to different phylogenetic clades, which supports the hypothesis of frequent horizontal gene transfer events for these *nifH* genes (Li, Wang et al. 2008). The most abundant *nifH* OTU (OTU 7) matched to *Rubrivivax gelatinosus*, a purple non-sulfur photosynthetic facultative heterotroph capable of growing photosynthetically using CO and N_2 as its sole C and N sources, or anaerobically in the dark (Hu, Lang et al. 2012). The absolute abundance of OTU 7 monotonously increased along soil depth within the organic layer (0–25 cm), suggesting that it lives by chemoheterotrophy rather than photosynthesis and warming significantly enhanced the abundance of OTU 7 in the middle and lower organic layers (5–25 cm) (Figure S7A). The primer set chosen in this study has been tested in recent studies (Collavino, Tripp et al. 2014, Penton, Yang et al. 2016). Although this primer set was evaluated as not capturing most diazotrophs *in silico* (Gaby and Buckley 2012), the evaluation might be limited in reliability. This concern may be valid because a pair of *in silico* high-performance (high binding efficiency for a broad spectrum of nifH) primers, nifH1/nifH2, generated non-specific products from soil DNA (Gaby and Buckley 2012). On the other hand, PolF/PolR (the primer set we used) was evaluated to be reliable in amplifying soil DNA (Poly, Monrozier et al. 2001).

In conclusion, this study revealed that warming resulted in a more abundant diazotrophic community, which provides valuable insights into the potential factors affecting future C and N availability in tundra regions. Therefore, research is

warranted to directly test whether this warming-increased diazotrophic community results in increased N_2-fixation activity and N availability to the ecosystem.

Chapter 4: **Warming exacerbates tundra soil lignin decomposition governed by *Proteobacteria***

4.1 Abstract

In a warmer world, microbial decomposition of previously frozen carbon (C) is one of the most likely positive climate feedbacks of permafrost regions to the atmosphere. However, mechanistic understanding of microbial mediation of biologically recalcitrant C instability is limited, impeding prediction of the strength of the C-cycle feedback to climate changes for this century and beyond. Using stable isotope probing of the active layer of Arctic tundra soils after depleting soil labile C through a 975-day laboratory incubation, here we reveal the identity of microbial decomposers of lignin and their responses to warming. The *β-Proteobacteria* genus *Burkholderia* accounted for 95.1% of total abundance of potential lignin decomposers. Consistently, *Burkholderia* isolated from our tundra soils could grow with lignin as the sole C source. Warming considerably increased total abundance and functional capacities of all potential lignin decomposers. In addition to *Burkholderia*, *α-Proteobacteria* capable of lignin decomposition (e.g. *Bradyrhizobium* and *Methylobacterium* genera) were stimulated by 82-fold. Those community changes collectively doubled the priming effect, i.e., decomposition of existing C after fresh C input to soil. Consequently, warming caused more intense decomposition of soil C, as verified by microbially-enabled Climate-C modeling. Our findings are alarming, which demonstrate that accelerated C decomposition under warming conditions will make tundra soils a larger biospheric C source than anticipated.

4.2 Introduction

Nearly half of global soil organic C is stored in the northern permafrost regions (1,330–1,580 Pg organic C) (Vonk, Sánchez-García et al. 2012, Xue, Yuan et al. 2016). With rapid increase of temperature occurring in higher latitudes, this large C pool becomes vulnerable to microbial decomposition (Natali, Schuur et al. 2011)**.** It was shown that an increase of 2^{o}C would accelerate the decomposition of biologically recalcitrant C by 21%, compared with only a 10% rise for biologically labile C, suggesting that biologically recalcitrant C storage is more vulnerable to global warming (Davidson and Janssens 2006). Therefore, the biologically recalcitrant C pool in tundra soil may act as an important source for accumulation of atmospheric greenhouse gases.

As a complex aromatic heteropolymer in plant cell walls and litter, lignin is an important component of biologically recalcitrant C (Romero-Olivares, Allison et al. 2017). In addition to fungi (Bugg, Ahmad et al. 2011), bacteria, such as *Streptomyces viridosporus* T7A, *Pseudomonas putida* MT-2, *Nocardia*, and *Rhodococcus sp.* RHA1 (Ramachandra, Crawford et al. 1988, Vicuña 1988, Zimmermann 1990, Masai, Katayama et al. 2007), have been demonstrated to be potent lignin decomposers. Given that bacteria grow faster than fungi under warming (Sistla, Moore et al. 2013) and more diverse terminal electron acceptors can be utilized by bacteria during recalcitrant C decomposition, bacteria may play a role as important as fungi in affecting soil C stability in warmed soil (DeAngelis, Pold et al. 2015, Pold, Melillo et al. 2015). However, the identity of bacterial lignin decomposers in tundra soils and their responses to warming remain elusive, which prevent accurate prediction of future C fate in tundra regions.

Warmer climate leads to permafrost soil thaw in tundra regions, which releases previously frozen organic C so as to be accessible for microbial decomposition (Natali, Schuur et al. 2011). In moist acidic tundra soils, microbial community subjected to warming treatment showed a higher C-decomposing capacity (Ernakovich and Wallenstein 2015). Abundances of biologically recalcitrant C-decomposing genes were also increased by warming in tundra soils, which corroborated with higher ecosystem respiration (Xue, Yuan et al. 2016). Moreover, warming in tundra regions promotes plant root exudates such as organic acids, sugars and amino acids (Yin, Li et al. 2013), which could exacerbate the biologically recalcitrant C vulnerability (termed the priming effect) (Mau, Dijkstra et al. 2018). Given that approximately 65% of total C in tundra soil is stored as lignin, chitin, and terpenes (Vonk, Sánchez-García et al. 2012, Xue, Yuan et al. 2016), we hypothesize that warming would cause faster decomposition of tundra C by shifting microbial community composition, increasing decomposer abundance and the decomposing capacity of biologically recalcitrant C.

4.3 Materials and Methods

4.3.1 Site description and soil sample preparation

The warming experiment was carried out at the Carbon in Permafrost Experimental Heating Research (CiPEHR) site, which was established in 2008. As described previously (Natali, Schuur et al. 2011), soils were warmed during winter months by increasing snow cover behind snow fences, which were perpendicular to the dominant south-easterly winter winds. Warmed plots were on the leeward side of snow fences while the control plots were on the windward side. Snow fences trapped and accumulated an insulating snow layer on the warmed plots. As a result, the warmed soil was at an average temperature of 2.3^{o}C higher than the control soil during winter.

Soil samples were collected in May 2010. Intact soil core was collected from a depth of 15–25 cm in order to avoid litter and course root that made up most of the tundra soil from 0–15 cm. Since extended soil incubation of soil is important for identifying potential lignin decomposers and measuring the priming effect of recalcitrant C (Schädel, Schuur et al. 2014), intact soil samples were incubated in lightproof jars for 975 days to deplete biologically labile C. As described previously (Bracho, Natali et al. 2016), soil was added to a perforated foil cup and placed over a bed of 3 mm glass beads inside the jar to allow drainage and maintain soil moisture. Because the temperature of surface soils at the CiPEHR site could reach 25^{o}C during the growing season (Bracho, Natali et al. 2016), jars were placed in a 25^{o}C water bath to ensure complete depletion of biologically labile C within 975 days. Jars were covered with perforated lids to allow air exchange.

4.3.2 The stable isotope probing experiment and CO_2 flux measurement

^{13}C-vanillin (vanillin-(*phenyl*-$^{13}C_6$); 99 atom% ^{13}C) and ^{12}C-vanillin were used as stable isotope probe substrates (Sigma-Aldrich, St. Louis, Missouri, USA). To ensure even addition to the soil, vanillin was dissolved in water as 0.8% solution, not exceeding the solubility of 1%, and then injected evenly to the soil. Three incubation groups, i.e., (1) with 0.345 ml of 0.8% ^{13}C-vanillin in 2.76 g of soil (1 mg/g w/w) as isotopic treatment, (2) with 0.345 ml of 0.8% ^{12}C-vanillin in 2.76 g of soil as isotopic control, and (3) with 0.345 ml of water in 2.76 g of soil as the background, were set up for both warming and control samples. Each group was set up in three biological replicates. The final water content did not exceed 70% of the water-holding capacity (WHC) of the soil, and each replicate was sealed in a 25-ml lightproof bottle and incubated at 25^{o}C for 6 days.

Headspace gas was collected daily into 12-ml evacuated vials (Labco Limited, Lampeter, UK), after which the bottle was opened and refreshed for 30 min. To generate positive pressure to atmosphere, sampled gas in vials was diluted by injecting 10 ml of N_2 gas into each vial. CO_2 and $^{13}CO_2$ concentration were measured at the Stable Isotope Facility, University of California, Davis.

The percentage of the CO_2-C derived from vanillin was calculated as:

$$\%C_{substrate} = \frac{\delta_C - \delta_T}{\delta_C - \delta_L} \times 100\%$$

where δ_C is the $\delta^{13}C$ value of respired CO_2 from the soil with no added vanillin, δ_T is the $\delta^{13}C$ value of respired CO_2 from the soil with ^{13}C-vanillin, and δ_L is the $\delta^{13}C$ value of ^{13}C-vanillin. Because vanillin was added to the soil in the form of water solution, the amount of soil organic matter C primed by vanillin was calculated as total soil respiration after vanillin addition minus the amount of C respired from vanillin, and then minus the amount of C primed by water (C respired from the soil with no added vanillin).

4.3.3 Soil DNA extraction

Soil DNA was extracted using a freeze-grinding method as described previously (Zhou, Bruns et al. 1996) and purified by a MOBIO PowerSoil kit (MO BIO Laboratories Inc., Carlsbad, CA, USA) according to the manufacturer's protocol. DNA quality was assessed by a NanoDrop ND-1000 Spectrophotometer (Thermo Fisher Scientific, Waltham, MA, USA) based on spectrometry absorbance at wavelengths of 230 nm, 260 nm and 280 nm. The absorbance ratios of 260/280 nm were larger than 1.8, and of 260/230 nm were around 1.7.

4.3.4 ^{13}C-DNA separation

Density gradient ultracentrifugation of ^{13}C-labelled DNA was performed according to a previous protocol with minor modifications (Neufeld, Vohra et al. 2007). In brief, we centrifuged 5.1 ml of a solution composed of 5 μg of soil DNA, 1.90 g ml^{-1} cesium chloride (CsCl) (MP Biomedicals, Santa Ana, CA, USA), and a gradient buffer of 1 mM EDTA, 0.1 M KCl, and 0.1 M Tris-HCl, reaching a final density of 1.725 g ml^{-1}. The solution was sealed in a polyallomer centrifuge tube (cat. No. 342412, Beckman Coulter, Brea, CA, USA) with a cordless tube topper, and centrifuged on a Vti 65.2 rotor of an Optima L-XP ultracentrifuge (Beckman Coulter, Brea, CA, USA) at 177,000 g and 20^{o}C for 48 hours. Solution from each centrifuged tube was then separated into twenty-four 220-ml fractions (14 drops per fraction) according to the density gradient. The buoyant density of each fraction was determined by an AR200 digital refractometer (Reichert, Depew, NY, USA). To this end, DNA in each fraction was precipitated with 20 μg of glycogen and 2 volumes of PEG solution (30% PEG 6000 and 1.6 M NaCl), washed with 70% ethanol, and re-suspended in 35 μl of ultrapure water.

Quantitative PCR (qPCR) was used to determine absolute abundances of 16S rRNA genes, thus identifying the fractions containing ^{13}C-DNA. Universal primers 515F (5'-GTGCCAGCMGCCGCGGTAA-3') and 806R (5'-GGACTACHVGGGTWTCTAAT-3') were used for targeting the V4 region of the 16S rRNA genes. qPCR was performed in triplicate 20-μl reactions containing 10 μl SsoAdvanced™ Universal SYBR® Green Supermix (Bio-Rad, Hercules, CA, USA), 350 nM each primer and 1 μl of template, using a thermocycler program of 35 cycles of 95^{o}C for 20 sec., 53^{o}C for 25 sec. and 72^{o}C for 30 sec. on an IQ5 Multicolor Real-time PCR Detection System (Bio-Rad, Hercules, CA, USA). Gene copy numbers

were determined by a standard curve constructed with 16S rRNA gene segment of *E. coli* JM109 competent cells and TA cloning vector (Promega, Madison, WI, USA). According to the buoyant density and 16S rRNA gene copy number, a light DNA peak was identified as ^{12}C-labelled DNA, and a heavy DNA peak was identified as ^{13}C-labelled DNA.

4.3.5 16S rRNA gene amplicon sequencing

A two-step PCR was performed prior to 16S rRNA gene sequencing (Wu, Wen et al. 2015). In the two-step PCR, the first step of the V4 region of 16S rRNA genes was amplified by the primer 515F and 806R in triplicate 25 μl reaction containing 2.5 μl of 10×AccuPrime PCR buffer (containing dNTPs) (Invitrogen, Grand Island, NY, USA), 1 μl of 10 μM forward and reverse primer, 2 μl of template DNA and 0.2 μl of AccuPrime High-Fidelity Taq Polymerase. The thermocycler program was as follows: 94^{o}C for 1 min, 10 cycles of 94^{o}C for 20 sec., 53^{o}C for 25 sec. and 68^{o}C for 45 sec., and a final extension at 68^{o}C for 10 min. The second step of PCR also used a 25-μl reaction containing 2.5 μl of 10×AccuPrime PCR buffer (including dNTPs), 1 μl of 10 μM 515F and 806R primer combined with the Illumina adaptor sequence, a pad and a linker of two bases, and a barcode sequences on the reverse primers, 15 μl of aliquot of the first step purified PCR product and 0.2 μl of AccuPrime High-Fidelity Taq Polymerase. The thermal cycling condition was the same as the first step except a cycle number of 20. PCR products from the second step were examined by agarose gel electrophoresis, and then triplicate PCR products were combined and quantified by Pico Green.

PCR products from each fraction were pooled at equal molarity and sequenced in the same MiSeq run. The pooled mixture was purified with a QIAquick Gel

Extraction kit (Qiagen Sciences, Germantown, MD, USA) and re-quantified with Pico Green. The detailed protocol for MiSeq sequencing had been described previously (Zhou, Deng et al. 2016).

The raw sequence reads were processed using an in-house pipeline built on the Galaxy platform. First, the FastQC (http://www.bioinformatics.babraham.ac.uk/projects/fastqc/) was used to evaluate the quality of raw sequence data. Second, the spiked PhiX reads were removed with E value<10^{-5}. Third, sequences were sorted to corresponding samples according to their barcodes on the primers, which allowed for 0 mismatch. Fourth, Btrim was performed for quality trimming (Kong 2011), then forward and reverse reads of the same sequence with at least 20-bp overlap and <5% mismatch were combined by FLASH v1.2.5 program (Magoč and Salzberg 2011). Combined sequences were removed if they contained ambiguous bases or were less than 240 bp, and then Uchime was used to remove the chimeric sequences (Edgar, Haas et al. 2011). Finally, OTUs were clustered using UPARSE at the 97% similarity level (Edgar 2013). Each fraction was randomly resampled according to the absolute abundance of 16S rRNA gene based on qPCR result, with a resampling size of 29,845. OTUs were annotated through Ribosomal Database Project (RDP) classifier 2.5 with minimal 50% confidence score (Wang, Garrity et al. 2007).

4.3.6 Identification of potential lignin decomposers

The minor peak on the right side of the major peak was identified as ^{13}C-labelled DNA from the abundance-density plot of ^{13}C-incubated samples. For each sample, four fractions contributing to the major peak were termed as the “heavy fractions”, and four fractions contributing to the minor peak were termed as the “light fractions”.

Not all OTUs detected in the heavy fraction can be labelled by ^{13}C due to interference of high GC content. In addition, OTUs are prone to sequencing errors. We developed a strictly filtering method to distinguish ^{13}C-labelled OTUs from false positives ascribed to high GC content or sequencing errors. This filtering method included three consecutive steps: (i) to exclude OTUs of high GC content, we performed a non-parametric *t*-test to determine the significance of sequence number difference assigned to each OTU found in heavy fractions between ^{13}C-incubated samples and ^{12}C-incubated samples. We removed OTUs with insignificant *P* values ($P>0.10$); (ii) we subtracted relative abundances of remaining OTUs with relative abundances in heavy fractions of the corresponding ^{12}C-incubated samples. We termed the difference as the modified sequence number in heavy fractions (MSNH); and (iii) to exclude OTUs from sequencing errors, we removed OTUs when its MSNH present in the heavy fractions was less than 20% of the total relative abundance. The remaining OTUs were regarded as potential lignin decomposers.

4.3.7 Isolation, identification and growth of Burkholderia isolates

Burkholderia AK1 and AK3 were isolated from soils after 975-day incubation by diluting nutrient broth media at 25^{o}C as previously described (Janssen, Yates et al. 2002). The 16S rRNA gene was amplified by universal bacterial 16S rRNA gene primers: 27F (5'-AGAGTTTGATCCTGGCTCAG-3') and 1492R (5'-GGTTACCTTGTTACGACTT-3'). Genomic DNA of isolates was extracted by GenElute^{TM} Bacterial Genomic DNA Kit (Sigma Aldrich, St. Louis, MO, USA), and sequenced by Illumina MiSeq platform. The ANI values were calculated by FastANI (Jain, Rodriguez-R et al. 2018).

The BMM defined medium (Woo, Hazen et al. 2014) is comprised of 0.80 g L^{-1} NaCl, 1.0 g L^{-1} NH_4Cl, 0.10 g L^{-1} KCl, 0.10 g L^{-1} KH_2PO_4, 0.80 g L^{-1} $MgCl_2 \cdot 6H_2O$, 4.0 g L^{-1} $CaCl_2 \cdot 2H_2O$, 10 g L^{-1} PIPES (pH=6.5), trace minerals (160 mg/L Nitrilotriacetic acid, pH6.5, 12.5 mg/L $FeCl_2 \cdot 4H_2O$, 6.25 mg/L $MnCl_2 \cdot 4H_2O$, 4.375 mg/L $CoCl_2 \cdot 6H_2O$, 2.5 mg/L $ZnCl_2$, 0.55 mg/L $Na_2MoO_4 \cdot 2H_2O$, 0.25 mg/L H_3BO_3, 1.25 mg/L $NiSO_4 \cdot 6H_2O$, 0.025 mg/L $CuCl_2.2H_2O$, 0.075 mg/L Na_2SeO_3, and 0.1 mg/L $Na_2WO_4.2H_2O$), vitamins solution (0.02 mg/L Biotin, 0.02 mg/L Folic acid, 0.1 mg/L Pyridoxine HCl, 0.05 mg/L Thiamine HCl, 0.05 mg/L Riboflavin, 0.05 mg/L Nicotinic acid, 0.05 mg/L DL pantothenic acid, 0.05 mg/L p-Aminobenzoic acid, 0.05 mg/L Lipoic acid, 2 mg/L choline chloride, and 0.01 mg/L Vitamin B12), and 0.05% (m/v) alkali lignin (Sigma Aldrich, St. Louis, MO, USA). Initially, isolated *Burkholderia* strains were inoculated into 50 ml of the BMM medium with 0.2 % yeast extract and incubated at 28^{o}C with constant shaking at 180 rpm to an OD_{600} (optical density at 600 nm) of approximately 1.0. Then, 1 ml of culture was aseptically inoculated into three parallel culture flasks containing 50 ml of the BMM defined medium. The flasks were incubated at 28^{o}C with constant shaking at 180 rpm for 9 days. Uninoculated medium was used as a control.

4.3.8 Draft Genome Reconstruction

Metagenomic paired-end reads were merged using PEAR (Zhang, Kobert et al. 2013) (options: -p 0.001). All merged and non-merged reads were then quality-trimmed with the SolexaQA package (Cox, Peterson et al. 2010) (options: -h 17). Merged and trimmed reads were assembled with IDBA-UD (Peng, Leung et al. 2012) (version 1.1.1; options: --mink 55 --maxk 107 --step 4 --min_contig 500). Contigs > 2 kb were used to calculate the mean coverage of each contig in each metagenome dataset (using

megablast in BLAST + version 2.2.25; cut-off used: ≥ 90% of length of the query sequence, ≥ 98% nucleotide identity) (Camacho, Coulouris et al. 2009). Resulting contigs (>2 kb) and coverage table were used with MetaBAT2 (options: --minCVSum 10) (Kang, Froula et al. 2015) to recover microbial population genomes. The quality of the resulted bins were assessed by CheckM (Parks, Imelfort et al. 2015). The bins with > 80% completeness and < 1% contamination were used for further analysis.

4.3.9 Functional annotation of pure culture genomes and metagenome binning

Genomic annotation was performed using Automatic Genomic Analysis Pipeline (AGAP, version 1.2, an internal pipeline). Genomic annotation was conducted using PROKKA (version 1.11) (Hyatt, Chen et al. 2010). First, finished genomes and draft genomes were submitted to gene calling using Prodigal (version 2.6) (Hyatt, Chen et al. 2010) with output of translated protein sequences, single mode and genetic code of bacteria and archaea. Then rRNA genes were predicted using Barrnap (version 0.7). Pseudogenes and coding sequences overlapping with tRNA and rRNA gene were removed by PROKKA. The 16S rRNA genes used for taxonomic classification were classified using RDP Classifier (version 2.12) (Wang, Garrity et al. 2007). Protein sequences were submitted to DIAMOND (Buchfink, Xie et al. 2015) search (BLASTp) against NCBI NR database (version Jan 2016) with E value cutoff of 1e-5, coverage cutoff of 0.5 and maximum target number of 50. The BLASTp results were imported into MEGAN6 (Ultimate Edition, version 6.6) (Huson, Auch et al. 2007) for functional profiling with output of SEED Subsystem, KEGG and COG categories. Exported tables of functional profiles were integrated for comparison of genomes. Genome binning (assigning the non-overlapping contigs to genomes) was performed

by tetra-nucleotide frequency and verified by differential coverage binning (Albertsen, Hugenholtz et al. 2013).

4.3.10 Experiments with GeoChip 5.0

Approximately 50 ng of DNA separated from heavy fractions in warming or control samples were amplified using a Templiphi kit (GE Healthcare, little Chalfont, UK). The amplified DNA (2 μg) was labelled with fluorescent dye (Cy-3) dUTP using random primers and Klenow fragment of DNA polymerase I at 37^{o}C for 6 h, followed by heating at 95^{o}C for 3 min. Labelled DNA was then purified, dried in a SpeedVac at 45^{o}C for 45 min, and resuspended in 43.1 μl of hybridization buffer containing 27.5 μl of 2X HI-RPM hybridization buffer, 5.5 μl of 10X CGH blocking agent, 2.4 μl of cot-1DNA, 2.2 μl of universal standard and 5.5 μl of formamide. DNA was hybridized with GeoChip 5.0 (60K) in a SL incubator (Shel Lab, Cornelius, OR, USA) at 67^{o}C for 24 h. Then GeoChip arrays were washed and scanned by an MS 200 Microarray Scanner (Roche, Basel, Switzerland) at 532 nm and 635 nm. Raw signals from the scanning were processed by an online pipeline as previously described (Yang, Wu et al. 2013).

4.3.11 Statistical and phylogenetic analyses

Differences of relative abundances between isotopic treatment and control groups were determined by Wilcoxon Rank Sum and Signed Rank Tests (Hollander). The two-tailed *t*-test was used to determine the difference of richness of active communities between warming and control samples. All analyses above were performed in R software (version 3.3.2). Unless otherwise stated, mean values are

given ± standard error of the mean; significant differences are determined by one-way ANOVA; and values of $P \leq 0.05$ were considered significant.

The maximum likelihood phylogenetic tree was constructed based on the representative sequence for each OTU, as determined by UPARSE. MEGA 6.05 (Hall 2013) was used to construct the phylogenetic tree with MUSCLE alignment, maximum likelihood method and a bootstrap value of 1,000. The visual of final tree was generated by iTOL (Life 2011).

4.3.12 Molecular ecological network analyses

Phylogenetic molecular ecological networks (pMENs) were constructed from the 16S rRNA gene sequencing data, using a random matrix theory (RMT)-based network approach (Deng, Jiang et al. 2012). To ensure reliability, only OTUs detected in at least 10 out of 12 samples were used for network construction. In brief, a matrix containing Pearson's rho correlation between any pair of OTUs was generated. The threshold for network construction was automatically determined when the nearest-neighbor spacing distribution of eigenvalues transitioned from GOE to Poisson distributions. Consequently, a threshold of 0.74 was used in both warming and control sample networks. Random networks corresponding to all pMENs were constructed using the Maslov-Sneppen procedure with the same network size and average number of links to verify the system-specificity, sensitivity and robustness of the empirical networks (Maslov and Sneppen 2002).

4.3.13 Microbially-enabled decomposition modeling

A Microbially-ENabled Decomposition model (MEND) (Wang, Jagadamma et al. 2015, Wang, Peng et al. 2017) was used in this study. The MEND model is a

sophisticated model with parameters representing microbial dormancy, resuscitation, and mortality. It simulates soil organic matter (SOM) decomposition in response to changes in environmental factors such as temperature (Wang, Jagadamma et al. 2015) by explicit microbe-mediated oxidative and hydrolytic processes. The temperature response is modeled by the Arrhenius equation characterized by the activation energy. Here, we initialized soil C pools by the measurements of soil organic C and microbial biomass C in the control and warmed samples at the beginning of the lab incubation experiments. To determine microbial parameters in soil samples, we combined the experimental data at two experimental incubation temperatures (i.e., 15^{o}C and 25^{o}C) since differential temperature allows for more accurate estimate of model parameters. We used the stochastic Shuffled Complex Evolution (SCE) algorithm (Wang, Jagadamma et al. 2015) to determine model parameters by achieving the highest goodness-of-fit between modeled and measured CO_2 fluxes. The microbial traits or parameters (e.g., microbial growth, maintenance, mortality, C use efficiency, and active versus dormant fractions) represent the microbial community characteristics related to soil C mineralization. We then ran model simulations with those parameters for 10 years to predict the long-term warming effect on SOM decomposition.

4.4 Results and Discussion

4.4.1 Strong warming effects on lignin decomposers

To identify potential lignin decomposers and their responses to warming, we collected tundra soils subjected to *in situ* warming for a 1.5-year period, in parallel with unwarmed/control soils. Since the turnover time of slow C pool of tundra soil is ~600 days (Hale, Feng et al. 2019), we starved soils by laboratory incubation for 975 days to completely deplete biologically labile C reserves, a practice also recommended for

helping accurate modeling of soil C kinetics (Schädel, Schuur et al. 2014). Subsequently, we performed stable isotope probing (SIP) experiments to label active bacterial decomposers in warmed and control samples. Intuitively, lignin should be used. However, it is difficult to label all of C atoms of lignin owing to its complex structure. More importantly, lignin is resistant to biochemical breakdown (Taylor, Hardiman et al. 2012), thus incubation time for the SIP experiment has to be extended, which inevitably causes cross-feeding. Therefore, we used vanillin, an intermediate of lignin decomposition widely used as a model aromatic substance to detect lignin depolymerization (Zak and Kling 2006, Taylor, Hardiman et al. 2012), as the SIP substrate to identify potential ligninolytic microorganisms. We use the word "potential" here because vanillin decomposers are not necessarily lignin decomposers.

The peak of ^{13}C-labelled DNA was detected around the density of 1.748 g/ml (heavy fractions, Figure S12), which was present only in samples incubated with ^{13}C-vanillin but not in samples incubated with ^{12}C-vanillin or no vanillin. The peak of ^{12}C-labelled DNA was detected around the density of 1.720 g/ml (light fractions). Total abundance of 16S rRNA genes in ^{13}C-labelled DNA was increased from $(2.7\pm0.5)\times10^5$ copies/g soil in control samples to $(1.0\pm0.3)\times10^6$ copies/g soil in warmed samples ($P<0.01$) (Figure 10a). As all variables except the field warming treatment were controlled between warming and control groups during the entire experimental workflow, this result suggests that warming stimulated potential lignin decomposers. High-throughput sequencing of ^{13}C-labelled DNA showed that there were 63 operational taxonomic units (OTUs) in warmed samples, which were significantly ($P<0.05$) higher than that of control samples (28 OTUs). In addition, warming enhanced total abundance of 16S rRNA genes in ^{12}C-labelled DNA from

$(4.7\pm1.6)\times10^5$ to $(1.4\pm0.4)\times10^6$ copies/g soil ($P<0.05$), suggesting that growth of the overall bacterial communities was also stimulated.

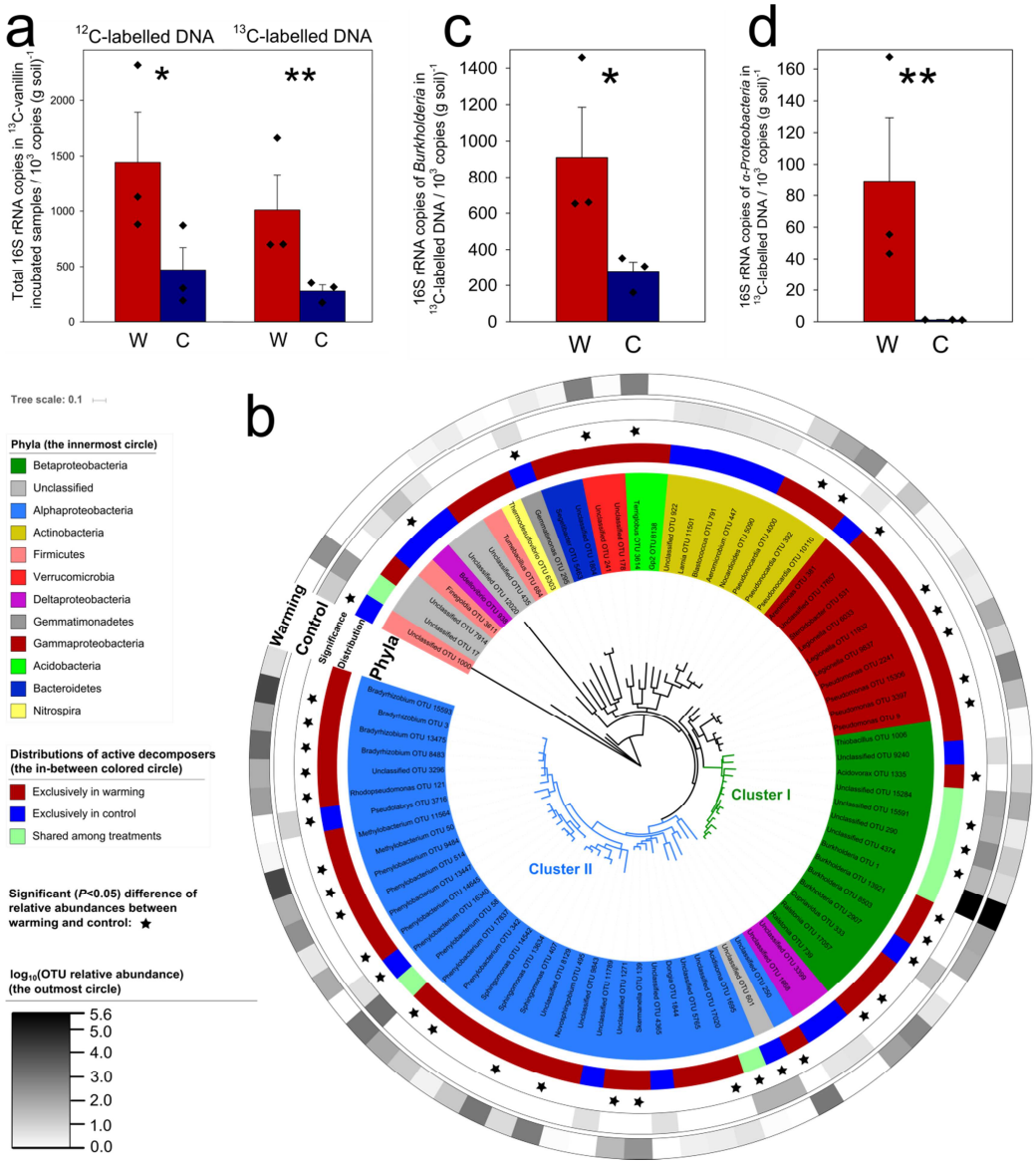

Figure 10. The absolute abundances of various taxa, measured by 16S rRNA genes, after incubation with ^{13}C-vanillin, determined by quantitative polymerase chain reaction (qPCR) and amplicon sequencing. (a) The numbers of total ^{12}C- and ^{13}C-labelled 16S rRNA gene copies in ^{13}C-vanillin incubated samples (n=3, biological replicates of warmed or control samples); (b) The circular maximum likelihood phylogenetic tree of the ^{13}C-labelled active decomposer operational taxonomic units (OTUs). Relative abundance is the modified sequence number in heavy fractions (MSNH; see Materials and Methods for details) of the OTU (n=3, biological replicates of warmed or control samples); (c) The number of ^{13}C-labelled 16S rRNA gene copies of *Burkholderia* (n=3, biological replicates of warmed or control samples); (d) The number of ^{13}C-labelled 16S rRNA gene copies of *α-Proteobacteria*

(n=3, biological replicates of warmed or control samples). Significance is indicated by *, $0.01<P\leq0.05$; and **, $0.001<P\leq0.01$, as determined by a two-tailed t-test. W: warmed soils; C: unwarmed/control soils. Data are shown as mean ± standard error.

Two major clusters were identified in the phylogenetic tree constructed for the potential lignin decomposers (Figure 10b). Cluster I contained 14 OTUs, of which 5 OTUs were shared by both warmed and control samples. Strikingly, Cluster I was solely composed of *β-Proteobacteria*, with 4 OTUs belonging to the genus *Burkholderia*. Warming slightly decreased relative abundance of *Burkholderia* in ^{13}C-labelled DNA from 99.4% to 90.8% (P<0.01, Figure S13a). In contrast, warming increased absolute abundance of ^{13}C-labelled *Burkholderia* from 2.6×10^5 to 9.1×10^5 copies/g soil (Figure 10c), reflecting strong stimulation. *Burkholderiales* dominated lignocellulosic decomposers in coniferous forest soils across North America (Wilhelm, Singh et al. 2019). It accounted for 64% of bacterial clone sequences in Canadian High Arctic soil (Harding, Jungblut et al. 2011), and was identified as keystone species in Arctic heathland soils using a network analysis (Hill, Saetnan et al. 2016). *Burkholderia* was abundant in our study site, which was significantly stimulated by *in situ* warming (P<0.05, Figure S14). Further, relative abundance of *Burkholderia* significantly increased by 31.5-fold after the 975-day incubation, and then increased by another 25.4-fold after addition of vanillin, demonstrating that *Burkholderia* is highly responsive to C substrate availability. Clearly, *Burkholderia* is a keystone taxon in Arctic tundra soils (Figure S15).

Given that the identified *Burkholderia* vanillin decomposers are not necessarily lignin decomposers, it is necessary to test whether *Burkholderia* species could decompose lignin. Both *Burkholderia* strains we isolated from tundra soils were able to grow with lignin as the sole C source (Figure S16). A number of peroxidases were annotated in the genomes, including multiple copies of a gene encoding catalase-

peroxidase well known in oxidizing lignin into small-molecule compounds (β-Aryl ether, Biphenyl, Diarylpropane, Ferulic acid, coumaric acid and Cinnamic acid) (Brown, Walker et al. 2011). We also identified 7 aromatic acid transporter genes and *β*-ketoadipate pathway genes that are downstream the catalase-peroxidase breakdown of lignin decomposition pathway, which potentially constitute a lignin metabolism pathway with the catalase-peroxidase (Figure S17).

Cluster II contained 35 OTUs. Only two of these OTUs were shared between warmed and control samples, with 26 OTUs exclusive to warmed samples. Thirty-two Cluster II OTUs belonged to *α-Proteobacteria*, including genera *Bradyrhizobium*, *Phenylobacterium*, *Sphingomonas, Novosphingobium*, and *Methylobacterium*. To provide further evidence for lignin-decomposing capacity, 7 *α-Proteobacterial* genomes, including 3 *Bradyrhizobium*, 3 *Phenylobacterium* and 1 *Sphingomonas*, were assembled from deep metagenomic sequencing data of starved soils despite their low abundance compared with Cluster I OTUs. Genes encoding catalase-peroxidases, which are capable for oxidizing lignin into small-molecule compounds, are present across all the genomes. Several genes associated with the *β*-ketoadipate pathway are also present, which are responsible for metabolizing intermediates during lignin decomposition.

Warming considerably enhanced total abundance of *α-Proteobacteria* in ^{13}C-labelled DNA from 1.1×10^3 to 8.9×10^4 copies/g soil (Figure 10d), and its relative abundance by 20.5-fold (Figure S13b). Among *α-Proteobacteria*, increases in representatives of genera *Bradyrhizobium* (from undetected to 4.0×10^4 copies/g soil) and *Methylobacterium* (from undetected to 3.2×10^4 copies/g soil) were most notable (Figure S18). Typically, *α-Proteobacteria* prefer to nutrient-rich environments and exhibit fast growth rates (Yergeau, Bokhorst et al. 2012). Tundra soil thawing by

warming exposes previously frozen organic C to microbial decomposition (Bracho, Natali et al. 2016), which stimulates *α-Proteobacteria*. Similarly, warming has increased the abundance of *α-Proteobacteria* in Antarctic environments (Yergeau, Bokhorst et al. 2012). However, bearing in mind a caveat that fast-growing bacteria may be preferably stimulated in the SIP experiment, since slow-growing bacteria may not incorporate sufficient ^{13}C-label within 6 days' incubation.

4.4.2 The priming effect doubled by warming

Changes in *α-Proteobacteria* abundance were positively correlated with soil CO_2 production in the High Arctic (Yergeau, Bokhorst et al. 2012). In this study, higher abundances of *α-Proteobacteria* in the warmed samples (Figure 10d) also corroborated with significantly higher total CO_2 production measured in the SIP experiment (182.6±6.2 μmol in warmed versus 174.9±4.0 μmol in control samples) (Figure 11). The ^{13}C content of $^{13}CO_2$ production after a 6-day incubation (92.7±1.1 μmol in warmed and 90.2±0.5 μmol in control samples) was close to that of added vanillin (82.6 μmol ^{13}C in warmed or control samples), indicating that added vanillin was depleted by the end of the incubation period. We detected a strong priming effect caused by supplementing with vanillin, as the C molar of total CO_2 production was substantially higher than the amount calculated from theoretical oxidation of vanillin (110.1 μmol). The C primed by vanillin under warming (19.1±2.2 μmol, the inset of Figure 11) was significantly more than that under the control condition (9.9±0.5 μmol). This result contrasts a previous study that detected no significant priming effect in the organic layer of tundra soil (De Baets, Van de Weg et al. 2016). This is likely attributed to our prolonged 975-day incubation of soils to deplete the

biologically labile C reserves (Bracho, Natali et al. 2016) prior to supplementing with vanillin.

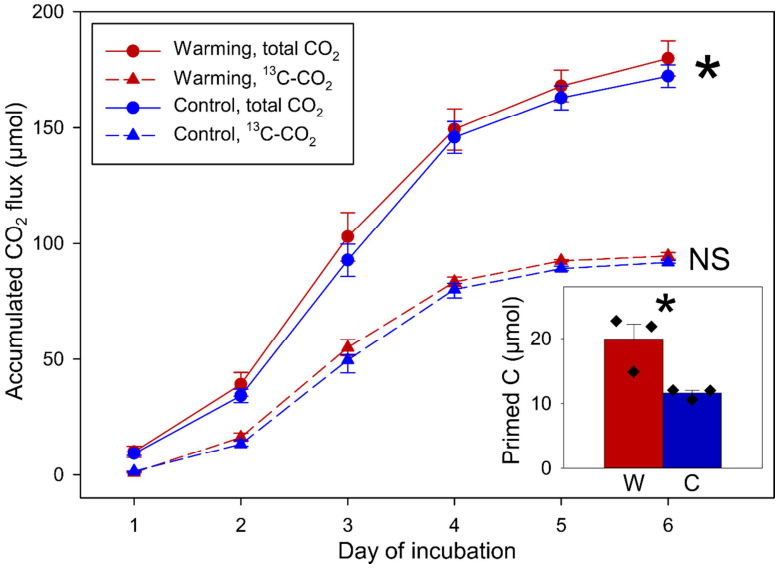

Figure 11. The accumulated CO_2 flux and the priming effect during the 6-day incubation trial. Red lines/symbols represent in situ warmed soils (W) and blue lines/symbols represent unwarmed/control soils (C). Solid lines represent total CO_2 and dashed lines represent ^{13}C-CO_2. The significance of the difference was determined by one-way ANOVA (n=3, biological replicates of warmed or control samples) on CO_2 amounts and primed C amounts between warmed and control samples (shown in the inset of the figure). W: warmed samples; C: control samples; NS: not significant. Data are shown as mean ± standard error.

To examine whether higher CO_2 production in warmed samples arises from changes in functional genes associated with C decomposition, especially of aromatics and lignin, relative abundances of related functional genes in ^{13}C-labelled DNA were quantified by GeoChip 5.0. Strikingly, almost all detected lignin-decomposing genes, including the *mnp* gene encoding peroxidase, *lcc* genes encoding phenol oxidase, *glx* gene encoding glyoxal oxidase, *vanA* gene encoding vanillate demethylase A, and *vdh* gene encoding vanillin dehydrogenase, increased by 10.1%–26.3% under warming (Figure 12a). This is consistent with higher ^{13}C ratio and greater total CO_2 flux under warming (Figure 11). More broadly, 32 out of 43 aromatic-decomposing genes also significantly increased by 4.9%–184.1% under warming (Figure 12a). Among them,

aromatic and lignin-decomposing genes derived from *Burkholderia* significantly increased by 11.9% (Figure 12b), suggesting higher decomposition potentials of *Burkholderia*. Interestingly, 83.5% of the other C-decomposing genes irrelevant to lignin decomposition, including those associated with decomposing chitin (e.g., chitinase), terpenes (e.g., *cdh* encoding carveol dehydrogenase), pectin (e.g., *pel* encoding pectin lyase), cellulose (e.g., endoglucanase), hemicellulose (e.g., xylanase) and starch (e.g., *amyA* encoding α-amylase), also significantly increased under warming by 5.7%–40.6% (Figure 12c). This is likely to arise from a broad functional response of priming to warming. In contrast, no C-decomposing gene was significantly decreased in abundance by warming. Given that warming may promote plant root exudation, releasing more biologically labile C substrates to the soil (Yin, Li et al. 2013), this strong priming effect implicates that there is an important positive feedback to global warming in tundra environments.

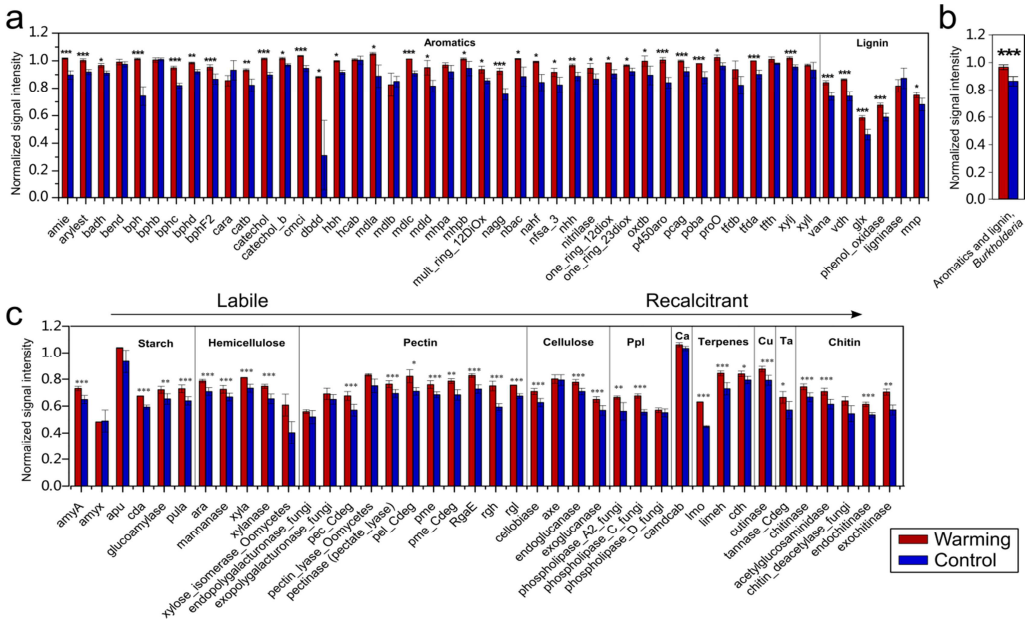

Figure 12. Normalized signal intensities of key C-decomposing genes in ^{13}C-labelled DNA. (a) Genes associated with aromatic and lignin decomposition; (b) Aromatic- and lignin-decomposing genes belonging to *Burkholderia* in ^{13}C-labelled DNA; (c) Genes associated with other key C-decomposing pathways. Ppl: phospholipids; Ca: Camphor; Cu: Cutin; and Ta: Terpenes. Differences in relative abundances were

determined using one-way ANOVA (n=3, biological replicates of warmed or control samples). Significance is indicated by *, $0.01<P\leq0.05$; **, $0.001<P\leq0.01$; and ***, $P\leq0.001$. Data are shown as mean ± standard error.

4.4.3 Model verification and data synthesis

To examine the scale of potential positive feedback of C cycling to warming, we implemented a Microbially-ENabled Decomposition (MEND) model (Wang, Jagadamma et al. 2015) to estimate the changes in C-decomposing rates. Simulated soil respiration for the 975-day laboratory incubation period agreed well with observed data ($R^2\geq0.85$, Figure 13a). Therefore, we proceeded to simulate the average soil respiration rate over the long term. We obtained significantly higher C-decomposing rates under warming (Figure 13b), which were verified by *in situ* respiration measurements in tundra regions (Pries, Schuur et al. 2016, Xue, Yuan et al. 2016). Accordingly, tundra soil organic C is projected to decrease significantly (Figure 13c), leading to greater net C loss under warming (Xue, Yuan et al. 2016). Higher soil respiration rates are consistent with the significantly more active microbial biomass (Figure 13d) and higher decomposition rates of oxidative enzymes (Figure 13e). Given that the oxidative enzymes mainly consist of ligninases (Wang, Post et al. 2012), these modeling results are consistent with our SIP results (Figure 10a), suggesting that warming would markedly increase the release of CO_2 from lignin or other biologically recalcitrant C sources to the atmosphere.

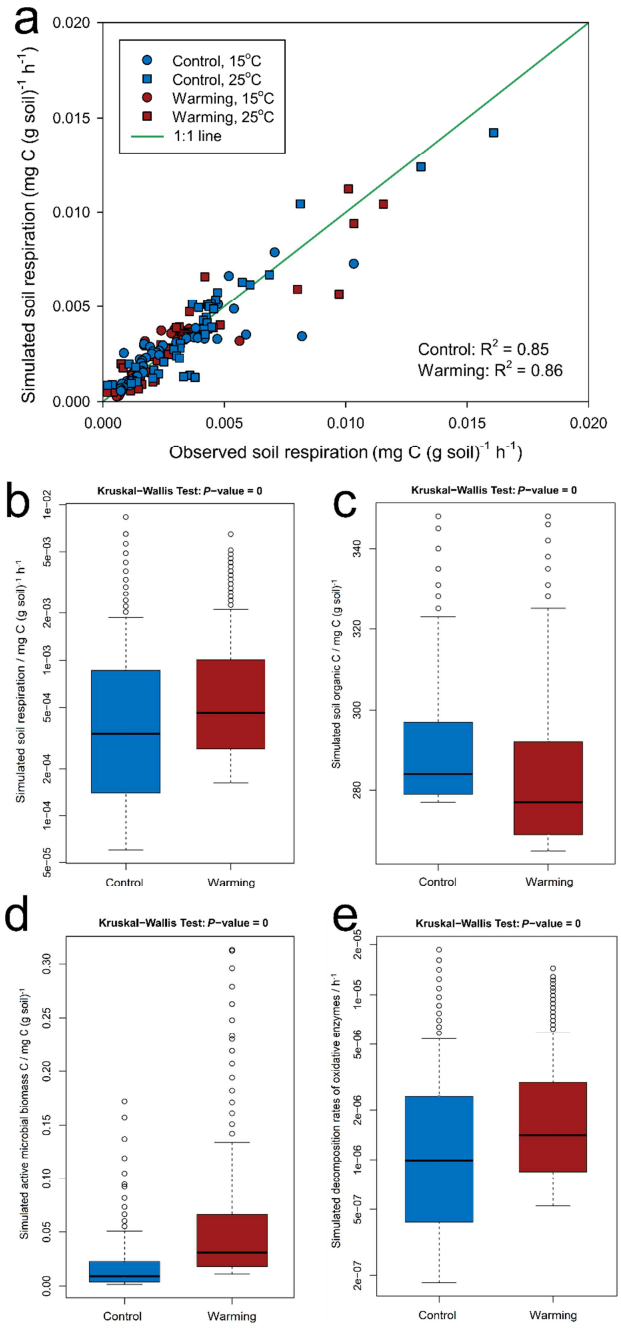

Figure 13. Soil and microbial variables simulated by MEND. Warming: *in situ* warmed soils; Control: unwarmed/control soils. (a) Simulated and observed soil respiration rates during the 975-day laboratory incubation period, showing high consistency. (b) Simulated soil heterotrophic respiration rates over 10 years. (c) Simulated soil organic C over 10 years. (d) Simulated active microbial biomass C over 10 years. (e) Simulated decomposition rates of oxidative enzymes over 10 years. The Kruskal-Wallis test was used to determine whether the parameter samples originated from significantly different distribution at a significance level of 0.05.

Combined, this study reveals important, positive feedbacks to climate warming in tundra regions, which can at least partially be attributed to higher lignin decomposer abundances and shifts in active ligninolytic community composition. To our knowledge, this is the first study directly investigating active recalcitrant C-decomposing bacteria in response to warming, leading to establishment of explicit linkages between soil respiration and microbial community composition and functional capacity. The stronger priming effect under warming is alarming, which indicates a previously overlooked mechanism that accelerates climate warming in tundra regions. Given that the past five years are the five warmest years on record since 1880, our study provides important insights into tundra soil C stability under global warming.

4.5 Author contributions

J.Z., E.A.G.S., Y.L., J.M.T., J.R.C., Y.Y. and K.T.K. developed the original concepts. M.M.Y. carried out the 16S rRNA gene amplicon experiments of the soil before the 975-day laboratory incubation. R.B. and E.A.G.S. performed the 975-day laboratory incubation experiment. L.H. carried out the 16S rRNA gene amplicon experiments of the soil after the 975-day laboratory incubation period. J.Y. and C.R.P. isolated and provided *Burkholderia* strains from the soil after the 975-day laboratory incubation period. E.R.J. assembled the genomes based on the metagenomic data from the soil the 975-day laboratory incubation period. R.T. conducted metagenomic assemblies and annotations. X.T., J.F. and F.F. carried out the 6-day incubation, and the related gas and 16S rRNA gene amplicon experiments and analyses. G.W. carried out the MEND model analysis. D.N. assisted with the statistical analyses. X.T., J.F., Y.Y., and J.Z. wrote the paper. C.T.B., LW.W., L.H., Q.G., LY.W., E.A.G.S., K.T.K., J.R.C.

and J.M.T. edited the manuscript. All authors were given the opportunity to review the results and comment on the manuscript.

Chapter 5: **Warming exacerbates grassland soil carbon degradation through activating *Firmicutes***

5.1 Abstract

Microbial decomposition of soil organic matter (SOM) has a strong impact on future atmospheric greenhouse gas concentrations, which serve as important feedbacks to climate warming. However, the underlying mechanisms remain poorly understood. In a stable-isotope probing incubation experiment using isotopically labelled straw to simulate grass litter, here we examined the composition and function of active bacterial communities subjected to a long-term (7 years) *in situ* warming treatment. Both bacterial abundance and carbon (C)-degrading potentials were stimulated by warming, concurrent with higher C degradation rates of both straw input and native SOM. Among them, a number of *Firmicutes* taxa, accounting for 18.5% of total bacterial abundance and well known to be efficient degraders of chemically labile and recalcitrant C compounds, were the most notable. Moreover, warming increased phylogenetic β-diversity among active bacterial communities, revealing a divergent pattern. Warming stimulated soil respiration by 13.3% and the priming effect on native SOM by 14.4%. Collectively, those results demonstrate that warming will accelerate soil C degradation by increasing active bacterial abundance, restructuring community composition, and increasing C-degradation potential.

5.2 Introduction

Global climate warming, resulted from unconscionable land utilization and accumulation of various greenhouse gases such as CO_2 and CH_4 due to fossil fuel combustion, has become the largest anthropogenic disturbance on natural systems (Deutsch, Tewksbury et al. 2008) and a major scientific and political issue worldwide (Stocker, Qin et al. 2013). As higher temperature is a primary driver of metabolic rates and biochemical processes (Gillooly, Brown et al. 2001, Brown, Gillooly et al. 2004), climate warming has affected biodiversity at all systematic levels, leading to restructured community (Xue, Yuan et al. 2016), enhanced abundance (Feng, Penton et al. 2019), divergent successional trajectories (Guo, Feng et al. 2018), and shifted geographic distribution (Chen, Hill et al. 2011) of organisms. Microbial communities, the most abundant, diverse and complex assemblage of the biosphere (Singh, Campbell et al. 2009), could also be stimulated to be a larger source of greenhouse gases such as CH_4 and CO_2 and thus a stronger positive feedback to warming (Xue, Yuan et al. 2016). Previous research has assessed phylogenetic and structural changes of microbial communities in response to warming (Xue, Yuan et al. 2016, Guo, Feng et al. 2018, Feng, Penton et al. 2019), and uncovered relationships between warming and CO_2 emissions from microbial communities (Luo, Wu et al. 2001, Mahecha, Reichstein et al. 2010, Carey, Tang et al. 2016), but the underlying mechanisms of microbial C degradation change in response to warming remain understudied, which are crucial for predicting future carbon (C) dynamics and thus global climate change (Wang, Jagadamma et al. 2015).

The grassland ecosystem is a large terrestrial C pool possessing about 12% of the global organic matter (Schlesinger 1977), where more than 90% is stored belowground in soil organic matter (SOM) and roots (Shahzad, Chenu et al. 2012).

This C reservoir derives from rhizodeposits (6%–40% of the net-photosynthesized C) (Lynch and Whipps 1990, Kuzyakov and Domanski 2000) and litter (Semmartin, Garibaldi et al. 2008) of the grasses. The rhizodeposits mainly consist of low-molecular-weight compounds such as organic acids, carbohydrates, amino acids and amides (Bürgmann, Meier et al. 2005), and herbaceous straw mainly consists of cellulose and hemicellulose which are relatively biologically more labile than recalcitrant C compounds such as lignin and chitin (Mood, Golfeshan et al. 2013). Therefore, this vital C reservoir could be vulnerable to the stimulated C degradation from soil microbial communities under climate warming. In addition to the microbial degradation of fresh deposited exogenous C, microbial degradation of soil organic C (SOC) induced by the fresh C input (Mau, Dijkstra et al. 2018), i.e. the priming effect, has also been observed as increased by warming in grassland soil (Cheng, Zhang et al. 2017), indicating that both fresh and old C of grassland soil could be more instable under warming. Nonetheless, microbes are often dormanct in the natural environment (Jones and Lennon 2010), which may mask the linkages between total microbial communities and soil C dynamics (Wang, Jagadamma et al. 2015). Therefore, investigations into active microbial communities, which are actually responsible for soil C degradation, and their mechanistic linkages with C degradation under warming is necessary for predicting the future C balance of grassland ecosystems.

Here, we carried out a long-term *in situ* warming experiment on a tall-grass prairie ecosystem and a subsequent stable-isotope probing (SIP) laboratory experiment incubating the soil samples with ^{13}C-straw of *Avena fatua* (common wild oat), which is similar to many other herbal plant species in chemical composition of shoot (Mood, Golfeshan et al. 2013), to simulate the grass litter and label the active microbial community. Bacteria have a higher growth rate and a wider variety of environmental

niches than fungi, and its cellulases are often more complex providing a higher function and synergy in the degradation of cellulose (Sadhu and Maiti 2013, DeAngelis, Pold et al. 2015, López-Mondéjar, Zühlke et al. 2016), which is the top abundant component of the crop straw (Mood, Golfeshan et al. 2013). Therefore, we targeted the active community of bacteria responsible for litter degradation, and investigated how its abundance, structures and functions were changed by *in situ* warming using integrated metagenomic technologies. Combined with incubation C flux data, we attempted to establish explicit linkages between dynamics of active bacterial community and grassland ecosystem C cycling. We hypothesize that warming would aggravate instabilities of both fresh C (litter) and old C (SOC, via priming effect) by shifting the abundance, composition and C-degrading capacities of active bacterial community.

5.3 Materials and Methods

5.3.1 Site description and field measurements

The warming experiment was carried out in the tall-grass prairie of Kessler Atmospheric and Ecological Field Station (KAEFS) in McClain County, Oklahoma (34° 58' 44" N, 97° 31' 15" W). The grassland of KAEFS is dominated by C_3 forbs (*Ambrosia trifida*, *Solanum carolinense* and *Euphorbia dentate*) and C_4 grasses (*Tridens flavus*, *Sporobolus compositus* and *Sorghum halapense*). Based on Oklahoma Climatological Survey data from 1948 to 1999, the mean annual air temperature was 16.3 °C and the mean annual precipitation was 967 mm (McManus and Shafer 2002). The soil type of this site is Port-Pulaski-Keokuk complex, which is a well-drained soil that is formed in loamy sediment on flood plains (Li, Zhou et al. 2013). The soil texture class is loam with 51% of sand, 35% of silt and 13% of clay,

with a soil bulk density of 1.2 g cm^{-3} (Li, Zhou et al. 2013). The soil has a high available water holding capacity (37%), neutral pH and a deep (about 70 cm), moderately penetrable root zone (Xu, Sherry et al. 2013).

The experimental design of the site was established in July 2009. It artificially manipulates temperature and precipitation, within which a clipping factor is nested. Each treatment is randomly repeated 4 times for a total of 24 plots of 2.5 m × 3.5 m each. The whole ecosystem warming treatment is achieved by infrared heaters. In each warmed plot, 2 infrared heaters (165 cm × 15 cm; Kalglo Electronics, Bethlehem, PA, USA) are suspended 1.5 m above the ground to warm the area of 2.5 m × 1.75 m. The no-warming (control) plot has 2 "dummy" heaters with same dimensions as the infrared heaters suspended at a similar height to simulate the shading effect of the heaters.

Constantan-copper thermocouples wired to a Campbell Scientific CR10x data logger (Campbell Scientific Inc., Logan, UT, USA) were used to measure and record soil temperature every 15 min at 7.5, 20, 45 and 75 cm at the center of each plot. To represent the microclimate of the soil samples in this study, the annual average temperature data of year 2016 (the sampling year) at 7.5 cm depth was used for analyses. Soil volumetric water content from the soil surface to a 15-cm depth was measured once a month using a portable time domain reflectometer (SoilMoisture Equipment Corp., Goleta, CA, USA). Three measurements of soil moisture were performed in every plot and the annual average values of year 2016 were used for analyses. Above-ground plant biomass investigations were conducted at peak biomass (September as in this site) by a modified pin-touch method as described previously (Xu, Sherry et al. 2013).

5.3.2 Soil sample preparation and chemical measurements

The 8 samples used in this study were collected in September 2016 (peak plant biomass) from the 0–15 cm depth of 4 warmed plots and 4 control plots (that is, 4 biological replicates for warming or control). Therefore, the total of 8 soil samples used in this study had been subjected to a long-term warming or control of 7 years.

After soil sampling, visible roots (>0.25 cm) and stones were removed from the soil by 2-mm-mesh metal sieves (Hogentogler Co. Inc., Columbia, MD, USA), and thoroughly homogenized by manually physical mixing. All soil samples were then analyzed for soil chemistry by the Soil, Water, and Forage Analytical Laboratory at Oklahoma State University (Stillwater, OK, USA). The organic C and total N contents in soil were determined using a dry combustion C and N analyzer (LECO Corp., St. Joseph, MI, USA). Soil pH was measured at a water-to-soil mass ratio of 2.5:1 using an Accumet XL15 pH meter with a calibrated combined glass electrode (Accumet Engineering Inc., Westford, MA, USA).

5.3.3 SIP incubation and priming effect calculation

^{13}C- and ^{12}C-straw of common wild oat (*Avena fatua*, grown by Mary K. Firestone's lab, University of California, Davis, CA, USA), were used as stable-isotope probe substrate to simulate the grass litter deposition to soil. Oats were grown to maturity in a $^{13}CO_2$-enriched atmosphere as previously described (Bird and Torn 2006). The ^{13}C atom% of the harvested ^{13}C-straw was 75.1%, as determined by the Stable Isotope Facility, University of California, Davis, CA, USA. Three incubation groups, i.e. (1) with 0.1 g of ^{13}C-straw in 5 g of soil (2% w/w) as isotopic treatment, (2) with 0.1 g of ^{12}C-straw in 5 g of soil (2% w/w) as isotopic control, and (3) with 5 g of soil as the background, were set up for both *in situ* warmed and control samples. To ensure even

distribution in the soil, the 3 incubation groups were thoroughly stirred with steel spoons. Each replicate was sealed in a 25-ml lightproof bottle and incubated at 25 °C. Because we are interested in the field natures of the soil microbial communities, duration of the incubation was set as short-term (7 days) to minimize the impact of the incubation on microbial community structures. This short-tern duration could also minimize the cross-feeding among microbes thus increasing the reliability of the identification of active degraders.

Headspace gas was collected daily into 12-ml evacuated vials (Labco Limited, Lampeter, UK), after which the bottles were opened and refreshed for 30 min in a clean bench with the maximum flow of wind. To avoid gas contamination by the atmosphere, sampled gas was then diluted by injecting 10 ml of N_2 gas into each vial, generating a positive pressure to the atmosphere. $^{12}CO_2$ and $^{13}CO_2$ concentration were measured at the Stable Isotope Facility, University of California, Davis.

The percent of the CO_2-C derived from ^{13}C-straw was calculated as:

$$\%C_{substrate} = \frac{\delta_C - \delta_T}{\delta_C - \delta_L} \times 100\%$$

where δ_C is the $\delta^{13}C$ value of respired CO_2 from the soil with no straw added, δ_T is the $\delta^{13}C$ value of respired CO_2 from the soil with ^{13}C-straw, and δ_L is the $\delta^{13}C$ value of the ^{13}C-straw. The amount of SOC primed by straw was calculated as total soil respiration after straw addition minus the amount of C respired from straw, and then minus the amount of C respired from the soil with no straw added.

5.3.4 Soil DNA extraction

After the 7-day incubation, soil DNA was extracted following the method of liquid N grinding method (Zhou, Bruns et al. 1996) followed by PowerMax Soil DNA Isolation Kit (MO BIO Laboratories, Inc., Carlsbad, CA, USA) according to the

manufacturer's protocol. DNA quality was assessed based on spectrometry absorbance at wavelengths of 230 nm, 260 nm and 280 nm by a NanoDrop ND-1000 Spectrophotometer (Thermo Fisher Scientific, Waltham, MA, USA). The absorbance ratios of 260/280 nm were all larger than 1.8 and 260/230 nm were about 1.7. The extracted DNA was quantified by PicoGreen using a FLUOstar OPTIMA fluorescence plate reader (BMG LabTech, Jena, Germany). PicoGreen showed that the DNA concentration extracted were 49.1 ± 2.6 ng/µl, with no significant difference among treatments or isotopic treatments. Soil DNA were then stored at -80 °C for further analyses.

5.3.5 Density-gradient ultracentrifugation of soil DNA

To reveal the effect of ^{13}C-straw incubation on soil DNA density, density-gradient ultracentrifugation was performed according to a previous protocol with minor modifications (Neufeld, Vohra et al. 2007). In brief, we centrifuged 5.1 ml of a solution composed of 3.6 µg of soil DNA (the minimum of total DNA amounts across all samples), 1.90 g ml^{-1} cesium chloride (CsCl) (MP Biomedicals, Santa Ana, CA, USA), and gradient buffer (1 mM EDTA, 0.1 M KCl, 0.1 M Tris-HCl), reaching a final density of 1.725 g ml^{-1}. The solution was sealed in a polyallomer centrifuge tube (cat. No. 342412, Beckman Coulter, Brea, CA, USA) with a cordless tube topper, and centrifuged on a Vti 65.2 rotor of an Optima L-XP ultracentrifuge (Beckman Coulter, Brea, CA, USA) at 177,000 g and 20 °C for 48 hours. Solution from each centrifuged tube was then separated into twenty-four 220-ml fractions (14 drops per fraction). The buoyant density of each fraction was determined by an AR200 digital refractometer (Reichert, Depew, NY, USA). DNA in each fraction was then precipitated with 20 µg

of glycogen and 2 volumes of PEG solution (30% PEG 6000 and 1.6 M NaCl), washed with 70% ethanol, and re-suspended in 35 µl of ultrapure water.

5.3.6 Quantitative PCR of 16S rRNA genes

Quantitative PCR (qPCR) was used to determine absolute abundances of 16S rRNA genes in each fraction. Universal primers 515F (5'-GTGCCAGCMGCCGCGGTAA-3') and 806R (5'-GGACTACHVGGGTWTCTAAT-3') were used for targeting the V4 region of the 16S rRNA genes. qPCR was performed in triplicate 20-µl reactions containing 10 µl of SsoAdvanced Universal SYBR Green Supermix (Bio-Rad, Hercules, CA, USA), 350 nM of each primer and 1 µl of template, using a thermocycler program of 35 cycles of 95 ℃ for 20 sec, 53 ℃ for 25 sec and 72 ℃ for 30 sec on an IQ5 Multicolor Real-time PCR Detection System (Bio-Rad, Hercules, CA, USA). Gene abundances (copy numbers) were determined by a standard curve constructed with 16S rRNA gene segment of *E. coli* JM109 competent cells and TA cloning vector (Promega, Madison, WI, USA).

5.3.7 Amplicon sequencing of 16S rRNA genes

A two-step PCR was performed to generate amplicon libraries of 16S rRNA genes (Wu, Wen et al. 2015). In brief, the first step of the V4 region of 16S rRNA genes was amplified by the primer 515F and 806R in triplicate 25-µl reactions containing 2.5 µl of 10× AccuPrime PCR buffer containing dNTPs (Invitrogen, Grand Island, NY, USA), 0.2 µl of AccuPrime High-Fidelity Taq Polymerase, 1 µl of 10 µM forward and reverse primer, and 10 ng of template DNA. The thermocycler program was as follows: 94 ℃ for 1 min, 10 cycles of 94 ℃ for 20 sec, 53 ℃ for 25 sec and 68 ℃ for 45 sec, and a final extension at 68 ℃ for 10 min. Bead purification was used to

retrieve the amplicons generated by the first step using AMPure XP magnetic particles (Agencourt Bioscience Corp., Beverly, MA, USA) with a 1:1 volume to the reactions. The second step of PCR also used triplicate 25-µl reactions, with each containing 2.5 µl of 10× AccuPrime PCR buffer containing dNTPs, 0.2 µl of AccuPrime High-Fidelity Taq Polymerase, 1 µl of 10 µM 515F and 806R primer combined with the Illumina adaptor sequence (a pad and a linker of two bases, and a unique barcode sequence on the reverse primer), and 15 µl of purified PCR product of the first step. The thermal cycling condition was the same as the first step except a cycle number of 20. Triplicate PCR products from the second step were combined, examined for band of 16S rRNA genes by agarose gel electrophoresis, and quantified by PicoGreen.

PCR products from all fractions were pooled at equal molarity and sequenced in the same MiSeq run as described previously (Zhou, Deng et al. 2016). The raw sequence reads underwent PhiX removing, assigning to corresponding samples according to barcodes with 0 mismatches, and trimming primers using a pipeline built on the Galaxy platform (http://zhoulab5.rccc.ou.edu:8080/). Next, high-resolution amplicon sequence variants (ASVs) with sequencing error filtered were identified from the reads using the DADA2 procedure (Callahan, McMurdie et al. 2016), with the package dada2 (v.1.12) on R software (v.3.5.2). The ASV table including all fractions was randomly resampled to the absolute abundance of 16S rRNA genes revealed by qPCR. Representative sequence of each ASV was annotated through Ribosomal Database Project (RDP) classifier (http://rdp.cme.msu.edu/classifier/classifier.jsp) with a confidence score of 50% (Wang, Garrity et al. 2007). Copy numbers of 16S *rrn* genes were also annotated through RDP classifier.

5.3.8 Identification of active degraders of straw

Active degraders of straw was identified following qSIP, a cutting-edge quantitative stable-isotope probing analysis method (Hungate, Mau et al. 2015) with minor modifications. Briefly, for an ASV (say ASV *i*), the density weighted by the absolute abundance determined by 16S rRNA genes sequencing and qPCR was calculated for both ^{13}C- and ^{12}C-straw incubated samples. The density shift (difference of density) of ASV *i* between ^{12}C-straw incubated sample and ^{13}C-straw incubated sample was calculated for all 4 biological replicates, and a 90% confidence interval (CI) was calculated for the density shift using bootstrap method with the package boot (v.1.3-22) in R software. ASV *i* would be considered as active degrader if the lower bound of the bootstrapped 90% CI of the density shift was above zero.

5.3.9 Determination of functional potentials using GeoChip microarray

Functional potentials of active community were determined by GeoChip 5.0S, a high-throughput microarray designed for investigations into microbial community functional profiles (Van Nostrand, Yin et al. 2016). Four fractions of each ^{13}C-straw incubated sample were selected and regarded as representative for active communities. The criterion of selection is that, if the 16S rRNA gene copies of the corresponding ^{12}C-straw-incubated samples at the densities of the fractions were close to zero, they would be regarded as the fractions of active communities (Figure S19). Approximately 50 ng of DNA separated from heavy fractions in warming or control samples were amplified using a Templiphi kit (GE Healthcare, little Chalfont, UK). The amplified DNA (2 μg) was labelled with fluorescent dye (Cy-3) dUTP using random primers and Klenow fragment of DNA polymerase I at 37 °C for 6 h,

followed by heating at 95 °C for 3 min. Labelled DNA for each sample was then purified with QIAquick PCR purification reagents (Qiagen) and SpinSmart columns (Denville at Thomas Scientific Inc., Swedesboro, NJ, USA), dried in a SpeedVac at 45 °C for 45 min, and resuspended in 43.1 µl of hybridization buffer containing 27.5 µl of 2× HI-RPM hybridization buffer, 5.5 µl of 10× CGH blocking agent, 2.4 µl of cot-1 DNA, 2.2 µl of universal standard and 5.5 µl of formamide. DNA was hybridized with GeoChip 5.0S (60K) in a SL incubator (Shel Lab, Cornelius, OR, USA) at 67 °C and 20 rpm for 24 hours. Then GeoChip arrays were washed and scanned by an MS 200 Microarray Scanner (Roche, Basel, Switzerland) at 532 nm and 635 nm. Raw signals from the scanning were processed by an online pipeline (http://ieg.ou.edu/microarray/) as previously described (Yang, Wu et al. 2013). Response ratio of signal intensities to warming was calculated as $\ln(I_{warming}/I_{control})$, where $I_{warming}$ and $I_{control}$ are the signal intensities of C-degrading genes of warmed and control samples.

5.3.10 Determination of carbohydrates utilization capacity using Biolog EcoPlates

Biolog EcoPlates (Biolog Inc., Hayward, CA, USA) containing 31 different labile carbon sources (and a control well with no carbon source) were used to assess the carbohydrates utilization capacity of soil microbial communities after the soil was sampled from the field site and stored in 4 °C for 1 day (before the SIP incubation). For each soil sample, 0.5 g of soil was mixed with 45 ml of 0.85% NaCl solution, shaken for 20 min at 180 rpm, and settled at 4 °C for 30 min. Subsequently, 1500 µl of supernatant was mixed with 13.5 ml of distilled water and added onto Biolog EcoPlates with 100 µl of supernatant per well. Then the Biolog EcoPlates were continuously incubated and read for 4.5 days using a Biolog Omnilog PM incubator

(Torcon Instruments Inc., Torrance, CA, USA) at 25 °C. The color changes of the wells were transmitted to absorbance-time curves. Area under the curves was calculated to represent utilization capacities of various C sources (Guckert, Carr et al. 1996).

5.3.11 Statistical and phylogenetic analyses

Most statistical analyses were performed in R software (version 3.5.2), such as difference among 16S rRNA gene abundances determined by permutation *t*-test conducted by the package Deducer (v.0.7-9), difference of respiration and priming effect determined by repeated measures ANOVA conducted by the package vegan (v.2.3-2), and linear models detecting correlations among microbial communities and C fluxes conducted by the package stats (v.3.5.2) and subsequently tested for significance by permutation tests with the package lmPerm (v.2.1.0). Unless otherwise stated, mean values are given ± standard error of the mean, and values of $p \leq 0.050$ were considered as significant.

The maximum likelihood phylogenetic tree was constructed based on the representative sequence for each active ASV. Previously reported cultured species of >99.6% 16S rRNA gene nucleotide identity with the 6 top abundant active ASVs was obtained from the nucleotide BLAST on NCBI (https://blast.ncbi.nlm.nih.gov/BlastAlign.cgi) and anchored into the tree as reference species. MEGA 6.05 (Hall 2013) was used to construct the phylogenetic tree with MUSCLE alignment, maximum likelihood method, and a bootstrap of 1,000 times. The visualization of the tree was generated by iTOL (http://itol.embl.de/) (Life 2011). Beta nearest taxon index (βNTI) was calculated by an online pipeline

(http://ieg3.rccc.ou.edu:8080/) as the phylogenetic β-diversity among samples (Stegen, Lin et al. 2012).

5.4 Results

5.4.1 Edaphic factors

The *in situ* warming significantly ($p < 0.001$) increased average soil temperature of year 2009–2016 by 2.2 °C (from 17.4 ± 0.2 °C to 19.6 ± 0.5 °C, Table S7), indicative of an effective experimental warming treatment. Warming did not significantly change other edaphic factors. Average C content of the sampled soils was 0.843 ± 0.043%, and average N content was 0.092 ± 0.004 (Table S7). Annual volumetric water content of year 2016 was lower under warming (10.02 ± 0.98%) than under control (11.75 ± 1.17%), albeit insignificantly ($p = 0.365$). Warming halved the aboveground plant biomass from 204.9 ± 60.6 g m^{-2} to 107.2 ± 22.7 g m^{-2} ($p = 0.239$) at the peak of plant biomass (September) of year 2016.

5.4.2 Warming enlarged and activated soil bacterial community

After the 7-day incubation with straw, compared to the ^{12}C-straw incubated soils, a considerable amount of 16S rRNA gene abundance shifted to heavier densities in the ^{13}C-straw incubated soil (Figure S19), suggestive of an effective labeling of SIP experiment. A total of 7,945 16S rRNA gene ASVs were identified across all samples and fractions. Among them, 147 ASVs was identified as active degraders of straw, accounting for 59.7% of the total bacterial abundance, indicating that the majority of the bacterial community was active. As determined by qPCR of 16S rRNA genes, the *in situ* warming significantly increased the abundance of the active community after straw addition by 50.9% (Figure 14a), and significantly increased the abundance of

total bacterial community after straw addition by 44.9% (Figure 14b), indicative of a considerable effect of warming on both active and total bacterial communities in grassland topsoil.

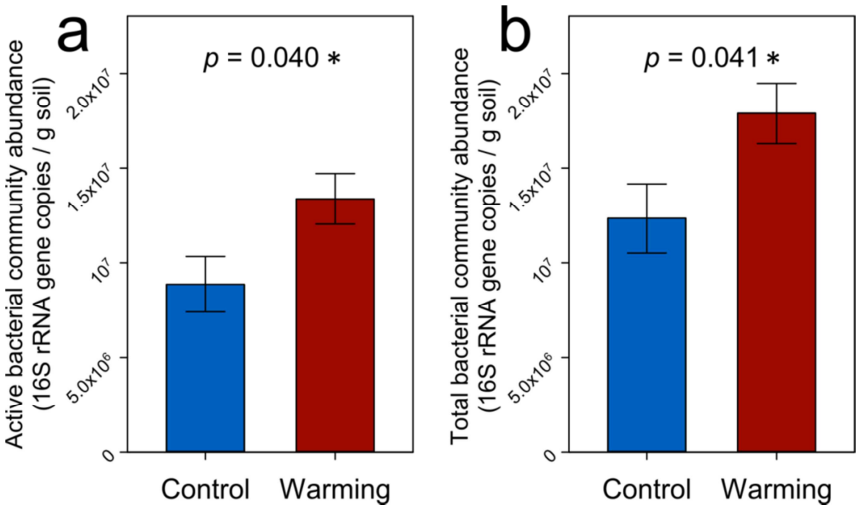

Figure 14. Absolute abundances of 16S rRNA genes of (a) active bacterial community and (b) total bacterial community of *in situ* warmed or control soils, after the 7-day incubation with plant litter. Each column represents average ± standard error of n = 4 biological replicates of *in situ* warming or control. Significances are indicated using * as $0.010 < p \leq 0.050$ as determined by permutation t-tests.

Among the 147 active bacterial ASVs, 121 ASVs were active under both warming and control, accounting for 33.8% of the total bacterial abundance. There were 21 ASVs active under warming but inactive under control, which accounted for 25.6% of total bacterial abundance, indicating a strong activation effect on previously inactive taxa by warming. Among the 21 ASVs that were only active under warming, 9 belonged to the phylum *Firmicutes* (Figure 15), occupying for 72.3% of the 21 degraders' abundance (or 18.5% of total bacterial abundance), implying a consistency between the lineage and ecological strategy of *Firmicutes*. On the other hand, only 5 bacterial ASVs among the total 147 were inactivated by warming, accounting for 0.2% of the total bacterial abundance. In addition, *Firmicutes* also possessed the highest copy numbers of *rrn* genes (Figure 15), indicating a faster response to resource input (Klappenbach, Dunbar et al. 2000).

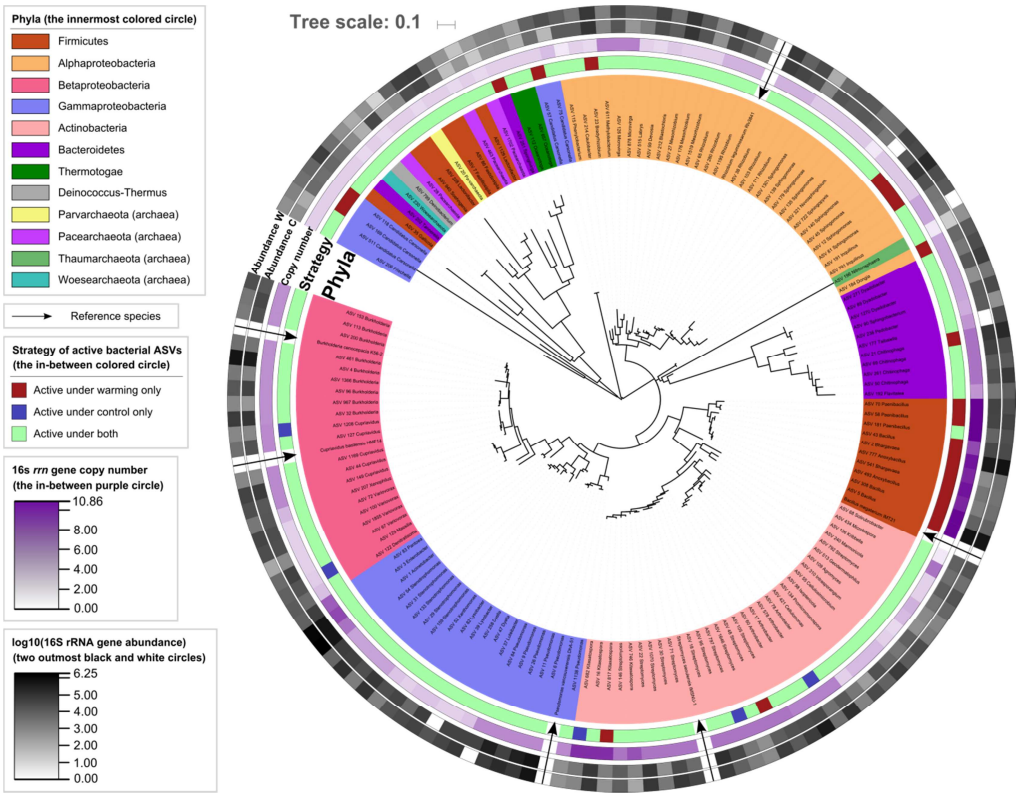

Figure 15. The maximum-likelihood phylogenetic tree of active bacterial ASVs (degraders). Abbreviations: W, *in situ* warmed samples; C, *in situ* control samples.

Beyond the abundance, warming also significantly increased the phylogenetic β-diversity (shown as weighted βNTI) among active bacterial communities (Figure S20a), indicative of a divergent succession pattern and thus more unpredictable dynamics of active bacterial communities under warming. On the contrary, warming did not significantly change the phylogenetic β-diversity among total bacterial communities (Figure S20b), indicative of a less divergent succession of the total bacterial communities under warming.

5.4.3 Warming enhanced C-degrading potentials of active community

To examine the C-degrading potential of the active community, genes involved in C degradation were quantified by GeoChip 5.0 experiment on the DNA fractions of

active communities. Among the total of 45 detected C-degrading genes, response ratios of 15 genes to warming showed significantly positive values, spanning both biologically labile and recalcitrant C (Figure 16), indicative of a general stimulation on the C-degrading genes of the active community by warming.

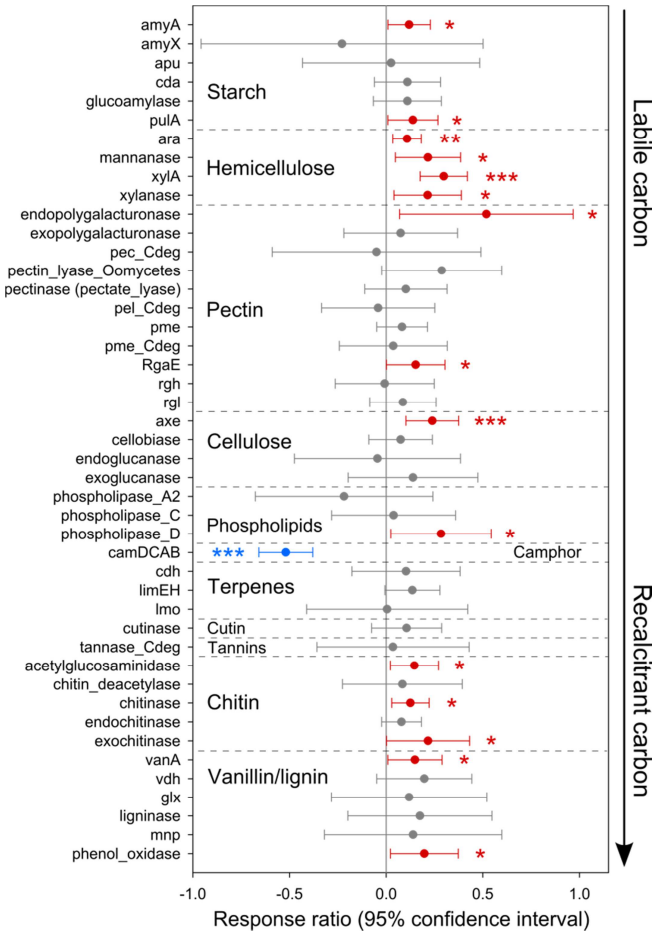

Figure 16. Response ratios of GeoChip signal intensities of active community C-degrading genes to *in situ* warming. Each symbol represents average ± standard error of $n = 4$ biological replicates of *in situ* warming or control. Red symbols represent significantly positive response ratios, and blue symbols represent significantly negative response ratios. Significances are indicated using * as $0.010 < p \leq 0.050$, ** as $0.001 < p \leq 0.010$, and *** as $p \leq 0.001$ as determined by confidence intervals.

Specifically, regarding that cellulose, hemicellulose and lignin are the top 3 abundant components of oat straw we added to the soil (Mood, Golfeshan et al. 2013), the gene *axe* encoding acetyl esterase, which is involved in cellulose degradation, was

significantly stimulated by warming (Figure 16). Similarly, the phenol oxidase was also significantly stimulated by warming, which is involved in lignin degradation. For genes involved in hemicellulose degradation, all 4 detected genes (xylanase, mannanase, *ara* encoding L-arabinose operon, and *xylA* encoding xylose isomerase) were significantly stimulated by warming, implying that in this short-term (7-day) incubation, the active community was very active on the degradation of hemicellulose, which is a biologically labile component of oat straw compared to cellulose and lignin. Among the C-degradation genes belonging to active *Firmicutes* species, *xylA* encoding xylose isomerase, *pme* encoding pectin methylesterase, and *vdh* encoding vanillin dehydrogenase were significantly stimulated by warming, which belong to categories hemicellulose, pectin, and vanillin respectively (Figure S21).

Additionally, Biolog EcoPlates were used to assess the capacity of carbohydrates utilization of soil microbial communities before the 7-day SIP incubation. Interestingly, microbial utilization capacity of xylose, a major component of hemicellulose xylan, showed a significantly positive response ratio to warming (Figure S22), suggestive of a higher capacity of hemicellulose degradation, which is consistent with the significantly positive response ratio of the *xylA* gene to warming (Figure 16).

5.4.4 Warming increased soil C-degrading activity and priming effect

To assess the actual C-degrading activities of soil microbial communities, we calculated soil respiration and priming effect on SOC during the 7-day SIP incubation with straw. In concert with the stimulated C-degrading potential by warming, soil respiration of warmed samples was significantly higher than control samples by 13.3% (Figure 17). Notably, the priming effect on SOC of warmed samples was also

significantly higher than control samples by 14.4% (Figure 17), indicative of a stimulation of warming on SOC degradation when fresh C was deposited. Regarding the data of individual days of the incubation, significant differences between warming and control were observed in the last 4 days instead of the first 3 days, suggestive of a stably stimulated SOC degradation by warming in the long term. Notably, the respiration deriving from the straw significantly and positively correlated with the total signal intensity of hemicellulose-degrading genes of active communities (Figure S23).

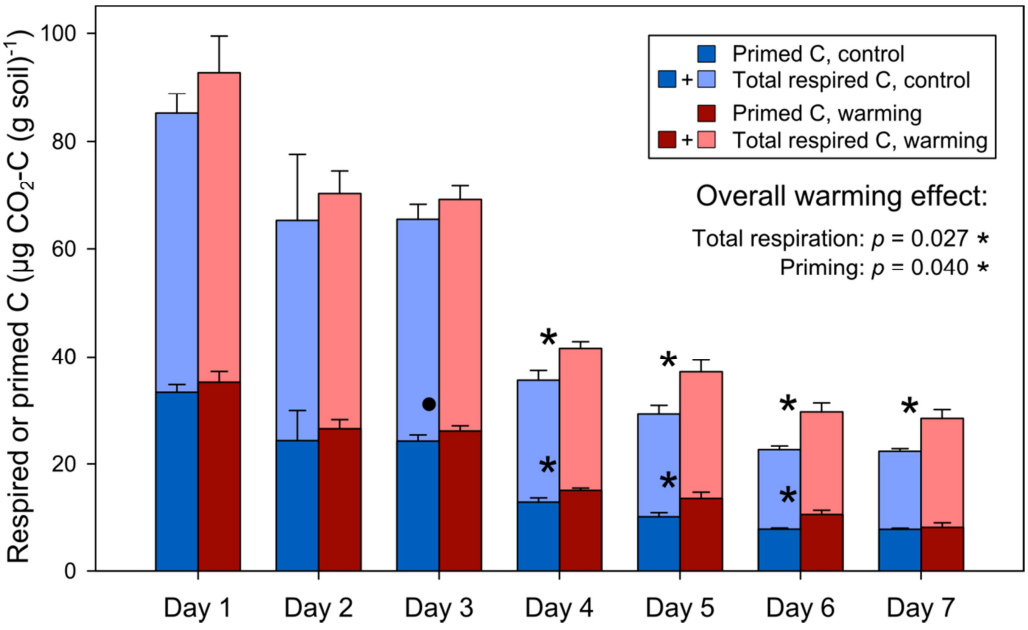

Figure 17. Soil daily respiration and priming effect during the 7-day incubation with plant litter. Each column represents average ± standard error of n = 4 biological replicates of *in situ* warming or control. Significances are indicated using · as $0.050 < p \leq 0.100$ and * as $0.010 < p \leq 0.050$ for total respiration or priming effect, as determined by permutation t-tests (individual days) or repeated measures ANOVA (overall warming effect).

5.5 Discussion

Our results showed that both soil respiration and priming effect on SOC were significantly higher in warmed soils than control during the 7-day incubation (Figure

17), leading to the concern that the topsoil microbial community of tall-grass prairie may serve as a positive feedback to climate warming. Topsoil SOC is vulnerable to microbial degradation under warming (Yergeau, Bokhorst et al. 2012, Karhu, Auffret et al. 2014, Crowther, Todd-Brown et al. 2016), and stimulations of warming on soil C emissions have been reported (Zhou, Xue et al. 2012, Yue, Wang et al. 2015, Carey, Tang et al. 2016). Our results have provided underlying microbial structural mechanisms, such as enhanced active bacterial abundance by warming (Figure 14). Higher active bacterial abundance has been reported as concomitant with higher soil respiration and priming effect in tundra soil (Tao et al. 2019). In contrast, reduced active microbial biomass by warming have also been reported in forest (Liu, Zhang et al. 2009) and semiarid grassland (Frey, Drijber et al. 2008) with soil C emissions unchanged, probably due to the stress from excessively dry conditions driven by warming. Therefore, the tall-grass prairie may serve as an advantageous environment for bacterial C degradation and thus providing a positive feedback to climate warming, where the enhanced active bacterial abundance could be one of the underlying structural mechanisms.

In the compositional angle, warming activated a lot of previously inactive taxa (21 ASVs, 25.6% of total bacterial abundance), suggestive of a compositional change of active communities, and thus an irreversible contribution to the positive feedback to climate warming driven by microbial communities. Most activated taxa belonged to the phylum *Firmicutes* (Figure 15), occupying for 72.3% of the activated abundance, implying a consistency between microbial lineage and strategy of activity for *Firmicutes*. Habitat preference of microbes has been observed as consistent with phylogenetic coherence (Von Mering, Hugenholtz et al. 2007, Hartman, Lough et al. 2009). For example, microbial resuscitation strategies to wetting after long-term

drying are deeply rooted in phylogenetic groups (Placella, Brodie et al. 2012). These studies analogously support the consistency between lineage and functional strategies in response to environmental changes. Interestingly, a mechanistic study in the same site of our study has shown that *Firmicutes* was the most stimulated phylum by warming due to the warming-induced selective stresses such as increased drought and reduced plant productivity (Daliang Ning et al., iCAMP). The order *Bacillales* (accounting for 73.6 ± 3.6% of abundance of the activated *Firmicutes* in our study) of *Firmicutes* can form endospores (Logan and Vos 2015) and is thus more competitive under selective stresses such as warming. The high *rrn* gene copy numbers of *Firmicutes* (the in-between purple circle of Figure 15) implies a more rapid response to resource input than other taxa (Klappenbach, Dunbar et al. 2000). Our observations after the input of straw indicate that warming may activate and promote such rapid responses of *Firmicutes* to resource input, leading to the compositional change and enlargement of active communities.

The increased microbial C-degrading potentials were the functional basis of the positive feedback to warming (Figure 16). Among the increased potentials, it is notable that all genes in the category of hemicellulose were significantly stimulated, including genes involved in both hydrolysis (xylanase) and monomer degradation (mannanase, *ara*, and *xylA*), suggestive of a larger contribution of hemicellulose than other SOC categories to the respiration (Figure S23), which also explains the observed faster utilization of xylose under warming (Figure S22). Hemicellulose is the second abundant component of the oat straw (~27% w/w, only less than cellulose) and is also a biologically labile component (Mood, Golfeshan et al. 2013). This relative lability of hemicellulose to degradation is consistent with the short duration of our incubation (7 days) and the rapid-responding nature of *Firmicutes* to resource

input (Klappenbach, Dunbar et al. 2000, Roller, Stoddard et al. 2016) under warming. In addition to hemicellulose degradation, *Firmicutes* has also been identified as effective in degrading cellulose (Desvaux 2005). However, *Bacillales* species of *Firmicutes* have been reported as capable for degrading more recalcitrant C compounds: strain IMT21 of *Bacillus megaterium*, a reference strain for *Bacillales* ASVs in the active community tree (Figure 15) possessing a 100% nucleotide identity with ASV-5, is efficient in degrading dichloroaniline, which is an aromatic compound (Yao, Khan et al. 2011); strain TN41 and TN42 of *Bacillus* sp., possessing >99.2% nucleotide identities with ASV-5, are capable of degrading many aromatic compounds including phenol, toluene, biphenyl and naphthalene (Đokić, Narančić et al. 2011). For the active communities overall, warming also promoted the degrading potentials of more recalcitrant C including chitin (chitinase and exochitinase), vanillin (*vanA*) and lignin (phenol oxidase) (Figure 16), indicative of a more comprehensive microbial C-degrading capability than hemicellulose degradation, which may contribute to a stronger positive feedback to climate warming.

Warming increased the phylogenetic β-diversity (βNTI) among active bacterial communities (Figure S20). Another study on this site has revealed the increasingly divergent succession of microbial communities under warming over time (Guo, Feng et al. 2018). Studies in Alaska tundra have observed increased dissimilarities among diazotrophic (Feng, Penton et al. 2019) and total bacterial communities (Feng et al., CiPEHR paper) under warming. Transplanting agricultural soils to warmer regions also increased the β-diversity among soil bacterial communities (Liang, Jiang et al. 2015). These studies collectively suggest that the divergent succession of bacterial communities under warming might be a ubiquitous phenomenon. The divergent

successional trajectories of active bacterial communities in grassland soil may lead to less predictable dynamics of the soil microbial positive feedback to climate warming.

Our study unveiled a comprehensive stimulation of warming on active bacterial communities of grassland soil in terms of abundance, functional potentials, and C-degrading rates of both resource input and SOC, indicative of an exacerbated positive feedback to climate warming. This stronger positive feedback could be irreversible because warming also caused the compositional change of active bacterial communities, where the major taxon turned into active, *Firmicutes*, could be efficient in the degradations of both biologically labile and recalcitrant C compounds. Moreover, the warming-induced divergent turnovers of active bacterial communities may lead to less predictable dynamics of the responsible microbial communities, and thus larger difficulties in projections for the magnitudes of this positive feedback. Further research should be devoted to examine whether the alarming changes and activations of soil bacterial communities induced by warming identified in this study are generalizable to other ecosystems.

5.6 Author contributions

J.Z., Y.Y. and J.F. developed the original concepts. X.T., J.F. and X.Z. carried out the 7-day incubation, headspace gas analysis and 16S rRNA gene amplicon experiment. X.T. performed the GeoChip hybridization experiment. X.G. performed the BioLog EcoPlate experiment. J.F. and X.T. analyzed experimental data and carried out statistical analyses. J.F., Y.Y. and X.T. wrote the paper. X.G. and J.Z. edited the manuscript. All authors were given the opportunity to review the results and comment on the manuscript.

Chapter 6**: Summary and output**

This dissertation provided several lines of field and lab evidence in supporting that the soil bacterial/diazotrophic community could be influenced by climate warming with changes in their community compositions, functional potentials, activities, interactions among themselves, interactions with environmental factors, and overall feedbacks to the warmer climate. This dissertation presented valuable observations of these profiles in terms of both total and active soil microbial communities, and compared tundra and grassland soil microbial communities. Findings of this work could be valuable arguments and implements for comprehensive and mechanistic understanding of ecosystem models in predicting future climate conditions and element cycling.

Overall, warming considerably altered soil bacterial communities, whose compositions or functional potentials were correlated to different warming-induced changes of environmental factors, but different ecosystems and taxonomic groups still exhibited distinct patterns of responses. The responses of total bacterial communities in Alaska tundra soil to warming were closely related to environmental factors, especially with thaw depth, soil moisture and aboveground plant biomass. Although less altered by warming in compositions, diazotrophic communities in Alaska tundra were highly enlarged by warming, indicating an important mechanism for supplementing biologically available N in the tundra system, and similarly, the responses of diazotrophic communities to warming were also related to soil moisture, soil thaw, and aboveground plant biomass. Our observations on soil active bacterial communities illustrated that lignin decomposing bacterial communities in Alaska tundra soil were enlarged by warming, and the major responsible taxonomic groups were *Burkholderia* (genus) and *Alphaproteobacteria* (class) species. However in

Oklahoma grassland soil, the active bacterial communities were *Firmicutes* (phylum) species instead. Functional potentials, especially signal intensities of C decomposing genes of both total and active microbial communities were generally enhanced by warming, and functional potentials of N fixing genes (*nifH*) were also stimulated by warming, indicating a generally activated metabolism and element cycling among microbially-mediated ecological processes.

This dissertation presented comparisons of taxonomic and functional profiles between soil total bacterial and diazotrophic communities in Alaska tundra, which is a crucial ecosystem in global C and N balances. We observed that, although the composition of diazotrophic communities were less altered than the total bacterial community (only significant altered in one soil layer), its abundance was enlarged by 86.3%, indicating an important mechanism for supplementing biologically available N in this tundra ecosystem, and thus an potential negative feedback to climate warming through the C fixation of plants. On the other hand, ecosystem respiration and methane flux were both significantly enhanced by warming in Alaska tundra, which strongly correlated with microbial community functional structures, indicating a positive feedback to the climate warming through microbial C decomposition. In addition, both total bacterial and diazotrophic communities were shaped by similar environmental factors, which were soil moisture, thaw depth, and aboveground plant biomass. Together, the observed positive value of net ecosystem exchange showed an overall C sink, which suggests that the C loss through ecosystem respiration was temporarily offset by plant C fixation.

However, we cannot expect long-term overall C sink in the Alaska tundra ecosystem because we have observed compositional succession and enlargement of the responsible active bacterial communities decomposing lignin under warming, a

major biologically recalcitrant component of Alaska tundra soil C, which implies an irreversible change of C decomposing communities under warming. These community changes also collectively doubled the priming effect, i.e., decomposition of existing C after fresh C input to soil. Consequently, warming alarmingly aggravated soil C instability as verified by microbially-enabled Climate-C modeling. In addition, we observed a more divergent succession of all of total bacterial communities, diazotrophic communities, and active lignin decomposing communities under warming, indicating a large difficulty in projections to the future dynamics of soil microbial communities and thus their feedbacks to warming.

Then, by comprehensive ecosystem and microbial analyses, we also focused on the research question whether different ecosystems, in this case Alaska tundra and Oklahoma grassland soils, respond similarly or differently to climate warming in terms of active decomposers of C input. Generally, active bacterial communities of Alaska tundra and Oklahoma grassland soils responded similarly to climate warming, in that their abundance were both enlarged by warming, their compositions were both altered by warming, and their microbial decomposition of both new and old C were enhanced by warming. The major difference of the two ecosystems was that the major taxonomic groups activated by warming were different, in that in tundra soil the *Alphaproteobacteria* species were activated, while in grassland soil the *Firmicutes* species were activated. In addition, the grassland soil active bacterial communities showed a consistency between the lineage and ecological strategy of *Firmicutes* when subjected to warming, while the tundra soil did not show explicit consistencies.

The subject of microbial ecology is a developing branch of science which is still in the stage of the accumulation of observation and attempts. The understanding of both the total microbial communities and their interactions with the earth's

environment, life and human beings are still uncertain and vague. As a small part exploring outside our existing knowledge, this dissertation provided novel insights into the future of soil microbes and their interactions to climate warming in a warmer world.

Below is the list of manuscripts related to this dissertation. Chapter 3 in this dissertation presented contents in the published journal article 1 below. The Publishers of the journals granted the author to re-use these published materials in this dissertation by copyright policies.

Peer reviewed journal papers published:

1. **Feng, J.**, Penton, C. R., He, Z., Van Nostrand, J. D., Yuan, M. M., Wu, L., ... & Schuur, E. A. (2019). Long-Term Warming in Alaska Enlarges the Diazotrophic Community in Deep Soils. ***mBio***, 10(1), e02521-18.
2. Guo, X.*, **Feng, J.***, Shi, Z., Zhou, X., Yuan, M., Tao, X., ... & Zhou, A. (2018). Climate warming leads to divergent succession of grassland microbial communities. ***Nature Climate Change***, 8(9), 813.

Manuscripts in preparation:

3. **Feng, J.***, Wang, C.*, Yang, Y., Yan, Q., Zhou, X., Tao, X., … & Zhou, J. Warming-accelerated thaw of permafrost-based tundra exacerbates soil carbon loss by restructuring the microbial community. ***Microbiome***. In review
4. Tao, X.*, **Feng, J.***, Fan, F., Yang, Y., Ning, D., Wu, L., He, Z., Van Nostrand, D. J., … & Zhou, J. Warming exacerbates tundra soil lignin decomposition governed by Proteobacteria. ***The ISME Journal***. Submitted

5. **Feng, J.**, Zou, D., Wu, L., Van Nostrand, D. J., He, Z., Yuan, M., Qin, Y., Shi, Z., and Zhou, J. Reproducibility of experimental workflows of MiSeq amplicon sequencing and GeoChip functional microarray. In preparation
6. **Feng, J.***, Tao, X.*, Wang, G., Zhou, X., and Zhou, J. Climate warming promotes grassland soil C degradation through enlarging and restructuring active bacterial communities. In preparation

Appendix A: Supplementary Figures

Figure S1 to **Figure S5** for Chapter 2: Warming-accelerated thaw of permafrost-based tundra exacerbates soil carbon loss by restructuring the microbial community

Figure S6 to **Figure S11** for Chapter 3: Long-term warming in Alaska enlarges the diazotrophic community in deep soils

Figure S12 to **Figure S18** for Chapter 4: Warming exacerbates tundra soil lignin decomposition governed by *Proteobacteria*

Figure S19 to **Figure S23** for Chapter 5: Warming exacerbates grassland soil carbon degradation through activating *Firmicutes*

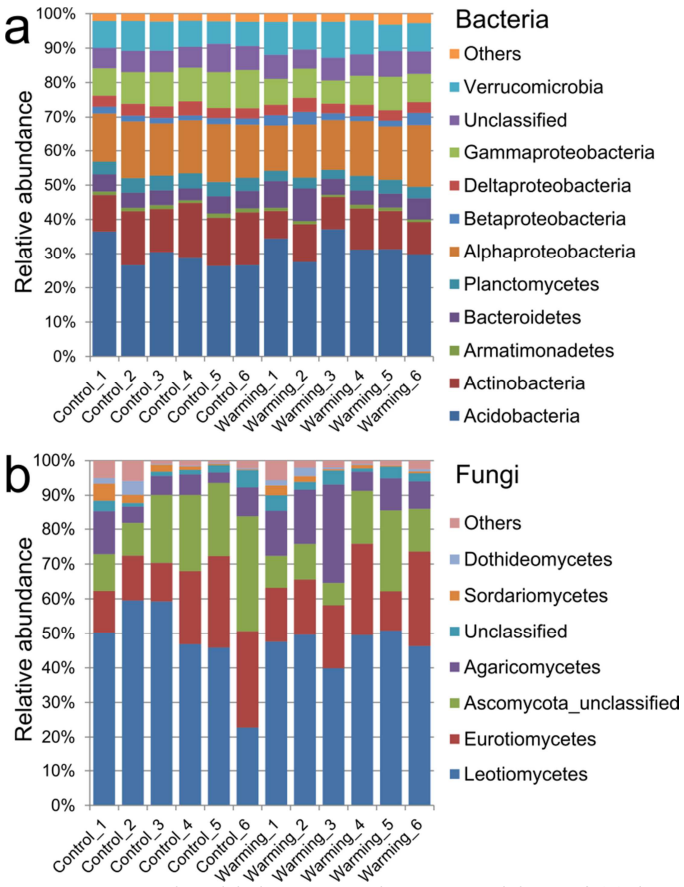

Figure S1. Microbial taxonomic composition of (a) bacterial communities and (b) fungal communities at the phylum level (for bacterial communities, *Proteobacterial* Classes are juxtaposed with other Phyla). Phyla with abundance less than 1% were combined to Others.

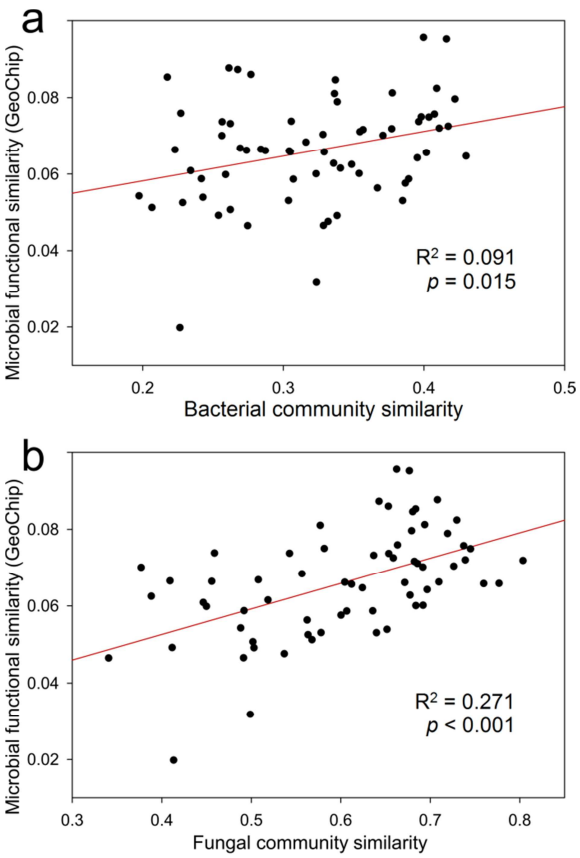

Figure S2. The linear regressions between pairwise similarities of (a) bacterial community composition and functional structure (GeoChip data), and (b) fungal community composition and functional structure. The black circles represent the 66 pairs of similarities generated from the 6 warming and 6 control samples. Bray-Curtis distance was used for the similarity calculations.

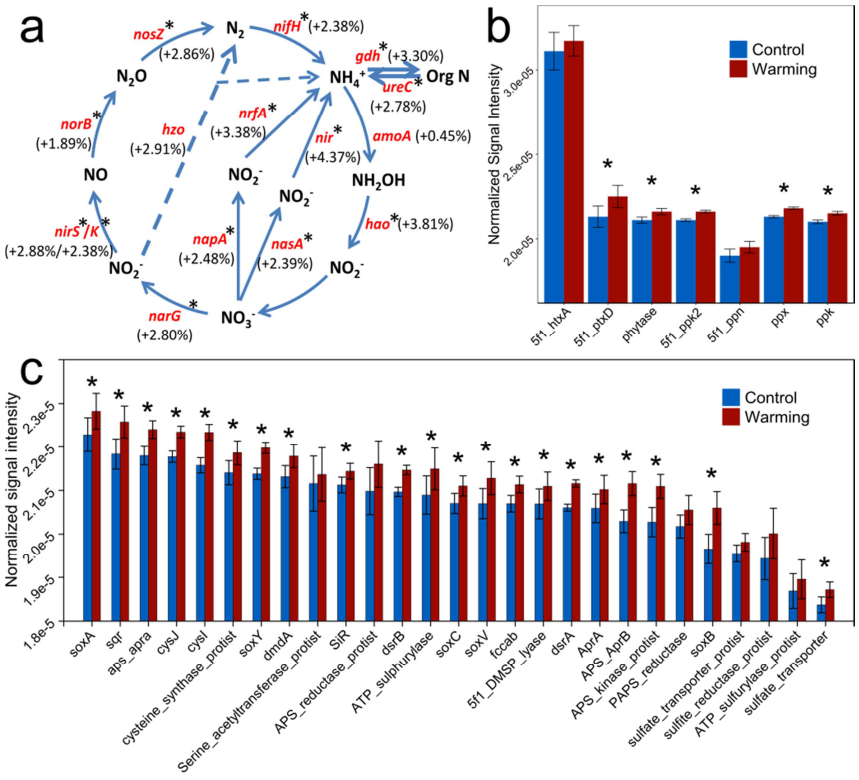

Figure S3. Differences of average normalized signal intensities (GeoChip data) of representative genes involved in (a) nitrogen cycling, (b) phosphorus cycling, and (c) sulfur cycling. Red gene names represent genes with a higher average normalized signal intensity in warming samples, percentage of increase indicated in parentheses. Blue bars represent the average normalized signal intensity of gene probes in control samples; red bars represent warming samples. Error bars represent standard error of the mean for n = 6 biological replicates. The differences between warming and control samples were tested using ANOVA, *, $p < 0.050$.

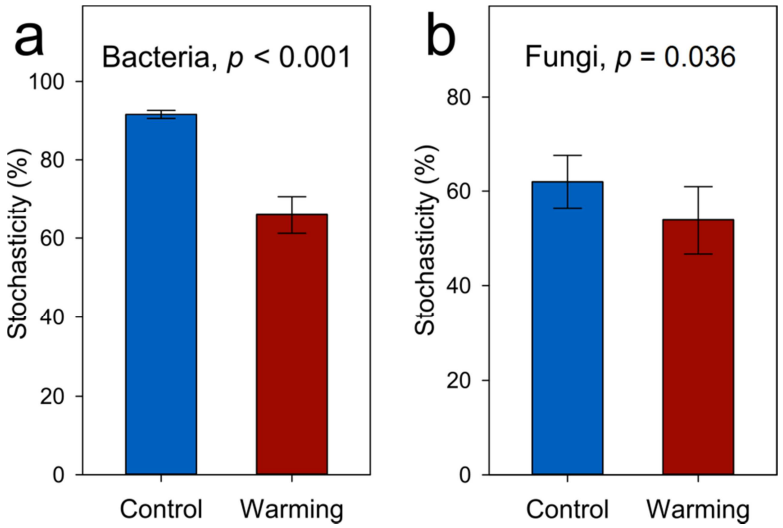

Figure S4. Overall community stochasticity on the basis of phylogenetic metric of (a) bacterial communities and (b) fungal communities under warming and control conditions. The data for each bar contains n = 15 within-group pairwise comparisons calculated from 6 biological replicates.

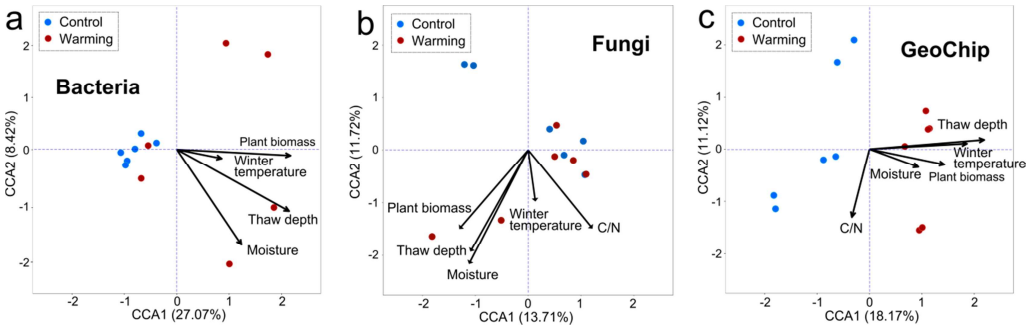

Figure S5. Relationship between microbial community composition or functional structure and environmental factors revealed by canonical correspondence analysis (CCA) of (a) bacterial communities (red dots, warming samples; blue dots, control samples) and environmental variables (arrows), (b) fungal communities and environmental variables; and (c) microbial functional structure and environmental variables. All CCA models were significant ($p < 0.050$).

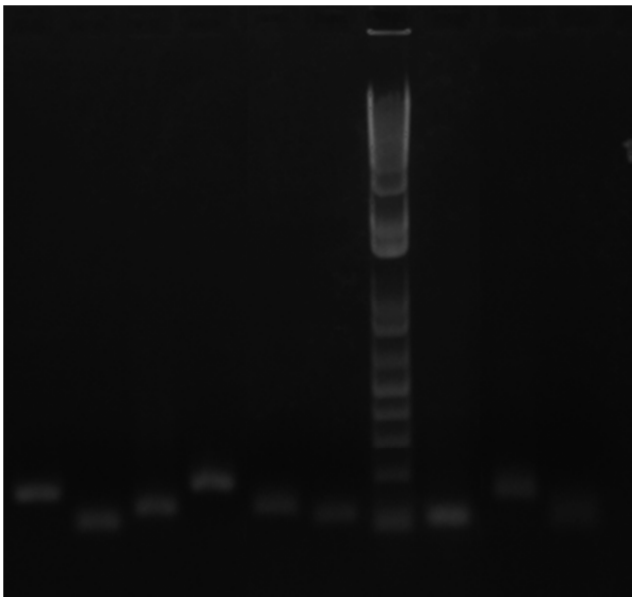

Figure S6. Gel plot showing the sizes of PCR products of specific *nifH* primers. Lanes from the left to the right are products of primers of OTU 109, OTU 35, OTU 7, OTU 67, OTU 188, OTU 277, the standard (the two bands at the bottom are 100 bp and 200 bp), OTU 539, OTU 25, and OTU 262.

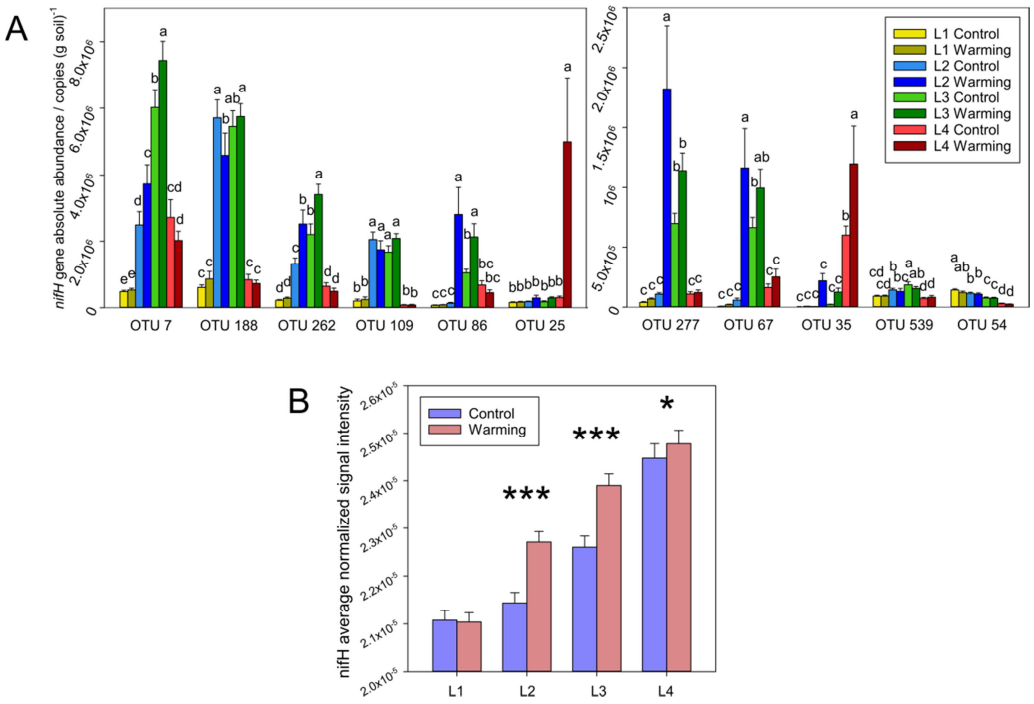

Figure S7. (A) Absolute abundance of the top 11 abundant *nifH* OTUs determined by qPCR. The two panes of the figure are different in the scales of Y-axes. Letters (i.e., a, b, bc, cd, de, and e) above the error bars show the results of ANOVA and LSD tests to examine the significant differences. (B) Average normalized signal intensity of *nifH* genes determined by GeoChip. Abbreviations: L1: the upper organic layer; L2: the middle organic layer; L3: the lower organic layer; L4: the upper mineral layer. Significance determined by ANOVA: *, $0.01<P\leq0.05$; **, $0.001<P\leq0.01$; ***, $P\leq0.001$.

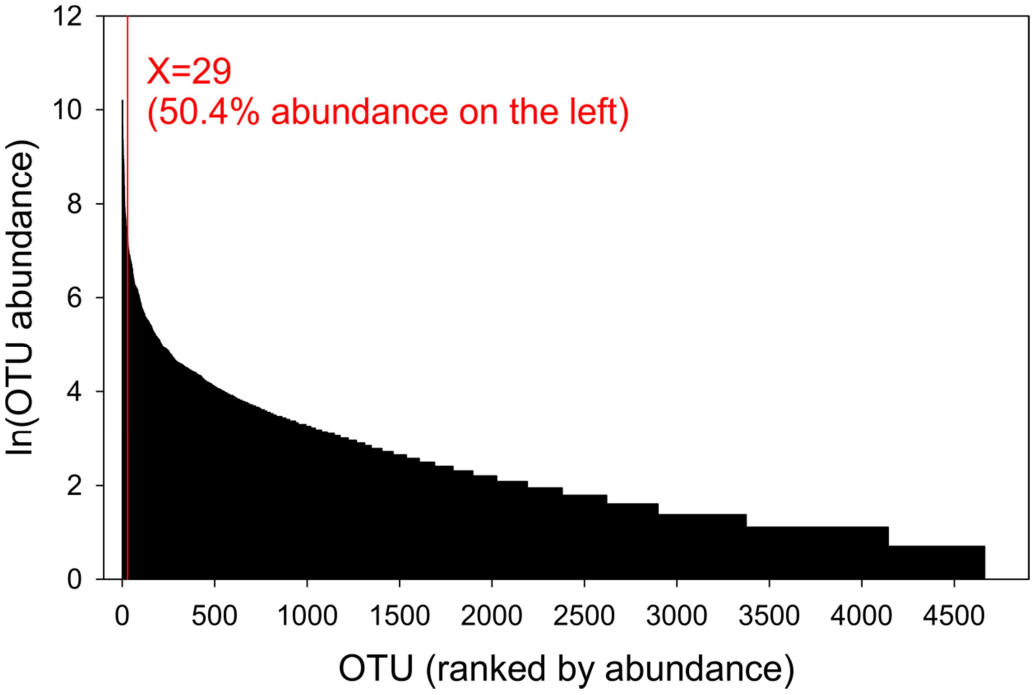

Figure S8. The long-tailed pattern of 4,663 *nifH* OTU relative abundance ranking and distribution based on sequencing data. The abundance of the OTUs on the left of the red line accounts for 50.4% of total abundance.

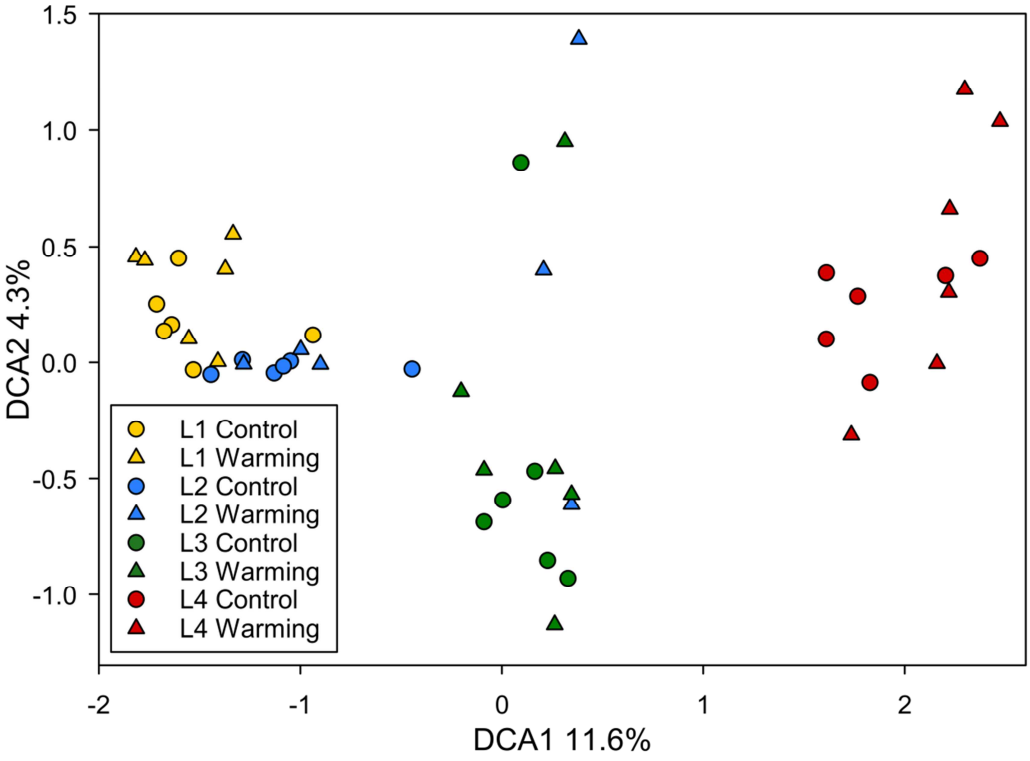

Figure S9. Detrended correspondence analysis (DCA) of *nifH* gene based on sequencing data. The values in the labels of X (11.6%) and Y (4.3%) axes are percentages that the axis can explain. Abbreviations: L1, the upper organic layer; L2, the middle organic layer; L3, the lower organic layer; L4, the upper mineral layer.

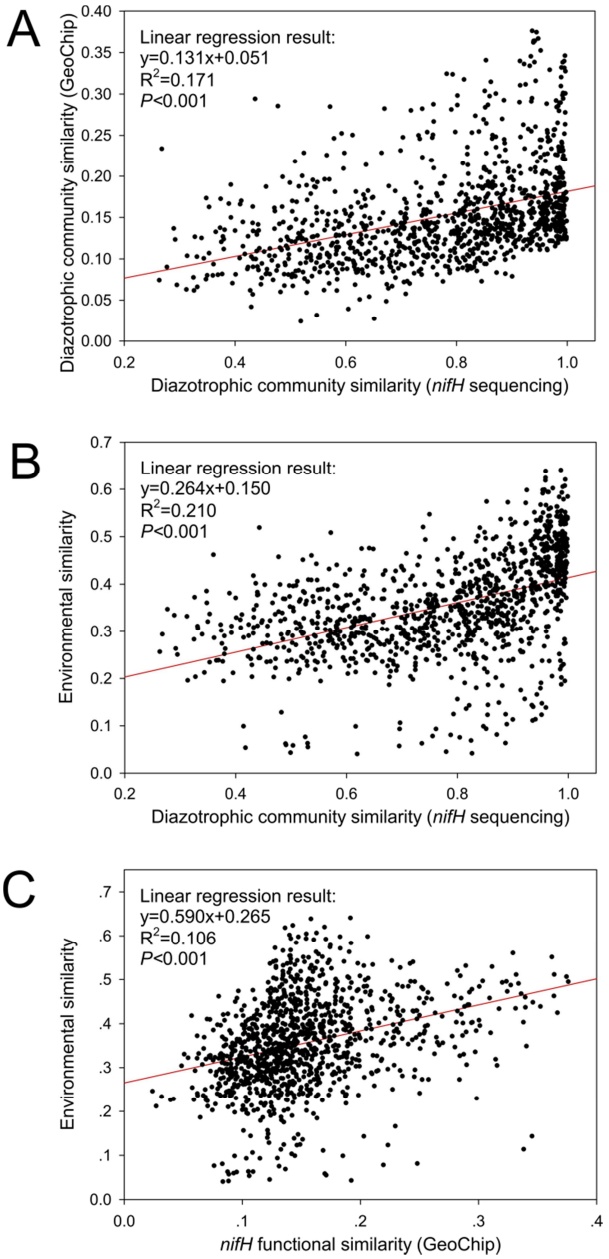

Figure S10. (A) The similarity test of diazotrophic community (Bray-Curtis distances are used) between *nifH* sequencing data and GeoChip data. Bray-Curtis distances are used for the similarity test. (B) The similarity test between diazotrophic community based on sequencing data and 30 environmental factors (Euclid distances are used). (C) The similarity test between diazotrophic community based on GeoChip data and 30 environmental factors.

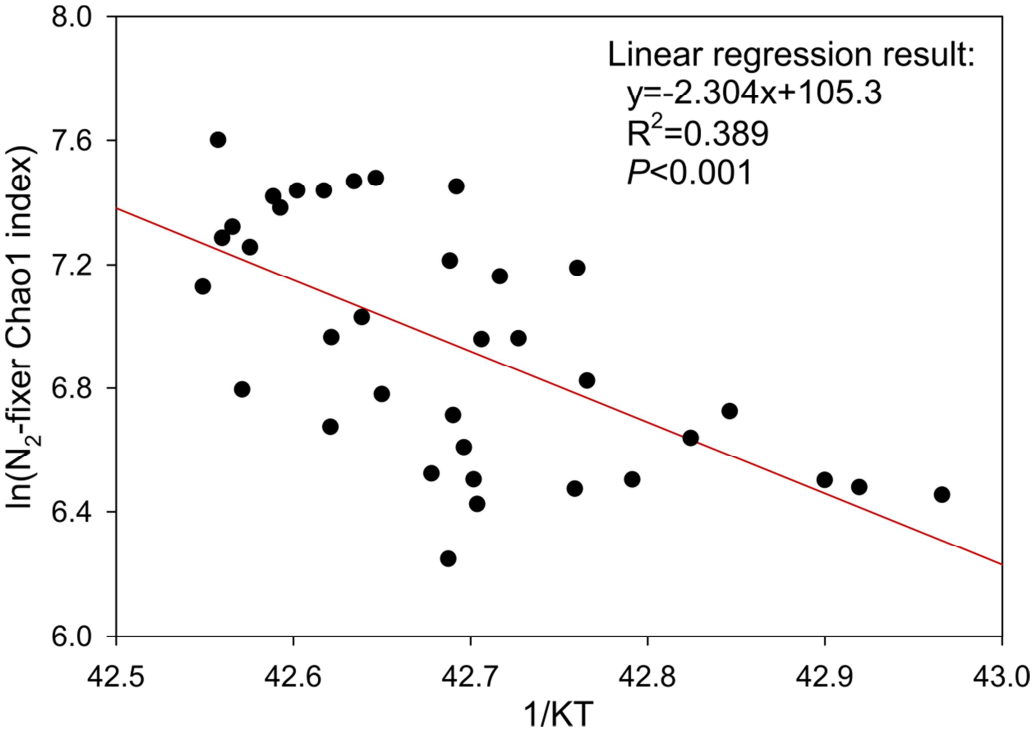

Figure S11. Relationships between diazotrophic richness and temperature. The sequences from all 48 samples were pooled together and calculated for theoretical Chao1 value (for individual samples). The natural log values of the Chao1 were used for analyzing the relationships between temperature and diazotrophic richness. The constant K (Boltzmann's constant) equals to 8.62×10^{-5} electron Volt/Kelvin.

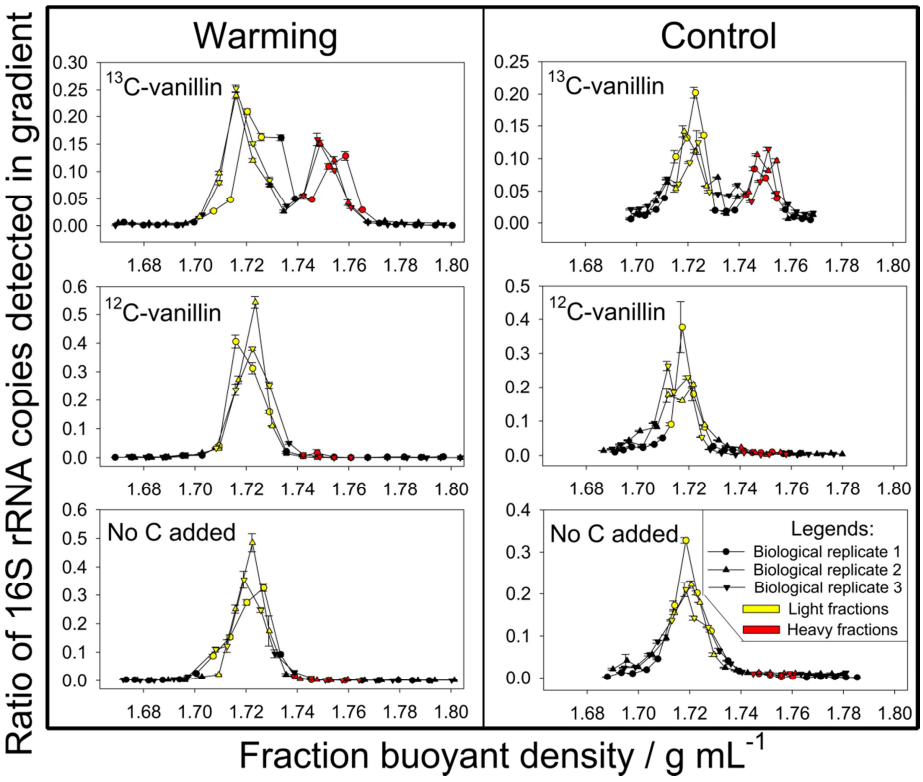

Figure S12. Distribution of 16S rRNA gene copy numbers along buoyant density of the samples in warmed and control samples. Each plot contains three biological replicates, as shown by circles, triangles, or inverted triangles. Each biological replicate value is shown as the average ± standard error of three technical replicates. Red symbols represent the heavy fractions and yellow symbols represent the light fractions.

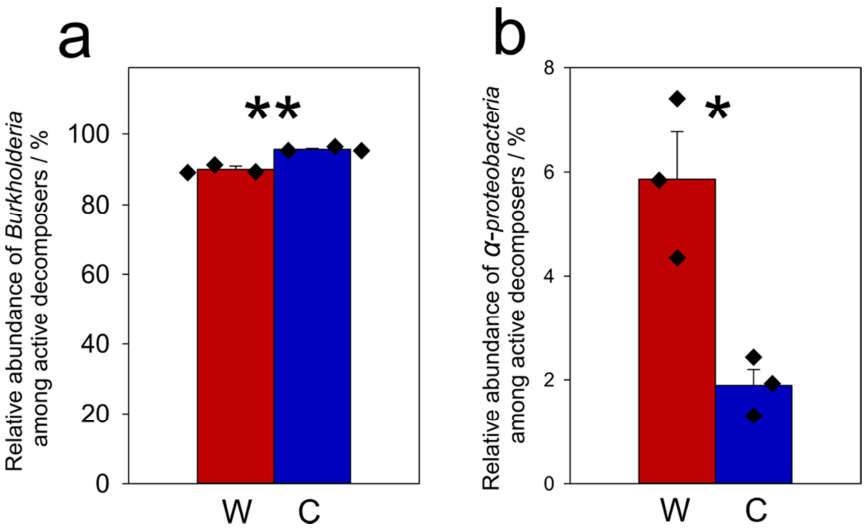

Figure S13. The average relative abundance of (a) *Burkholderia* and (b) *Alphaproteobacteria* among ^{13}C-labelled DNA in ^{13}C-vanillin incubated samples. Significance is indicated using: *, $0.01<P\leq0.05$; **, $0.001<P\leq0.01$; ***, $P\leq0.001$ as determined by two-tailed *t*-test (n=3, biological replicates of warming or control). W: warmed sample; C: control samples. Data are shown as mean ± standard error.

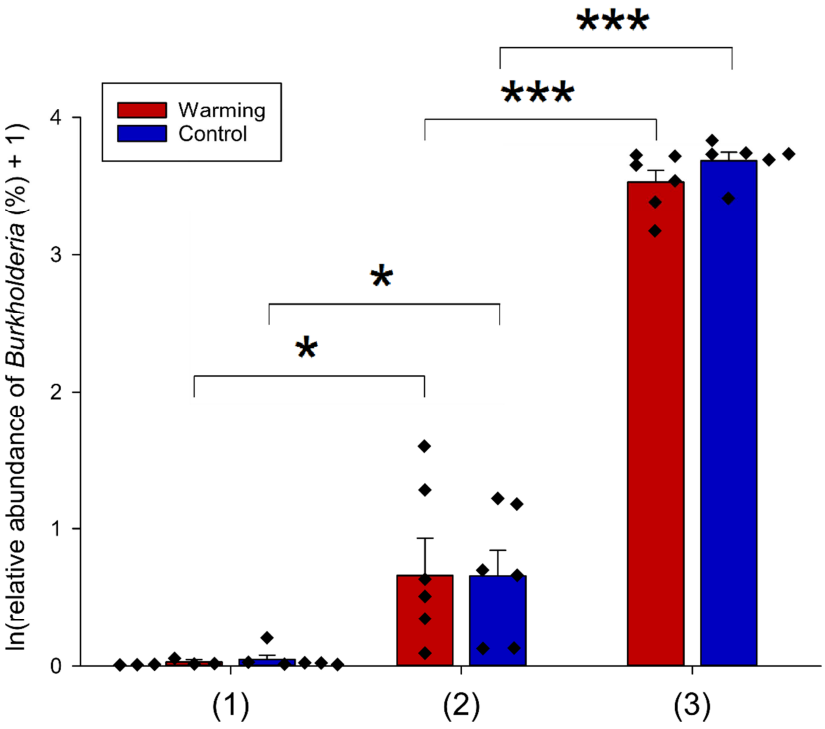

Figure S14. The Napierian logarithm of relative abundances of *Burkholderia* at different time points of the experiment, as revealed by 16S rRNA gene amplicon sequencing. The X axis indicates microbial communities at experimental time points of (1) before the 975-day lab incubation, (2) after the 975-day lab incubation, and (3) after the 6-day SIP incubation. Significance is shown as *, $0.01<P\leq0.05$; **, $0.001<P\leq0.01$; ***, $P\leq0.001$, as determined by two-tailed *t*-test (n=6 for microbial communities before and after 975-day laboratory incubation, and n=3 for active communities identified by the SIP experiment). Data are shown as mean ± standard error.

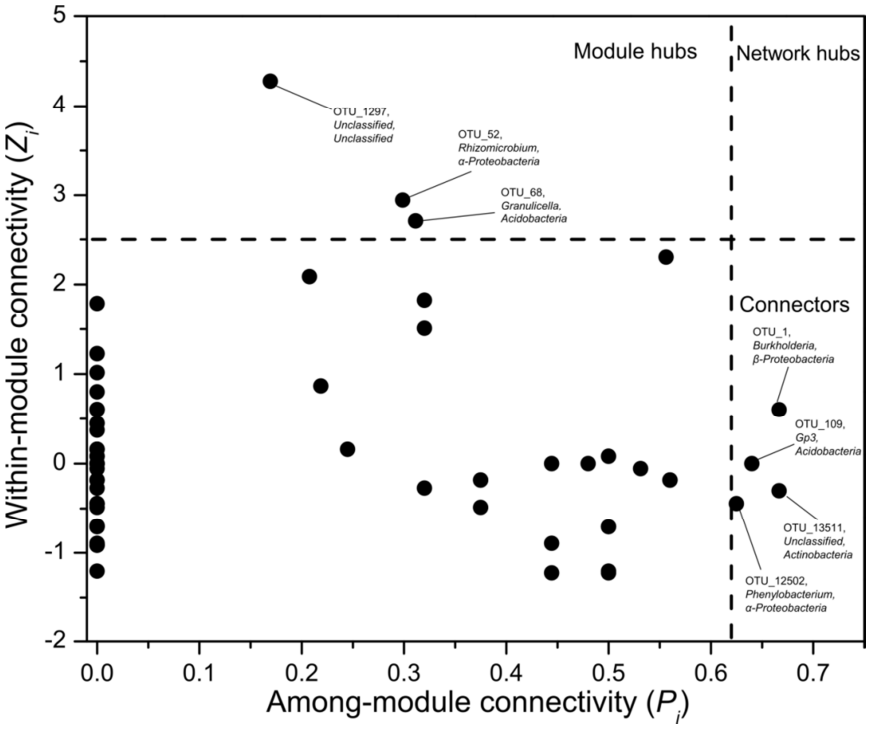

Figure S15. *Z-P* plot showing the distribution of OTUs based on their topological roles. Each symbol represents an OTU. The topological role of each OTU was determined according to the scatter plot of within-module connectivity (Z_i) and among-module connectivity (P). The module hubs and connectors are labeled with OTU numbers.

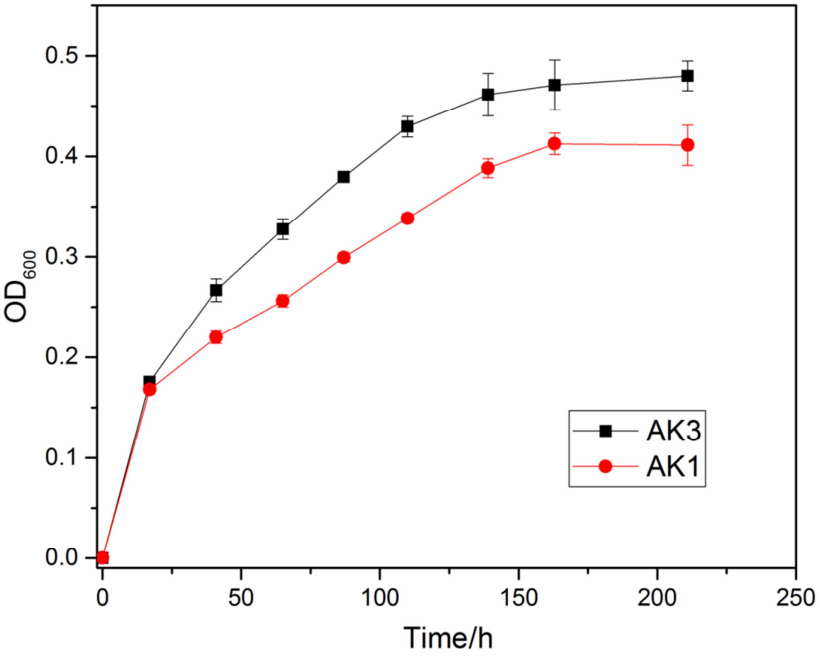

Figure S16. Growth curves of *Burkholderia* strains AK3 and AK1 in defined BMM medium with alkaline lignin as the sole C source (*n*=3).

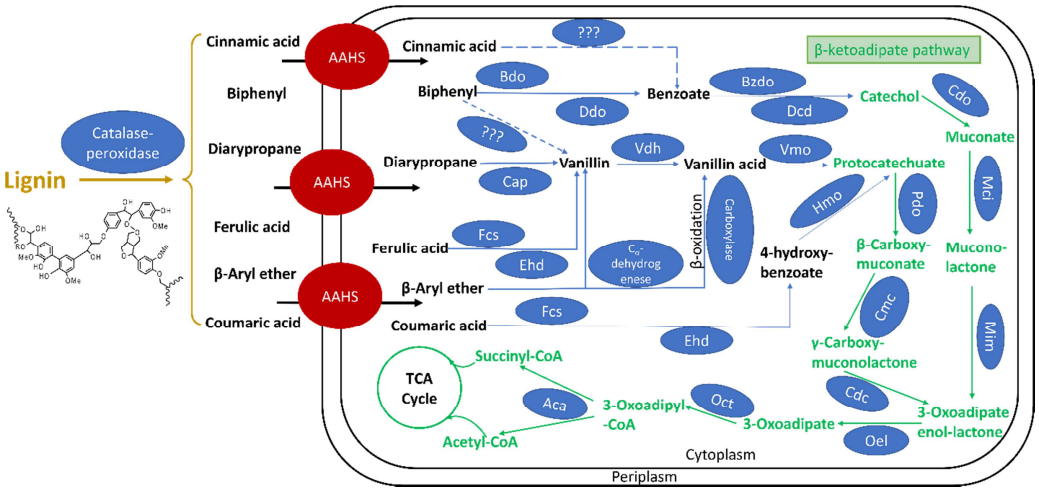

Figure S17. Predicted lignin degradation pathway in *Burkholderia* AK1 and AK3. The lignin is initially oxidized into small compounds (β-Aryl ether, Biphenyl, Diarylpropane, Ferulic acid, coumaric acid and Cinnamic acid) by catalase-peroxidases, and those small molecular compounds may be transported by Aromatic acid: H^+ symporter (AAHS) family transporters into cell. Cinnamic acid and Biphenyl can be oxidized to benzoate and furthered oxidized to Catechol; Diarylpropane, ferulic acid and β-Aryl ether can be oxidized to vanillin firstly and then further oxidized to protocatechuate. Coumaric acid can be oxidized to 4-hydroxy-benzoate and then further oxidized to protocatechuate. The catechol and protocatechuate can be oxidized to succinyl-CoA and acetyl-CoA by β-ketoadipate pathway (Green) and enter into TCA cycle. Enzymes potentially involve in the lignin deploymerization are indicated: Cap, Catalase-peroxidase; Bdo , biphenyl dioxygenase; Ddo, 2,3-dihydroxybiphenyl dioxygenase; Fcs, feruloyl-CoA synthase; Ehd, enoyl-CoA hydratase; Vdh, Vanillin dehydrogenase; Vmo, vanillate monooxygenase; Bzdo, benzoate/toluate 1,2-dioxygenase; Dcd, dihydroxycyclohexadiene carboxylate dehydrogenase; Hmo, hydroxybenzoate 3-monooxygenase; Cdo, catechol 1,2-dioxygenase; pdo, protocatechuate 3,4-dioxygenase; Mci, muconate cycloisomerase;

Cmc, 3-carboxy-cis,cis-muconate cycloisomerase; Mim, muconolactone D-isomerase; Cdc, 4-carboxymuconolactone decarboxylase; Oel, 3-oxoadipate enol-lactonase.

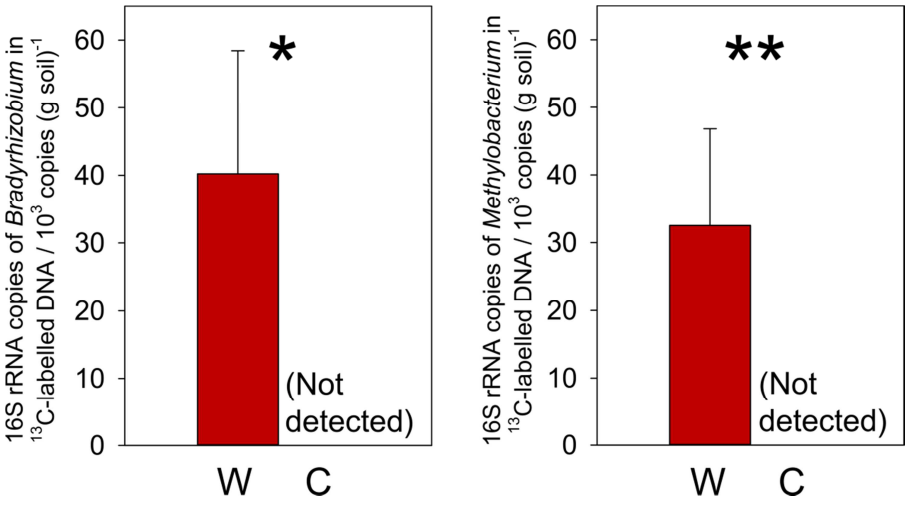

Figure S18. (a) The number of ^{13}C-labelled 16S rRNA gene copies of *Bradyrhizobium*; (b) The number of ^{13}C-labelled 16S rRNA gene copies of *Methylobacterium*. Significance is shown as *, $0.01<P\leq0.05$ as determined by two-tailed *t*-test (n=3, biological replicates of warming or control). Data are shown as mean ± standard error.

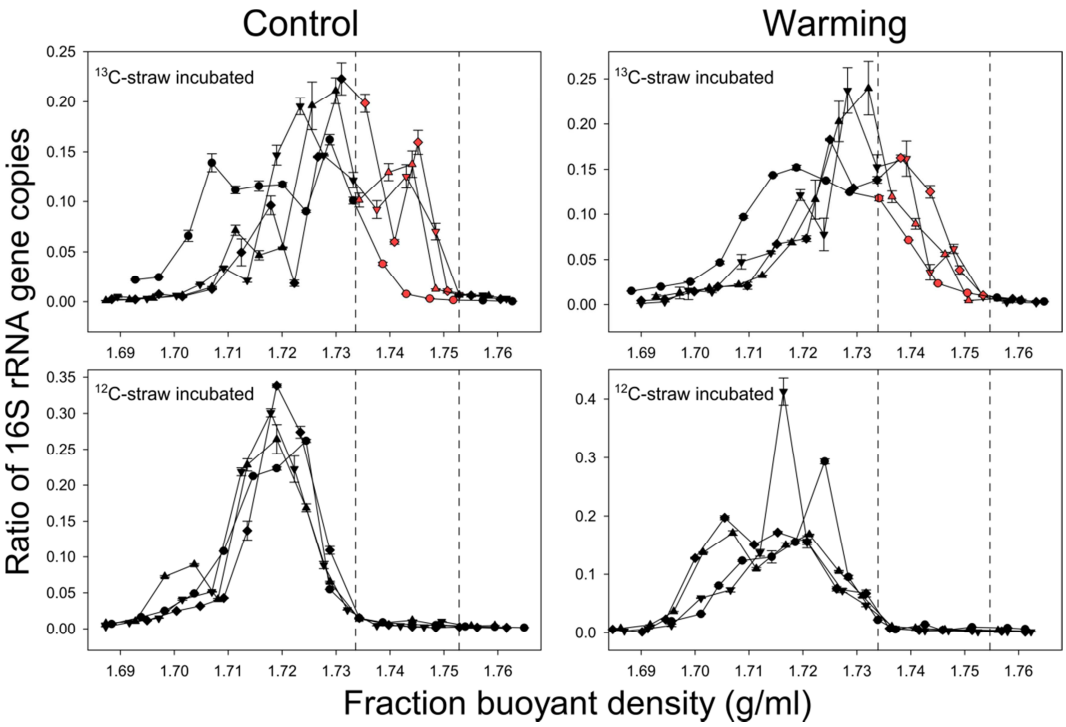

Figure S19. Distribution of 16S rRNA gene abundance along buoyant density. In each pane, symbols of the shapes triangles up, triangles down, diamonds, and circles represent fractions of biological replicate (plot) 1, 2, 3, and 4, respectively. Red symbols in panes of ^{13}C-plant litter represent fractions of active communities, where the corresponding ^{12}C-plant-litter-incubated samples at the same densities were close to zero. Symbols represent average ± standard error of 3 technical replicates of qPCR.

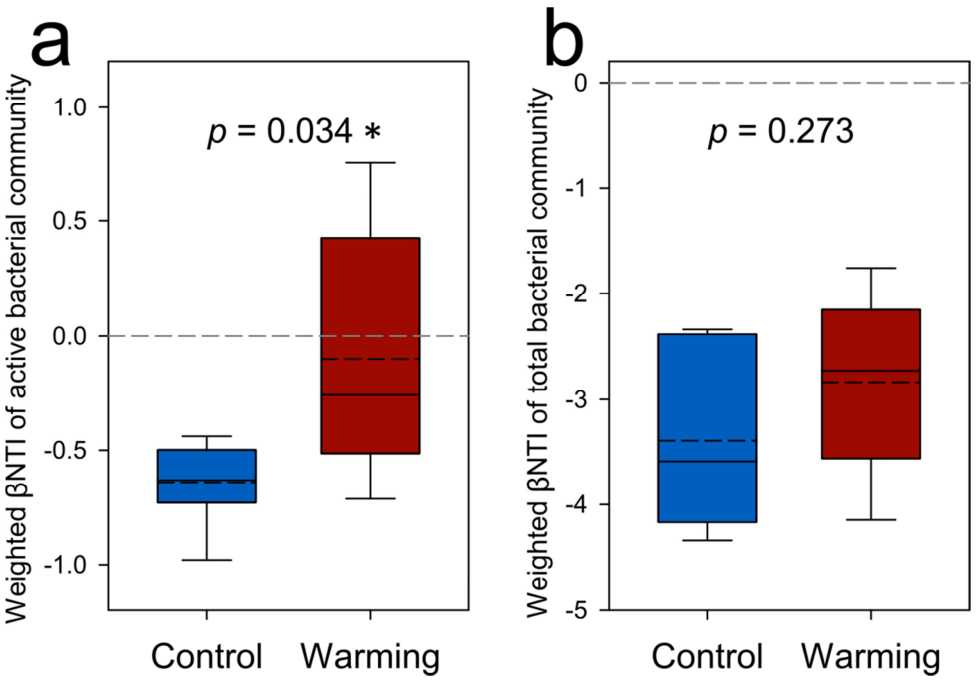

Figure S20. Weighted βNTI (phylogenetic β-diversity) among (a) active communities and (b) total communities. Average values are shown as black dashed lines in the boxes. Each box was plotted from the $n = 6$ pairwise differences among the 4 *in situ* warmed samples or 4 control samples. Significance is indicated using * as $0.010 < p \leq 0.050$ as determined by permutation *t*-test.

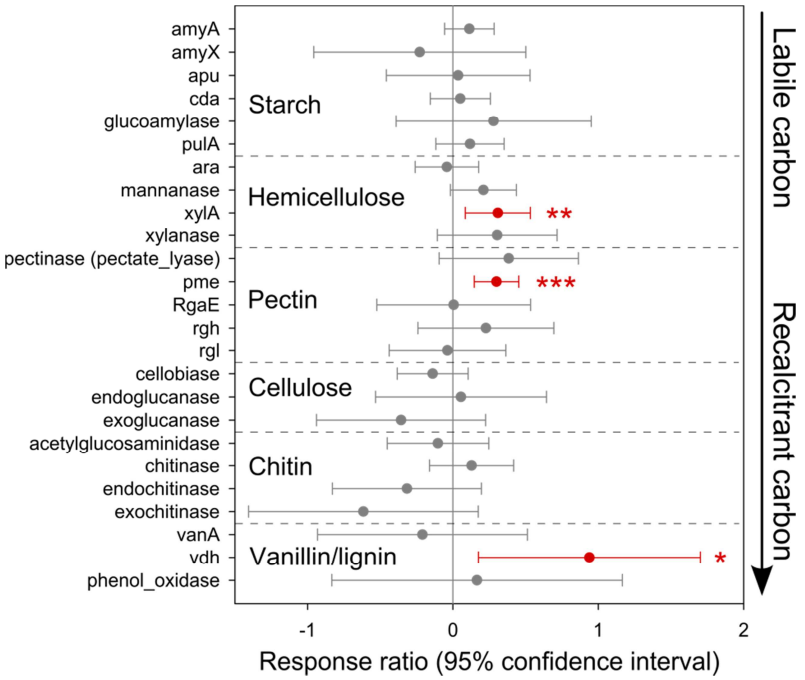

Figure S21. Response ratios of GeoChip signal intensities of active *Firmicutes* C-degrading genes to *in situ* warming. Each symbol represents average ± standard error of n = 4 biological replicates of *in situ* warming or control. Red symbols represent significantly positive response ratios. Significances are indicated using * as $0.010 < p \leq 0.050$, ** as $0.001 < p \leq 0.010$, and *** as $p \leq 0.001$ as determined by confidence intervals.

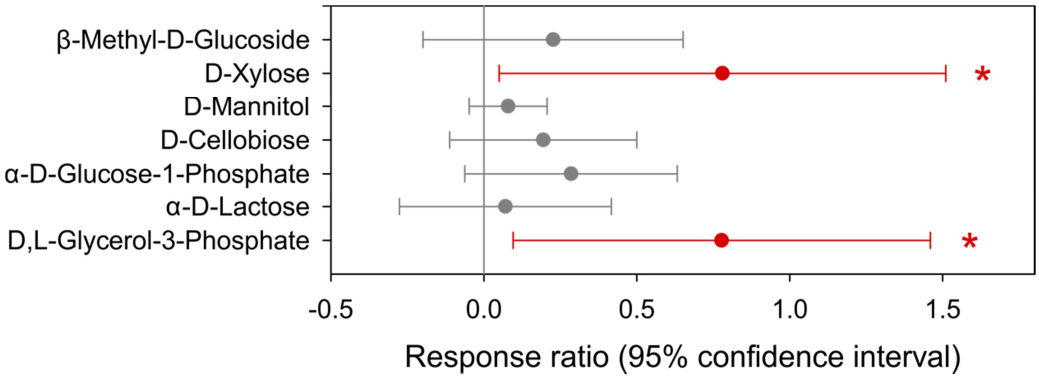

Figure S22. Response ratios of capacity of carbohydrates utilization of soil microbial community to *in situ* warming, as determined by Biolog EcoPlates. Each symbol represents average ± standard error of $n = 4$ biological replicates of *in situ* warming or control. Red symbols represent significantly positive response ratios. Significances are indicated using * as $0.010 < p \leq 0.050$ as determined by confidence intervals.

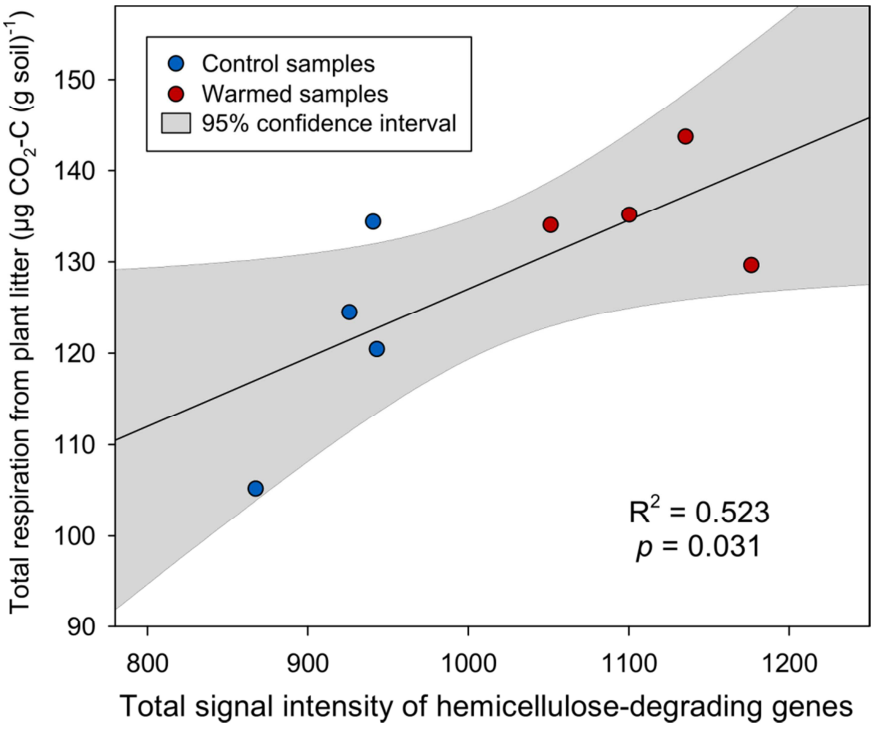

Figure S23. Linear regression between total signal intensity of hemicellulose-degrading genes of active communities revealed by GeoChip and total respiration from straw during the 7-day incubation.

Appendix B: Supplementary Tables

Table S1 for Chapter 2: Warming-accelerated thaw of permafrost-based tundra exacerbates soil carbon loss by restructuring the microbial community

Table S2 to **Table S6** for Chapter 3: Long-term warming in Alaska enlarges the diazotrophic community in deep soils

Table S7 for Chapter 5: Warming exacerbates grassland soil carbon degradation through activating *Firmicutes*

Table S1. Summary of environmental factors.

Environmental factors[a]	Control	Warming
Winter soil temperature (°C)[b]	**-1.95 ± 0.25**	**-1.32 ± 0.13**
Growing season soil temperature (°C)	6.15 ± 0.46	6.20 ± 0.33
Soil moisture (%)	37.77 ± 1.39	42.54 ± 2.90
Water table depth (cm)	23.82 ± 1.19	21.79 ± 1.90
Thaw depth (cm)	**40.98 ± 0.70**	**52.35 ± 2.65**
Aboveground plant biomass (g/m^2)	**1619.0 ± 69.2**	**2025.0 ± 179.5**
Soil carbon/nitrogen ratio	30.03 ± 2.52	30.41 ± 2.08
Ecosystem respiration (mg (CO_2-C) m^{-2} h^{-1})	**94.74 ± 6.02**	**163.68 ± 9.85**
Soil CH_4 flux (µg C m^{-2} h^{-1})[c]	**96.97 ± 32.28**	**309.10 ± 49.62**

[a]Winter soil temperature was measured during the winter of 2012–2013. Growing season soil temperature, soil moisture, water table depth, thaw depth, ecosystem respiration, and CH_4 flux were measured during the 2012 growing season. Data was time-averaged within each plot for analyses.

[b]Mean value and standard error of 6 biological replicates are shown. Differences between warming and control plots were examined by two-tailed permutation *t*-tests. Bold values indicate $p < 0.050$.[c]There were n = 6 biological replicates of control and n = 4 of warming plots. One missing data point (warming biological replicate 1) and one data point identified as an outlier by boxplot (1871.58 µg C m^{-2} h^{-1}, warming biological replicate 2) were excluded. The difference between warming and control plots were tested using two-tailed permutation *t*-test.

Table S2. Environmental factors.

Treatments/layers	Winter temperature (°C)	Growing season temperature (°C)	Soil thaw duration (day per year)	Moisture (VWC within 0–20 cm)	Thaw depth (cm)	Plant biomass (g/m^2)
Average control L1[a]	**-2.3**[b]	7.4	**142.0**	-	-	-
Average warming L1	**-1.6**	7.4	**149.3**	-	-	-
Average control L2	**-1.6**	5.1	118.8	-	-	-
Average warming L2	**-1.0**	5.5	127.0	-	-	-
Average control L3	**-1.2**	**2.6**	**104.2**	-	-	-
Average warming L3	**-0.7**	**3.6**	**112.2**	-	-	-
Average control L4	**-0.9**	**1.1**	**45.5**	-	-	-
Average warming L4	**-0.4**	**2.2**	**79.3**	-	-	-
Average control	-1.5	4.1	102.6	28.1%	**18.3**	**1617**
Average warming	-0.9	4.7	117.0	29.2%	**23.0**	**2025**
Control p1 L1	-2.9	7.8	141.0			
Control p1 L2	-1.8	5.8	111.0	28.6%	20.3	1729
Control p1 L3	-1.4	3.0	103.0			
Control p1 L4	-1.2	1.5	46.0			
Warming p1 L1	-1.5	7.0	147.0			
Warming p1 L2	-0.9	5.3	135.0	29.7%	29.6	2720
Warming p1 L3	-0.6	3.5	117.0			
Warming p1 L4	-0.3	1.5	99.0			
Control p2 L1	-2.4	8.5	144.0			
Control p2 L2	-1.5	5.7	125.0	28.3%	18.7	1633
Control p2	-1.0	2.3	107.0			

L3						
Control p2 L4	-0.9	1.4	46.0			
Warming p2 L1	-1.8	8.1	148.0	31.5%	25.5	2027
Warming p2 L2	-1.1	5.9	128.0			
Warming p2 L3	-0.6	4.2	116.0			
Warming p2 L4	-0.5	3.9	94.0			
Control p3 L1	-1.4	5.5	138.0	28.1%	17.5	1508
Control p3 L2	-1.0	3.4	117.0			
Control p3 L3	-0.8	1.7	100.0			
Control p3 L4	-0.4	0.3	42.0			
Warming p3 L1	-1.4	7.4	151.0	27.8%	19.7	1882
Warming p3 L2	-0.8	5.7	121.0			
Warming p3 L3	-0.6	3.6	107.0			
Warming p3 L4	-0.3	2.2	75.0			
Control p4 L1	-1.5	7.5	143.0	27.9%	17.0	1344
Control p4 L2	-1.1	5.1	125.0			
Control p4 L3	-0.7	2.5	111.0			
Control p4 L4	-0.6	2.0	56.0			
Warming p4 L1	-1.3	7.5	153.0	29.4%	19.9	1390
Warming p4 L2	-0.6	5.3	121.0			
Warming p4 L3	-0.5	3.3	107.0			
Warming p4 L4	-0.4	2.6	68.0			
Control p5 L1	-2.7	6.7	143.0	27.9%	18.2	1820
Control p5 L2	-1.9	4.8	118.0			
Control p5 L3	-1.4	2.3	100.0			

Control p5 L4	-0.9	0.3	26.0			
Warming p5 L1	-1.4	7.4	151.0	29.0%	20.4	1900
Warming p5 L2	-1.1	5.4	132.0			
Warming p5 L3	-0.8	3.4	114.0			
Warming p5 L4	-0.4	1.2	71.0			
Control p6 L1	-3.1	8.4	143.0	27.6%	18.3	1671
Control p6 L2	-2.3	5.8	117.0			
Control p6 L3	-1.6	3.8	104.0			
Control p6 L4	-1.1	1.1	57.0			
Warming p6 L1	-2.0	7.1	146.0	28.0%	22.7	2231
Warming p6 L2	-1.6	5.5	125.0			
Warming p6 L3	-1.0	3.7	112.0			
Warming p6 L4	-0.5	1.7	69.0			

[a]Abbreviations: L1, the upper organic layer; L2, the middle organic layer; L3, the lower organic layer; L4, the upper mineral layer; p1–p6, plot 1–plot 6; N, nitrogen; C, carbon; VWC, volumetric water content; Thaw depth, soil thaw depth when sampled in May 2013; Plant biomass, peak growing season aboveground plant biomass. This table shows the absolute lengths of soil thaw durations instead of the differences between warming and control.

[b]Significance of $P \leq 0.05$, as determined by two-tailed *t*-test between warming and control, is shown by bold values.

Table S3. Adonis tests of the effects of warming on diazotrophic community composition based from sequencing data and functional structure from GeoChip data for *nifH* genes[a].

Layers	*nifH* sequencing[b]		*nifH* GeoChip[c]	
	F	*P*-value	F	*P*-value
All[d]	0.685	0.516	1.353	0.190
L1	0.521	0.657	1.541	0.191
L2	7.850	**0.028**[e]	2.120	***0.057***
L3	1.074	0.414	2.336	**0.047**
L4	1.870	0.222	0.951	0.396

[a]Adonis, permutational Multivariate Analysis of Variance using distance matrices.

[b]Weighted Chao dissimilarity index is used for the dissimilarity analysis of diazotrophic communities based from sequencing data.

[c]Weighted Bray-Curtis dissimilarity index is used for the dissimilarity analysis of diazotrophic communities based on GeoChip data.

[d]All, all of 4 layers combined; L1, the upper organic layer; L2, the middle organic layer; L3, the lower organic layer; L4, the upper mineral layer.

[e]Significance: bold values, $P \leq 0.05$; bold and italic values, $0.05 < P < 0.1$.

Table S4. α-diversity indices, within-treatment β-diversity, and relative abundances (sequence numbers) of *nifH* genes based on sequencing data[a].

Indices/relative abundances	Layer	Control	Warming
Richness	L1[b]	457.50[bc]	443.67[c]
	L2	599.17[bc]	817.50[a]
	L3	873.83[a]	845.17[a]
	L4	612.33[b]	456.67[bc]
Chao1 index	L1	699.44[c]	658.86[c]
	L2	956.06[bc]	1413.27[a]
	L3	1494.71[a]	1481.36[a]
	L4	1037.62[b]	754.43[bc]
Shannon index	L1	3.86[c]	3.88[c]
	L2	4.15[bc]	4.60[ab]
	L3	4.93[a]	4.88[a]
	L4	4.16[bc]	3.51[c]
Within-treatment *nifH* β-diversity (Bray-Curtis distance)	L1	0.591	0.589
	L2	**0.44**[c]	**0.648**
	L3	**0.548**	**0.606**
	L4	0.576	0.659
Within-treatment *nifH* β-diversity (UniFrac distance)	L1	0.352	0.314
	L2	**0.24**	**0.438**
	L3	**0.331**	**0.406**
	L4	0.369	0.429
Relative abundance of Alphaproteobacteria	L1	20420	24094
	L2	14873	16967
	L3	14263	15008
	L4	**10682**	**7669**
	Sum	60238	63738
Relative abundance of Betaproteobacteria	L1	8300	8302
	L2	**17710**	**11768**
	L3	11907	9935
	L4	**4053**	**2745**
	Sum	41970	32750
Relative abundance of Gammaproteobacteria	L1	5182	1507
	L2	**1183**	**2716**
	L3	4591	4254
	L4	16297	21230
	Sum	27253	29707

Relative abundance of Deltaproteobacteria	L1	439	339
	L2	**1080**	**2018**
	L3	1949	2253
	L4	**2617**	**1623**
	Sum	6085	6233
Relative abundance of Verrucomicrobia	L1	**55**	**124**
	L2	**117**	**979**
	L3	**1426**	**2150**
	L4	**1098**	**1781**
	Sum	2696	5034
Relative abundance of Cyanobacteria	L1	935	900
	L2	242	193
	L3	182	124
	L4	**87**	**17**
	Sum	1446	1234
Relative abundance of Firmicutes	L1	56	57
	L2	**94**	**321**
	L3	525	470
	L4	385	133
	Sum	1060	981
Relative abundance of Bacteroidetes	L1	10	67
	L2	78	145
	L3	464	600
	L4	75	55
	Sum	627	867
Relative abundance of Chlorobi	L1	1	23
	L2	7	268
	L3	13	521
	L4	13	18
	Sum	34	830
Relative abundance of Spirochaetes	L1	16	15
	L2	**4**	**35**
	L3	38	54
	L4	11	6
	Sum	69	110
Relative abundance of Actinobacteria	L1	10	0
	L2	33	1
	L3	26	8
	L4	71	8
	Sum	140	17
Relative abundance of Acidobacteria	L1	0	0
	L2	**4**	**16**

	L3	18	36
	L4	12	47
	Sum	34	99
Relative abundance of Nitrospirae	L1	1	0
	L2	0	3
	L3	2	5
	L4	**24**	**94**
	Sum	27	102
Relative abundance of Chloroflexi	L1	0	0
	L2	3	0
	L3	24	7
	L4	5	2
	Sum	32	9
Relative abundance of Epsilonproteobacteria	L1	5	2
	L2	2	0
	L3	0	1
	L4	0	2
	Sum	7	5
Relative abundance of Euryarchaeota	L1	0	0
	L2	0	0
	L3	2	4
	L4	0	0
	Sum	2	4

[a]Lower case superscript letters that is not italic (e.g., [a], [b], [c], and [ab]) in the table show the grouping result of ANOVA and LSD tests, verifying the significant differences among all values within each index. When the two numbers do not share the same lower-case letter, they are significantly different, and vice versa.

[b]Abbreviations: L1, the upper organic layer; L2, the middle organic layer; L3, the lower organic layer; L4, the upper mineral layer.

[c]Significance: bold values, $P \leq 0.05$ as determined by two-tailed *t*-test between warming and control.

Table S5. Pearson correlation of diazotrophic abundance between qPCR result and environmental variables.

R	All layers	L1[a]	L2	L3	L4
Thaw duration (day per year)	-0.047	0.168	***0.571***[b]	0.041	**0.677**
Moisture (VWC percentage within 0–20 cm)	**0.302**	-0.425	0.391	0.206	**0.828**
Plant biomass (g/m^2)	***0.264***	0.349	**0.678**	-0.074	***0.515***

[a]Abbreviations: L1, the upper organic layer; L2, the middle organic layer; L3, the lower organic layer; L4, the upper mineral layer.

[b]Significance: bold values, $P \leq 0.05$; bold and italic values, $0.05 < P < 0.1$.

Table S6. Sequences, product sizes, and melting temperatures (T_m) of qPCR primers of the top 11 abundant OTUs.

nifH OTU ID	Forward primer	Reverse primer	Product size/bp	T_m/^oC (forward, reverse)
OTU 109	CGAGGACCTG GAACTCGATG	CCAACACGTC GTAGGACACA	179	59.9, 59.97
OTU 35	GTTTCGGCGG TATCAAGTGC	ATCGTCATAC GCGCCTTCTT	116	59.9, 59.9
OTU 7	CGGCGTTATC ACCTCGATCA	GTAGATTTCC TGCGCCTTGC	142	59.97, 59.62
OTU 67	CGGAGAAGG GCACTATCGAG	CCGAGCACGT CATAGGAGAC	196	59.69, 59.97
OTU 54	ATGAGAAGGC CCAGAACACG	GCCGAAGTCG ACCTTCATCA	95	60.04, 60.11
OTU 188	AGGGCATCAA GTGTGTCGAG	CGCCGAGCAC ATCATAGGAA	141	60.04, 60.25
OTU 277	CTGGACGAGA TCCTCAAGCC	AGCTGCTCCA GCATGTTGAT	122	59.9, 60.03
OTU 539	GACGTGATGA AGGTCGGCTT	TCGAGGGAGT TGATCGAGGT	110	60.39, 60.03
OTU 86	AGGCCCAGAA CAGCATTCTC	GATGCGCTGA TAGCCGTACT	95	60.03, 60.04
OTU 25	CTGCACTCGAA GGCACAAAC	TCTTCGAGGA AGTTGACGGC	188	60.04, 60.04
OTU 262	GGACCTGGAA CTCGAAGACG	GCACGTCGTA GGAGACGTAG	173	60.11, 59.97

Table S7. Edaphic factors.

Edaphic factors	Control	Warming	Average	*p* value[a]
Soil carbon content (%)[b]	0.798 ± 0.051[c]	0.888 ± 0.060	0.843 ± 0.043	0.359
Soil nitrogen content (%)[b]	0.088 ± 0.005	0.096 ± 0.006	0.092 ± 0.004	0.384
Soil pH[b]	7.30 ± 0.13	7.19 ± 0.18	7.25 ± 0.11	0.666
Soil temperature (°C)[d]	**17.4 ± 0.2**	**19.6 ± 0.5**	**18.5 ± 0.4**	**0.001**
Annual volumetric water content (%)	11.75 ± 1.17	10.02 ± 0.98	10.89 ± 0.82	0.365
Aboveground plant biomass (g m^{-2})[e]	204.9 ± 60.6	107.2 ± 22.7	156.1 ± 36.7	0.239

[a]The *p* value of permutation *t*-tests between edaphic factors of *in situ* warming and control.

[b]Measured using the soil samples used in this study.

[c]Values shown in this table are average ± standard error of $n = 4$ biological replicates.

[d]The average of years 2009–2016. Bold font represents significant difference ($p < 0.050$) between warming and control.

[e]Measured right before soil sampling (September 2016).

References

Abram, N. J., et al. (2016). "Early onset of industrial-era warming across the oceans and continents." Nature **536**(7617): 411-418.

Aeronautics, N. and S. Administration (2017). "Scientific consensus: Earth's climate is warming."

Albertsen, M., et al. (2013). "Genome sequences of rare, uncultured bacteria obtained by differential coverage binning of multiple metagenomes." Nature biotechnology **31**(6): 533.

Bardgett, R. D., et al. (2008). "Microbial contributions to climate change through carbon cycle feedbacks." The ISME Journal **2**(8): 805-814.

Barsdate, R. J. and V. Alexander (1975). "The nitrogen balance of arctic tundra: pathways, rates, and environmental implications." Journal of Environmental Quality **4**(1): 111-117.

Bassin, S., et al. (2007). "Nitrogen deposition but not ozone affects productivity and community composition of subalpine grassland after 3 yr of treatment." New Phytologist **175**(3): 523-534.

Belnap, J. (2002). "Nitrogen fixation in biological soil crusts from southeast Utah, USA." Biology and fertility of soils **35**(2): 128-135.

Bird, J. A. and M. S. Torn (2006). "Fine roots vs. needles: a comparison of 13 C and 15 N dynamics in a ponderosa pine forest soil." Biogeochemistry **79**(3): 361-382.

Bracho, R., et al. (2016). "Temperature sensitivity of organic matter decomposition of permafrost-region soils during laboratory incubations." Soil Biology and Biochemistry **97**: 1-14.

Bradford, M. A. (2013). "Thermal adaptation of decomposer communities in warming soils." Front Microbiol **4**: 333.

Brown, J. H., et al. (2004). "Toward a metabolic theory of ecology." Ecology **85**(7): 1771-1789.

Brown, M. E., et al. (2011). "Discovery and characterization of heme enzymes from unsequenced bacteria: application to microbial lignin degradation." Journal of the American Chemical Society **133**(45): 18006-18009.

Buchfink, B., et al. (2015). "Fast and sensitive protein alignment using DIAMOND." Nature Methods **12**(1): 59-60.

Bugg, T. D., et al. (2011). "The emerging role for bacteria in lignin degradation and bio-product formation." Current opinion in biotechnology **22**(3): 394-400.

Bürgmann, H., et al. (2005). "Effects of model root exudates on structure and activity of a soil diazotroph community." Environmental microbiology **7**(11): 1711-1724.

Byrne, B. M. (2016). Structural equation modeling with AMOS: Basic concepts, applications, and programming, Routledge.

Callahan, B. J., et al. (2016). "DADA2: high-resolution sample inference from Illumina amplicon data." Nature methods **13**(7): 581.

Camacho, C., et al. (2009). "BLAST+: architecture and applications." BMC bioinformatics **10**(1): 421.

Carey, J. C., et al. (2016). "Temperature response of soil respiration largely unaltered with experimental warming." Proceedings of the National Academy of Sciences **113**(48): 13797-13802.

Castro, H. F., et al. (2010). "Soil Microbial Community Responses to Multiple Experimental Climate Change Drivers." Applied and Environmental Microbiology **76**(4): 999-1007.

Cavaleri, M. A., et al. (2015). "Urgent need for warming experiments in tropical forests." Glob Chang Biol **21**(6): 2111-2121.

Chapin, D. M. and C. S. Bledsoe (1992). "Nitrogen fixation in arctic plant communities." Arctic ecosystems in a changing climate: an ecophysiological perspective: 301-319.

Chen, I.-C., et al. (2011). "Rapid range shifts of species associated with high levels of climate warming." Science **333**(6045): 1024-1026.

Cheng, L., et al. (2017). "Warming enhances old organic carbon decomposition through altering functional microbial communities." The ISME journal **11**(8): 1825.

Chu, H., et al. (2016). "Bacterial community dissimilarity between the surface and subsurface soils equals horizontal differences over several kilometers in the western Tibetan Plateau." Environmental microbiology **18**(5): 1523-1533.

Cieslinski, G., et al. (1997). "Low molecular weight organic acids released from roots of durum wheat and flax into sterile nutrient solutions." Journal of plant nutrition **20**(6): 753-764.

CLARKE, K. R. (1993). "Non ‐ parametric multivariate analyses of changes in community structure." Australian journal of ecology **18**(1): 117-143.

Collavino, M. M., et al. (2014). "nifH pyrosequencing reveals the potential for location ‐ specific soil chemistry to influence N2 ‐ fixing community dynamics." Environmental microbiology **16**(10): 3211-3223.

Comiso, J. C., et al. (2008). "Accelerated decline in the Arctic sea ice cover." Geophysical Research Letters **35**(1): n/a-n/a.

Coolen, M. J. L. and W. D. Orsi (2015). "The transcriptional response of microbial communities in thawing Alaskan permafrost soils." Frontiers in Microbiology **6**.

Cornwell, W. K., et al. (2006). "A trait ‐ based test for habitat filtering: convex hull volume." Ecology **87**(6): 1465-1471.

Cox, M. P., et al. (2010). "SolexaQA: At-a-glance quality assessment of Illumina second-generation sequencing data." BMC bioinformatics **11**(1): 485.

Crowther, T. W., et al. (2015). "Biotic interactions mediate soil microbial feedbacks to climate change." Proc Natl Acad Sci U S A **112**(22): 7033-7038.

Crowther, T. W., et al. (2016). "Quantifying global soil carbon losses in response to warming." Nature **540**(7631): 104.

Davidson, E. A. and I. A. Janssens (2006). "Temperature sensitivity of soil carbon decomposition and feedbacks to climate change." Nature **440**(7081): 165-173.

De Baets, S., et al. (2016). "Investigating the controls on soil organic matter decomposition in tussock tundra soil and permafrost after fire." Soil Biology and Biochemistry **99**: 108-116.

Deane-Coe, K. K., et al. (2015). "Experimental Warming Alters Productivity and Isotopic Signatures of Tundra Mosses." Ecosystems **18**(6): 1070-1082.

DeAngelis, K. M., et al. (2015). "Long-term forest soil warming alters microbial communities in temperate forest soils." Frontiers in microbiology **6**.

DeAngelis, K. M., et al. (2015). "Long-term forest soil warming alters microbial communities in temperate forest soils." Frontiers in microbiology **6**: 104.

Deng, J., et al. (2015). "Shifts of tundra bacterial and archaeal communities along a permafrost thaw gradient in A laska." Molecular ecology **24**(1): 222-234.

Deng, J., et al. (2015). "Shifts of tundra bacterial and archaeal communities along a permafrost thaw gradient in Alaska." Molecular Ecology **24**(1): 222-234.

Deng, Y., et al. (2012). "Molecular ecological network analyses." BMC bioinformatics **13**(1): 113.

Desvaux, M. (2005). "Clostridium cellulolyticum: model organism of mesophilic cellulolytic clostridia." FEMS microbiology reviews **29**(4): 741-764.

Deutsch, C. A., et al. (2008). "Impacts of climate warming on terrestrial ectotherms across latitude." Proceedings of the National Academy of Sciences **105**(18): 6668-6672.

Ding, J., et al. (2015). "Soil organic matter quantity and quality shape microbial community compositions of subtropical broadleaved forests." Molecular ecology **24**(20): 5175-5185.

Dobbelaere, S., et al. (2003). "Plant growth-promoting effects of diazotrophs in the rhizosphere." Critical reviews in plant sciences **22**(2): 107-149.

Docherty, K. M., et al. (2012). "Soil microbial responses to fire and interacting global change factors in a California annual grassland." Biogeochemistry **109**(1): 63-83.

Đokić, L., et al. (2011). "Four Bacillus sp. soil isolates capable of degrading phenol, toluene, biphenyl, naphthalene and other aromatic compounds exhibit different aromatic catabolic potentials." Arch. Biol. Sci., Belgrade **63**(4): 1057-1067.

Dufresne, J. L., et al. (2002). "On the magnitude of positive feedback between future climate change and the carbon cycle." Geophysical Research Letters **29**(10): 43-41-43-44.

Eaton, W. D., et al. (2012). "Differences in soil moisture, nutrients and the microbial community between forests on the upper Pacific and Caribbean slopes at Monteverde, Cordillera de Tilaran: implications for responses to climate change." Tropical Ecology **53**(2): 235-240.

Edgar, R. C. (2013). "UPARSE: highly accurate OTU sequences from microbial amplicon reads." Nature methods **10**(10): 996-998.

Edgar, R. C., et al. (2011). "UCHIME improves sensitivity and speed of chimera detection." Bioinformatics **27**(16): 2194-2200.

el Zahar Haichar, F., et al. (2008). "Plant host habitat and root exudates shape soil bacterial community structure." The ISME journal **2**(12): 1221.

Elberling, B., et al. (2013). "Long-term CO 2 production following permafrost thaw." Nature Climate Change **3**(10): 890.

Eliasson, P. E., et al. (2005). "The response of heterotrophic CO2 flux to soil warming." Global Change Biology **11**(1): 167-181.

Ernakovich, J. G. and M. D. Wallenstein (2015). "Permafrost microbial community traits and functional diversity indicate low activity at in situ thaw temperatures." Soil Biology and Biochemistry **87**: 78-89.

Farrar, J., et al. (2003). "How roots control the flux of carbon to the rhizosphere." Ecology **84**(4): 827-837.

Feng, J., et al. (2019). "Long-Term Warming in Alaska Enlarges the Diazotrophic Community in Deep Soils." mBio **10**(1): e02521-02518.

Frey, S., et al. (2008). "Microbial biomass, functional capacity, and community structure after 12 years of soil warming." Soil Biology and Biochemistry **40**(11): 2904-2907.

Friedlingstein, P., et al. (2001). "Positive feedback between future climate change and the carbon cycle." Geophysical Research Letters **28**(8): 1543-1546.

Gaby, J. C. and D. H. Buckley (2012). "A comprehensive evaluation of PCR primers to amplify the nifH gene of nitrogenase." PloS one **7**(7): e42149.

Gaskins, M., et al. (1985). "Rhizosphere bacteria and their use to increase plant productivity: a review." Agriculture, ecosystems & environment **12**(2): 99-116.

Gebauer, R. L., et al. (1995). "Growth and allocation of the arctic sedges Eriohorum angustifolium and E. vaginatum: effects of variable soil oxygen and nutrient availability." Oecologia **104**(3): 330-339.

Gillooly, J. F., et al. (2001). "Effects of size and temperature on metabolic rate." Science **293**(5538): 2248-2251.

Graham, D. E., et al. (2012). "Microbes in thawing permafrost: the unknown variable in the climate change equation." The ISME journal **6**(4): 709.

Grosse, G., et al. (2011). "Vulnerability of high‐latitude soil organic carbon in North America to disturbance." Journal of Geophysical Research: Biogeosciences **116**(G4).

Guckert, J. B., et al. (1996). "Community analysis by Biolog: curve integration for statistical analysis of activated sludge microbial habitats." Journal of Microbiological Methods **27**(2-3): 183-197.

Guo, X., et al. (2018). "Climate warming leads to divergent succession of grassland microbial communities." Nature Climate Change **8**(9): 813.

Hadri, A.-E., et al. (1998). Diversity of root nodulation and rhizobial infection processes. The Rhizobiaceae, Springer**:** 347-360.

Hale, L., et al. (2019). "Tundra microbial community taxa and traits predict decomposition parameters of stable, old soil organic carbon." The ISME journal: 1-15.

Hall, B. G. (2013). "Building phylogenetic trees from molecular data with MEGA." Molecular biology and evolution **30**(5): 1229-1235.

Hansen, J., et al. (2006). "Global temperature change." Proceedings of the National Academy of Sciences **103**(39): 14288-14293.

Harding, T., et al. (2011). "Microbes in high Arctic snow and implications for the cold biosphere." Applied and Environmental Microbiology **77**(10): 3234-3243.

Harms, T. K. and J. B. Jones (2012). "Thaw depth determines reaction and transport of inorganic nitrogen in valley bottom permafrost soils." Global Change Biology **18**(9): 2958-2968.

Hartley, I. P., et al. (2007). "Effects of three years of soil warming and shading on the rate of soil respiration: substrate availability and not thermal acclimation mediates observed response." Global Change Biology **13**(8): 1761-1770.

Hartman, A. L., et al. (2009). "Human gut microbiome adopts an alternative state following small bowel transplantation." Proceedings of the National Academy of Sciences **106**(40): 17187-17192.

Heller, P., et al. (2014). "ARBitrator: a software pipeline for on-demand retrieval of auto-curated nifH sequences from GenBank." Bioinformatics **30**(20): 2883-2890.

Hill, R., et al. (2016). "Temporal and spatial influences incur reconfiguration of Arctic heathland soil bacterial community structure." Environmental Microbiology **18**(6): 1942-1953.

Hines, J., et al. (2014). "Genotypic trait variation modifies effects of climate warming and nitrogen deposition on litter mass loss and microbial respiration." Global Change Biology **20**(12): 3780-3789.

Hobbie, S. E. (1992). "Effects of plant species on nutrient cycling." Trends in ecology & evolution **7**(10): 336-339.

Hobbie, S. E., et al. (2012). "Response of decomposing litter and its microbial community to multiple forms of nitrogen enrichment." Ecological Monographs **82**(3): 389-405.

Hodge, A., et al. (2000). "Are microorganisms more effective than plants at competing for nitrogen?" Trends in plant science **5**(7): 304-308.

Hollander, M. l. "DA WOLFE. 1973. Nonparametric statistical methods." John Wiley and Sons Perry, P. and S. Wolff **1074**: 156-158.

Hu, P., et al. (2012). "Draft genome sequence of Rubrivivax gelatinosus CBS." Journal of bacteriology **194**(12): 3262-3262.

Huang, L.-N., et al. (2011). "Biodiversity, abundance, and activity of nitrogen-fixing bacteria during primary succession on a copper mine tailings." FEMS microbiology ecology **78**(3): 439-450.

Hungate, B. A., et al. (2015). "Quantitative microbial ecology through stable isotope probing." Appl. Environ. Microbiol. **81**(21): 7570-7581.

Huson, D. H., et al. (2007). "MEGAN analysis of metagenomic data." Genome Research **17**(3): 377-386.

Hütsch, B. W., et al. (2002). "Plant rhizodeposition—an important source for carbon turnover in soils." Journal of Plant Nutrition and Soil Science **165**(4): 397-407.

Hyatt, D., et al. (2010). "Prodigal: prokaryotic gene recognition and translation initiation site identification." BMC Bioinformatics **11**(1): 119.

IPCC (2007). Climate change 2007: Synthesis report. Contribution of working groups i, ii and iii to the fourth assessment report of the Intergovernmental Panel on Climate Change. I. P. o. C. Change. Geneva, Switzerland**:** 104.

Iversen, C. M., et al. (2015). "The unseen iceberg: plant roots in arctic tundra." New Phytologist **205**(1): 34-58.

Jain, C., et al. (2018). "High throughput ANI analysis of 90K prokaryotic genomes reveals clear species boundaries." Nature communications **9**(1): 5114.

Janssen, P. H., et al. (2002). "Improved culturability of soil bacteria and isolation in pure culture of novel members of the divisions Acidobacteria, Actinobacteria, Proteobacteria, and Verrucomicrobia." Applied and Environmental Microbiology **68**(5): 2391-2396.

Jassey, V. E., et al. (2013). "Above- and belowground linkages in Sphagnum peatland: climate warming affects plant-microbial interactions." Glob Chang Biol **19**(3): 811-823.

Jones, D. L., et al. (2003). "Associative nitrogen fixation and root exudation-What is theoretically possible in the rhizosphere?" Symbiosis **35**(1): 19-38.

Jones, S. E. and J. T. Lennon (2010). "Dormancy contributes to the maintenance of microbial diversity." Proceedings of the National Academy of Sciences **107**(13): 5881-5886.

Kang, D. D., et al. (2015). "MetaBAT, an efficient tool for accurately reconstructing single genomes from complex microbial communities." PeerJ **3**: e1165.

Karhu, K., et al. (2014). "Temperature sensitivity of soil respiration rates enhanced by microbial community response." Nature **513**(7516): 81.

Keuper, F., et al. (2012). "A frozen feast: Thawing permafrost increases plant‐available nitrogen in subarctic peatlands." Global Change Biology **18**(6): 1998-2007.

Kirschbaum, M. U. F. (2004). "Soil respiration under prolonged soil warming: are rate reductions caused by acclimation or substrate loss?" Global Change Biology **10**(11): 1870-1877.

Klappenbach, J. A., et al. (2000). "rRNA operon copy number reflects ecological strategies of bacteria." Appl. Environ. Microbiol. **66**(4): 1328-1333.

Kline, R. B. (2015). Principles and practice of structural equation modeling, Guilford publications.

Knorr, W., et al. (2005). "Long-term sensitivity of soil carbon turnover to warming." Nature **433**(7023): 298-301.

Kong, Y. (2011). "Btrim: a fast, lightweight adapter and quality trimming program for next-generation sequencing technologies." Genomics **98**(2): 152-153.

Kortsch, S., et al. (2012). "Climate-driven regime shifts in Arctic marine benthos." Proceedings of the National Academy of Sciences **109**(35): 14052-14057.

Kuzyakov, Y. and G. Domanski (2000). "Carbon input by plants into the soil. Review." Journal of Plant Nutrition and Soil Science **163**(4): 421-431.

Lawrence, D. M., et al. (2012). "Simulation of present-day and future permafrost and seasonally frozen ground conditions in CCSM4." Journal of Climate **25**(7): 2207-2225.

Leake, J. R., et al. (2006). "Carbon fluxes from plants through soil organisms determined by field 13CO2 pulse-labelling in an upland grassland." Applied Soil Ecology **33**(2): 152-175.

Lenton, T. M., et al. (2008). "Tipping elements in the Earth's climate system." Proceedings of the National Academy of Sciences **105**(6): 1786-1793.

Li, D., et al. (2013). "Contrasting responses of heterotrophic and autotrophic respiration to experimental warming in a winter annual‐dominated prairie." Global Change Biology **19**(11): 3553-3564.

Li, J. H., et al. (2008). "Genetic diversity and potential for promotion of plant growth detected in nodule endophytic bacteria of soybean grown in Heilongjiang province of China." Soil Biology and Biochemistry **40**(1): 238-246.

Liang, Y., et al. (2015). "Long-term soil transplant simulating climate change with latitude significantly alters microbial temporal turnover." The ISME journal **9**(12): 2561-2572.

Liebner, S., et al. (2011). "Methane oxidation associated with submerged brown mosses reduces methane emissions from Siberian polygonal tundra." Journal of Ecology **99**(4): 914-922.

Liengen, T. and R. A. Olsen (1997). "Seasonal and site-specific variations in nitrogen fixation in a high arctic area, Ny-Ålesund, Spitsbergen." Canadian Journal of Microbiology **43**(8): 759-769.

Life, I. T. O. (2011). "v2: online annotation and display of phylogenetic trees made easy Letunic, Ivica; Bork, Peer." Nucleic Acids Research **39**: W475-W478.

Lipson, D. A. and R. K. Monson (1998). "Plant-microbe competition for soil amino acids in the alpine tundra: effects of freeze-thaw and dry-rewet events." Oecologia **113**(3): 406-414.

Lipson, D. A., et al. (2015). "Changes in microbial communities along redox gradients in polygonized Arctic wet tundra soils." Environmental Microbiology Reports **7**(4): 649-657.

Liu, S., et al. (2015). "The interactive effects of soil transplant into colder regions and cropping on soil microbiology and biogeochemistry." Environ Microbiol **17**(3): 566-576.

Liu, W., et al. (2016). "Precipitation regime drives warming responses of microbial biomass and activity in temperate steppe soils." Biology and Fertility of Soils: 1-9.

Liu, W., et al. (2009). "Predominant role of water in regulating soil and microbial respiration and their responses to climate change in a semiarid grassland." Global Change Biology **15**(1): 184-195.

Loewenstein, Y., et al. (2008). "Efficient algorithms for accurate hierarchical clustering of huge datasets: tackling the entire protein space." Bioinformatics **24**(13): i41-i49.

Logan, N. A. and P. D. Vos (2015). "Bacillus." Bergey's Manual of Systematics of Archaea and Bacteria: 1-163.

López-Mondéjar, R., et al. (2016). "Cellulose and hemicellulose decomposition by forest soil bacteria proceeds by the action of structurally variable enzymatic systems." Scientific reports **6**: 25279.

Luo, Y. (2007). "Terrestrial carbon–cycle feedback to climate warming." Annu. Rev. Ecol. Evol. Syst. **38**: 683-712.

Luo, Y., et al. (2001). "Acclimatization of soil respiration to warming in a tall grass prairie." Nature **413**(6856): 622-625.

Luo, Y., et al. (2001). "Elevated CO2 differentiates ecosystem carbon processes: deconvolution analysis of Duke Forest FACE data." Ecological Monographs **71**(3): 357-376.

Lynch, J. and J. Whipps (1990). "Substrate flow in the rhizosphere." Plant and soil **129**(1): 1-10.

Mack, M. C., et al. (2004). "Ecosystem carbon storage in arctic tundra reduced by long-term nutrient fertilization." Nature **431**(7007): 440-443.

Mack, M. C., et al. (2004). "Ecosystem carbon storage in arctic tundra reduced by long-term nutrient fertilization." Nature **431**(7007): 440-443.

Mackelprang, R., et al. (2011). "Metagenomic analysis of a permafrost microbial community reveals a rapid response to thaw." Nature **480**(7377): 368-371.

Magoč, T. and S. L. Salzberg (2011). "FLASH: fast length adjustment of short reads to improve genome assemblies." Bioinformatics **27**(21): 2957-2963.

Mahecha, M. D., et al. (2010). "Global convergence in the temperature sensitivity of respiration at ecosystem level." Science **329**(5993): 838-840.

Masai, E., et al. (2007). "Genetic and biochemical investigations on bacterial catabolic pathways for lignin-derived aromatic compounds." Bioscience, Biotechnology, and Biochemistry **71**(1): 1-15.

Maslov, S. and K. Sneppen (2002). "Specificity and stability in topology of protein networks." Science **296**(5569): 910-913.

Mau, R. L., et al. (2018). "Warming induced changes in soil carbon and nitrogen influence priming responses in four ecosystems." Applied Soil Ecology **124**: 110-116.

Mauritz, M., et al. (2017). "Nonlinear CO 2 flux response to 7 years of experimentally induced permafrost thaw." Global Change Biology **23**(9): 3646-3666.

McManus, G. D. and M. Shafer (2002). "Oklahoma Climatological Survey."

McMichael, A. J. (2003). "Global climate change and health: an old story writ large." Climate change and human health: Risks and responses. Geneva, Switzerland: World Health Organization.

Melillo, J., et al. (2002). "Soil warming and carbon-cycle feedbacks to the climate system." Science **298**(5601): 2173-2176.

Melle, C., et al. (2015). "Microbial activity is not always limited by nitrogen in Arctic tundra soils." Soil Biology and Biochemistry **90**: 52-61.

Mood, S. H., et al. (2013). "Lignocellulosic biomass to bioethanol, a comprehensive review with a focus on pretreatment." Renewable and Sustainable Energy Reviews **27**: 77-93.

Mus, F., et al. (2016). "Symbiotic nitrogen fixation and the challenges to its extension to nonlegumes." Appl. Environ. Microbiol. **82**(13): 3698-3710.

Natali, S. M., et al. (2011). "Effects of experimental warming of air, soil and permafrost on carbon balance in Alaskan tundra." Global Change Biology **17**(3): 1394-1407.

Natali, S. M., et al. (2014). "Permafrost degradation stimulates carbon loss from experimentally warmed tundra." Ecology **95**(3): 602-608.

Natali, S. M., et al. (2015). "Permafrost thaw and soil moisture driving CO2 and CH4 release from upland tundra." Journal of Geophysical Research-Biogeosciences **120**(3): 525-537.

Natali, S. M., et al. (2012). "Increased plant productivity in Alaskan tundra as a result of experimental warming of soil and permafrost." Journal of Ecology **100**(2): 488-498.

Natali, S. M., et al. (2011). "Effects of experimental warming of air, soil and permafrost on carbon balance in Alaskan tundra." Global Change Biology **17**(3): 1394-1407.

National Academies of Sciences, E. and Medicine (2018). Joint science academies' Statement: Global response to climate change.

Neufeld, J. D., et al. (2007). "DNA stable-isotope probing." Nature protocols **2**(4): 860.

Nie, M., et al. (2013). "Positive climate feedbacks of soil microbial communities in a semi-arid grassland." Ecology Letters **16**(2): 234-241.

Nordin, A., et al. (2004). "Nitrogen uptake by arctic soil microbes and plants in relation to soil nitrogen supply." Ecology **85**(4): 955-962.

O'Donnell, J. A., et al. (2012). "The Effects of Permafrost Thaw on Soil Hydrologic, Thermal, and Carbon Dynamics in an Alaskan Peatland." Ecosystems **15**(2): 213-229.

Oechel, W. C., et al. (2000). "Acclimation of ecosystem CO2 exchange in the Alaskan Arctic in response to decadal climate warming." Nature **406**(6799): 978-981.

Okon, Y., et al. (1995). Advances in agronomy and ecology of the Azospirillum/plant association. Nitrogen fixation: Fundamentals and applications, Springer**:** 635-640.

Oksanen, J. and P. R. Minchin (1997). "Instability of ordination results under changes in input data order: explanations and remedies." Journal of Vegetation Science **8**(3): 447-454.

Osterkamp, T. (2007). "Characteristics of the recent warming of permafrost in Alaska." Journal of Geophysical Research: Earth Surface **112**(F2).

Osterkamp, T., et al. (2009). "Physical and ecological changes associated with warming permafrost and thermokarst in interior Alaska." Permafrost and Periglacial Processes **20**(3): 235-256.

Pailler, A., et al. (2014). "Forest soil microbial functional patterns and response to a drought and warming event: Key role of climate–plant–soil interactions at a regional scale." Soil Biology and Biochemistry **70**: 1-4.

Parks, D. H., et al. (2015). "CheckM: assessing the quality of microbial genomes recovered from isolates, single cells, and metagenomes." Genome research **25**(7): 1043-1055.

Patz, J. A., et al. (2005). "Impact of regional climate change on human health." Nature **438**(7066): 310.

Pecl, G. T., et al. (2017). "Biodiversity redistribution under climate change: Impacts on ecosystems and human well-being." Science **355**(6332).

Peltoniemi, K., et al. (2015). "Microbial ecology in a future climate: effects of temperature and moisture on microbial communities of two boreal fens." FEMS Microbiol Ecol **91**(7).

Peng, Y., et al. (2012). "IDBA-UD: a de novo assembler for single-cell and metagenomic sequencing data with highly uneven depth." Bioinformatics **28**(11): 1420-1428.

Penton, C. R., et al. (2015). "Denitrifying and diazotrophic community responses to artificial warming in permafrost and tallgrass prairie soils." Frontiers in microbiology **6**: 746.

Penton, C. R., et al. (2016). "NifH-Harboring Bacterial Community Composition across an Alaskan Permafrost Thaw Gradient." Frontiers in Microbiology **7**.

Placella, S. A., et al. (2012). "Rainfall-induced carbon dioxide pulses result from sequential resuscitation of phylogenetically clustered microbial groups." Proceedings of the National Academy of Sciences **109**(27): 10931-10936.

Pold, G., et al. (2015). "Two decades of warming increases diversity of a potentially lignolytic bacterial community." Frontiers in microbiology **6**.

Pold, G., et al. (2015). "Two decades of warming increases diversity of a potentially lignolytic bacterial community." Frontiers in microbiology **6**: 480.

Poly, F., et al. (2001). "Improvement in the RFLP procedure for studying the diversity of nifH genes in communities of nitrogen fixers in soil." Research in Microbiology **152**(1): 95-103.

Pries, C. E. H., et al. (2012). "Holocene carbon stocks and carbon accumulation rates altered in soils undergoing permafrost thaw." Ecosystems **15**(1): 162-173.

Pries, C. E. H., et al. (2013). "Thawing permafrost increases old soil and autotrophic respiration in tundra: Partitioning ecosystem respiration using δ13C andΔ 14C." Global Change Biology **19**(2): 649-661.

Pries, C. E. H., et al. (2016). "Old soil carbon losses increase with ecosystem respiration in experimentally thawed tundra." Nature Climate Change **6**(2): 214.

Ramachandra, M., et al. (1988). "Characterization of an extracellular lignin peroxidase of the lignocellulolytic actinomycete Streptomyces viridosporus." Applied and Environmental Microbiology **54**(12): 3057-3063.

Raymond, J., et al. (2004). "The natural history of nitrogen fixation." Molecular biology and evolution **21**(3): 541-554.

Reed, S. C., et al. (2011). "Functional ecology of free-living nitrogen fixation: a contemporary perspective." Annual review of ecology, evolution, and systematics **42**: 489-512.

Reed, S. C., et al. (2010). "Microbial community shifts influence patterns in tropical forest nitrogen fixation." Oecologia **164**(2): 521-531.

Roller, B. R., et al. (2016). "Exploiting rRNA operon copy number to investigate bacterial reproductive strategies." Nature microbiology **1**(11): 16160.

Romero-Olivares, A. L., et al. (2017). "Decomposition of recalcitrant carbon under experimental warming in boreal forest." PloS one **12**(6): e0179674.

Rousk, J., et al. (2012). "Temperature adaptation of bacterial communities in experimentally warmed forest soils." Global Change Biology **18**(10): 3252-3258.

Rousk, J., et al. (2013). "Investigating the long-term legacy of drought and warming on the soil microbial community across five European shrubland ecosystems." Glob Chang Biol **19**(12): 3872-3884.

Rustad, L., et al. (2001). "A meta-analysis of the response of soil respiration, net nitrogen mineralization, and aboveground plant growth to experimental ecosystem warming." Oecologia **126**(4): 543-562.

Sadhu, S. and T. K. Maiti (2013). "Cellulase production by bacteria: a review." British Microbiology Research Journal **3**(3): 235.

Salmon, V. G., et al. (2015). "Nitrogen availability increases in a tundra ecosystem during five years of experimental permafrost thaw." Global Change Biology.

Salmon, V. G., et al. (2016). "Nitrogen availability increases in a tundra ecosystem during five years of experimental permafrost thaw." Global Change Biology **22**(5): 1927-1941.

Sangkhobol, V. and V. Skerman (1981). "Chitinophaga, a new genus of chitinolytic myxobacteria." International Journal of Systematic and Evolutionary Microbiology **31**(3): 285-293.

Schädel, C., et al. (2014). "Circumpolar assessment of permafrost C quality and its vulnerability over time using long‐term incubation data." Global change biology **20**(2): 641-652.

Scheffer, M., et al. (2006). "Positive feedback between global warming and atmospheric CO_2 concentration inferred from past climate change." Geophysical Research Letters **33**(10).

Schlesinger, W. H. (1977). "Carbon balance in terrestrial detritus." Annual review of ecology and systematics **8**(1): 51-81.

Schuur, E. A., et al. (2008). "Vulnerability of permafrost carbon to climate change: Implications for the global carbon cycle." BioScience **58**(8): 701-714.

Schuur, E. A., et al. (2007). "Plant species composition and productivity following permafrost thaw and thermokarst in Alaskan tundra." Ecosystems **10**(2): 280-292.

Schuur, E. A. G., et al. (2011). "High risk of permafrost thaw." Nature **480**(7375): 32-33.

Schuur, E. A. G., et al. (2008). "Vulnerability of permafrost carbon to climate change: Implications for the global carbon cycle." Bioscience **58**(8): 701-714.

Schuur, E. A. G., et al. (2015). "Climate change and the permafrost carbon feedback." Nature **520**(7546): 171-179.

Schuur, E. A. G., et al. (2009). "The effect of permafrost thaw on old carbon release and net carbon exchange from tundra." Nature **459**(7246): 556-559.

Semenova, T. A., et al. (2015). "Long-term experimental warming alters community composition of ascomycetes in Alaskan moist and dry arctic tundra." Mol Ecol **24**(2): 424-437.

Semmartin, M., et al. (2008). "Grazing history effects on above-and below-ground litter decomposition and nutrient cycling in two co-occurring grasses." Plant and Soil **303**(1-2): 177-189.

Shahzad, T., et al. (2012). "Plant clipping decelerates the mineralization of recalcitrant soil organic matter under multiple grassland species." Soil Biology and Biochemistry **51**: 73-80.

Simons, M., et al. (1997). "Amino acid synthesis is necessary for tomato root colonization by Pseudomonas fluorescens strain WCS365." Molecular plant-microbe interactions **10**(1): 102-106.

Singh, B. K., et al. (2009). "Soil genomics." Nature Reviews Microbiology **7**(10): 756-756.

Sistla, S. A., et al. (2013). "Long-term warming restructures Arctic tundra without changing net soil carbon storage." Nature **497**(7451): 615-618.

Stegen, J. C., et al. (2012). "Stochastic and deterministic assembly processes in subsurface microbial communities." The ISME journal **6**(9): 1653.

Steven, B., et al. (2015). "Climate Change and Physical Disturbance Manipulations Result in Distinct Biological Soil Crust Communities." Appl Environ Microbiol **81**(21): 7448-7459.

Stewart, K. J., et al. (2013). "How is nitrogen fixation in the high arctic linked to greenhouse gas emissions?" Plant and soil **362**(1-2): 215-229.

Stewart, K. J., et al. (2011). "Bryophyte-cyanobacterial associations as a key factor in N2-fixation across the Canadian Arctic." Plant and Soil **344**(1-2): 335-346.

Stocker, T. (2014). Climate change 2013: the physical science basis: Working Group I contribution to the Fifth assessment report of the Intergovernmental Panel on Climate Change, Cambridge University Press.

Stocker, T. F., et al. (2013). Climate change 2013: The physical science basis, Cambridge University Press Cambridge.

Stocker, T. F., et al. (2014). Climate Change 2013: The physical science basis. contribution of working group I to the fifth assessment report of IPCC the intergovernmental panel on climate change, Cambridge University Press.

Streit, K., et al. (2014). "Soil warming alters microbial substrate use in alpine soils." Glob Chang Biol **20**(4): 1327-1338.

Tarnocai, C., et al. (2009). "Soil organic carbon pools in the northern circumpolar permafrost region." Global biogeochemical cycles **23**(2).

Taş, N., et al. (2014). "Impact of fire on active layer and permafrost microbial communities and metagenomes in an upland Alaskan boreal forest." ISME J **8**(9): 1904-1919.

Taylor, C. R., et al. (2012). "Isolation of bacterial strains able to metabolize lignin from screening of environmental samples." Journal of applied microbiology **113**(3): 521-530.

Teepe, R., et al. (2004). "Emissions of N2O from soils during cycles of freezing and thawing and the effects of soil water, texture and duration of freezing." European Journal of Soil Science **55**(2): 357-365.

Tucker, C. L., et al. (2013). "Does declining carbon-use efficiency explain thermal acclimation of soil respiration with warming?" Global Change Biology **19**(1): 252-263.

Van Nostrand, J. D., et al. (2016). Hybridization of environmental microbial community nucleic acids by GeoChip. Microbial Environmental Genomics (MEG), Springer**:** 183-196.

Van Sickle, J. (1997). "Using mean similarity dendrograms to evaluate classifications." Journal of Agricultural, Biological, and Environmental Statistics: 370-388.

Vartapetian, B. B. and M. B. Jackson (1997). "Plant adaptations to anaerobic stress." Annals of Botany **79**(suppl_1): 3-20.

Vicuña, R. (1988). "Bacterial degradation of lignin." Enzyme and Microbial Technology **10**(11): 646-655.

Von Mering, C., et al. (2007). "Quantitative phylogenetic assessment of microbial communities in diverse environments." Science **315**(5815): 1126-1130.

Vonk, J. E., et al. (2012). "Activation of old carbon by erosion of coastal and subsea permafrost in Arctic Siberia." Nature **489**(7414): 137.

Walker, M. (1996). "Community baseline measurements for ITEX studies." ITEX manual **2**: 39-41.

Walker, M. D., et al. (2006). "Plant community responses to experimental warming across the tundra biome." Proc Natl Acad Sci U S A **103**(5): 1342-1346.

Walter, J., et al. (2013). "Combined effects of multifactor climate change and land-use on decomposition in temperate grassland." Soil Biology and Biochemistry **60**: 10-18.

Walter, K. M., et al. (2006). "Methane bubbling from Siberian thaw lakes as a positive feedback to climate warming." Nature **443**(7107): 71-75.

Wang, G., et al. (2015). "Microbial dormancy improves development and experimental validation of ecosystem model." The ISME journal **9**(1): 226.

Wang, G., et al. (2012). "Parameter estimation for models of ligninolytic and cellulolytic enzyme kinetics." Soil Biology and Biochemistry **48**: 28-38.

Wang, K., et al. (2017). "Modeling Global Soil Carbon and Soil Microbial Carbon by Integrating Microbial Processes into the Ecosystem Process Model TRIPLEX - GHG." Journal of Advances in Modeling Earth Systems **9**(6): 2368-2384.

Wang, Q., et al. (2007). "Naive Bayesian classifier for rapid assignment of rRNA sequences into the new bacterial taxonomy." Applied and Environmental Microbiology **73**(16): 5261-5267.

Wang, Q., et al. (2013). "Ecological patterns of nifH genes in four terrestrial climatic zones explored with targeted metagenomics using FrameBot, a new informatics tool." MBio **4**(5): e00592-00513.

Wang, X., et al. (2014). "Effects of short-term and long-term warming on soil nutrients, microbial biomass and enzyme activities in an alpine meadow on the Qinghai-Tibet Plateau of China." Soil Biology and Biochemistry **76**: 140-142.

Webb, C. O., et al. (2002). "Phylogenies and community ecology." Annual review of ecology and systematics **33**(1): 475-505.

Webb, E. E., et al. (2016). "Increased wintertime CO2 loss as a result of sustained tundra warming." Journal of Geophysical Research: Biogeosciences **121**(2): 249-265.

White, J., et al. (2007). "Nutrient sharing between symbionts." Plant Physiology **144**(2): 604-614.

Wigley, T. M. L. and S. C. B. Raper (1990). "Natural variability of the climate system and detection of the greenhouse effect." Nature **344**(6264): 324.

Wild, B., et al. (2014). "Input of easily available organic C and N stimulates microbial decomposition of soil organic matter in arctic permafrost soil." Soil Biology and Biochemistry **75**: 143-151.

Wilhelm, R. C., et al. (2019). "Bacterial contributions to delignification and lignocellulose degradation in forest soils with metagenomic and quantitative stable isotope probing." The ISME journal **13**(2): 413.

Woo, H. L., et al. (2014). "Enzyme activities of aerobic lignocellulolytic bacteria isolated from wet tropical forest soils." Systematic and applied microbiology **37**(1): 60-67.

Wu, L., et al. (2015). "Phasing amplicon sequencing on Illumina Miseq for robust environmental microbial community analysis." BMC microbiology **15**(1): 125.

Wu, L., et al. (2017). "Microbial functional trait of rRNA operon copy numbers increases with organic levels in anaerobic digesters." ISME J **11**(12): 2874-2878.

Wu, L., et al. (2017). "Microbial functional trait of rRNA operon copy numbers increases with organic levels in anaerobic digesters." The ISME journal **11**(12): 2874.

Xu, W., et al. (2014). "Distinct temperature sensitivity of soil carbon decomposition in forest organic layer and mineral soil." Scientific reports **4**.

Xu, X., et al. (2013). "Net primary productivity and rain‐use efficiency as affected by warming, altered precipitation, and clipping in a mixed‐grass prairie." Global Change Biology **19**(9): 2753-2764.

Xue, K., et al. (2016). "Tundra soil carbon is vulnerable to rapid microbial decomposition under climate warming." Nature Climate Change **6**(6): 595.

Yang, Y., et al. (2009). "Snapshot of iron response in Shewanella oneidensis by gene network reconstruction." BMC genomics **10**: 131.

Yang, Y., et al. (2013). "Responses of the functional structure of soil microbial community to livestock grazing in the Tibetan alpine grassland." Global Change Biology **19**(2): 637-648.

Yao, X.-F., et al. (2011). "Degradation of dichloroaniline isomers by a newly isolated strain, Bacillus megaterium IMT21." Microbiology **157**(3): 721-726.

Yergeau, E., et al. (2012). "Shifts in soil microorganisms in response to warming are consistent across a range of Antarctic environments." The ISME journal **6**(3): 692-702.

Yin, H., et al. (2013). "Enhanced root exudation stimulates soil nitrogen transformations in a subalpine coniferous forest under experimental warming." Global change biology **19**(7): 2158-2167.

Yoshitake, S., et al. (2015). "Soil microbial response to experimental warming in cool temperate semi-natural grassland in Japan." Ecological Research **30**(2): 235-245.

Yue, H., et al. (2015). "The microbe-mediated mechanisms affecting topsoil carbon stock in Tibetan grasslands." The ISME journal **9**(9): 2012.

Yue, H., et al. (2015). "The microbe-mediated mechanisms affecting topsoil carbon stock in Tibetan grasslands." ISME J **9**: 2012-2020.

Zak, D. R. and G. W. Kling (2006). "Microbial community composition and function across an arctic tundra landscape." Ecology **87**(7): 1659-1670.

Zapala, M. A. and N. J. Schork (2006). "Multivariate regression analysis of distance matrices for testing associations between gene expression patterns and related variables." Proceedings of the national academy of sciences **103**(51): 19430-19435.

Zehr, J. P., et al. (2003). "Nitrogenase gene diversity and microbial community structure: a cross‐system comparison." Environmental microbiology **5**(7): 539-554.

Zhang, J., et al. (2013). "PEAR: a fast and accurate Illumina Paired-End reAd mergeR." Bioinformatics **30**(5): 614-620.

Zhang, N., et al. (2013). "Soil microbial responses to warming and increased precipitation and their implications for ecosystem C cycling." Oecologia **173**(3): 1125-1142.

Zhang, W., et al. (2005). "Soil microbial responses to experimental warming and clipping in a tallgrass prairie." Global Change Biology **11**(2): 266-277.

Zhou, J., et al. (1996). "DNA recovery from soils of diverse composition." Applied and environmental microbiology **62**(2): 316-322.

Zhou, J., et al. (2016). "Temperature mediates continental-scale diversity of microbes in forest soils." Nature communications **7**: 12083.

Zhou, J., et al. (2016). "Temperature mediates continental-scale diversity of microbes in forest soils." Nature Communications **7**.

Zhou, J., et al. (2014). "Stochasticity, succession, and environmental perturbations in a fluidic ecosystem." Proceedings of the National Academy of Sciences **111**(9): E836-E845.

Zhou, J., et al. (2012). "Microbial mediation of carbon-cycle feedbacks to climate warming." Nature Climate Change **2**(2): 106.

Zhou, J., et al. (2012). "Microbial mediation of carbon-cycle feedbacks to climate warming." Nature Climate Change **2**(2): 106-110.

Zhou, J. Z., et al. (1996). "DNA recovery from soils of diverse composition." Applied and Environmental Microbiology **62**(2): 316-322.

Ziegler, S. E., et al. (2013). "Warming alters routing of labile and slower-turnover carbon through distinct microbial groups in boreal forest organic soils." Soil Biology and Biochemistry **60**: 23-32.

Zielke, M., et al. (2005). "Nitrogen fixation in the high arctic: role of vegetation and environmental conditions." Arctic, Antarctic, and Alpine Research **37**(3): 372-378.

Zimmermann, W. (1990). "Degradation of lignin by bacteria." Journal of Biotechnology **13**(2-3): 119-130.